

**SOME INTERACTIONS BETWEEN SURFACE WATER  
WAVES AND RIPPLES AND DUNES ON THE SEABED**

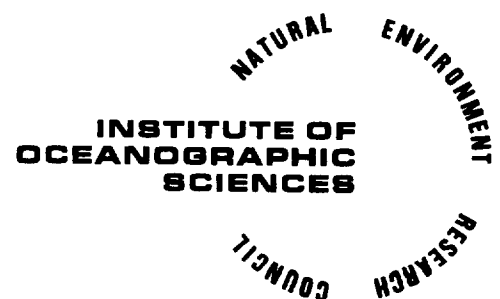
by

**A G Davies**

- Part 1    The wave-induced flow over seabed  
          topography**  
**Part II   The reflection of incident wave energy  
          by seabed topography**

**Report No 108**

**1980**



**INSTITUTE OF OCEANOGRAPHIC SCIENCES**

**Wormley, Godalming,  
Surrey, GU8 5UB.  
(0428 - 79 - 4141)**

**(Director: Dr. A.S. Laughton)**

**Bidston Observatory,  
Birkenhead,  
Merseyside, L43 7RA.  
(051 - 653 - 8633)**

**(Assistant Director: Dr. D.E. Cartwright)**

**Crossway,  
Taunton,  
Somerset, TA1 2DW.  
(0823 - 86211)**

**(Assistant Director: M.J. Tucker)**

---

*On citing this report in a bibliography the reference should be followed by  
the words UNPUBLISHED MANUSCRIPT.*

SOME INTERACTIONS BETWEEN SURFACE WATER  
WAVES AND RIPPLES AND DUNES ON THE SEABED

by

A G Davies

- Part I    The wave-induced flow over seabed  
          topography  
Part II   The reflection of incident wave energy  
          by seabed topography

Report No 108

1980

Institute of Oceanographic Sciences  
Crossway  
Taunton  
Somerset





# TABLE OF CONTENTS

	Page
Abstract	4
General Introduction	5
1 Summary	5
2 Literature review	7
2.1 Solutions of the classical wave equations	8
2.2 Solutions for long waves and small bottom slopes	12
2.3 Solutions for long barotropic coastal waves	16
2.4 Solutions for internal tidal waves and planetary waves	19
2.5 Interactions between surface waves and internal waves	22
2.6 Conclusions	22
Part I: The wave-induced flow over seabed topography	
1 Introduction	24
2 Justification for the use of the linearized equations	25
3 Statement of the problem	26
3.1 Solution of the first order problem	30
3.2 The second order problem	31
3.3 Solution of Problem 1	32
3.4 Solution of Problem 2	33
3.5 Limitations on the first order solution	34
3.6 Results to second order for the velocity field	36
3.7 The influence of the free surface	38
3.8 The accuracy of a quasi-uniform flow assumption	41
4 Energy fluxes	45
4.1 The resonant interaction at $\ell = 2k$	48
5 The third order problem	49
5.1 Limitations on the second order solution	54
6 Application of the method to naturally occurring seabed topography	55
6.1 Results for sand ripples in deep flow	56
6.2 Results for sandwaves in shallow water	67
7 Discussion	75
8 Conclusions	78

	Page
Part II: The reflection of incident wave energy by seabed topography	81
1 Introduction	81
2 The steady state formulation and solution	84
2.1 The evaluation of $\varphi(x, y, t)$ by contour integration	87
2.1.1 Solution in the asymptotic limit $x \rightarrow -\infty$	91
2.1.2 Solution in the asymptotic limit $x \rightarrow +\infty$	93
2.2 Limitations on the solution for $\varphi(x, y, t)$	94
2.3 Discussion of the steady state problem	95
3 The initial value problem and its solution	95
4 Applications of the theory	105
4.1 A simple piston action at the bottom boundary	105
4.2 A patch of ripples on an otherwise flat bed	106
4.3 A single sand bar or sandbank	116
4.4 The general result	118
4.5 Discussion	120
5 Correction procedure to establish a proper energy balance in the solution	120
5.1 Application in the case of a patch of ripples on an otherwise flat bed	122
6 Discussion	125
6.1 Consequences for sediment transport	125
6.2 Momentum flux considerations	126
7 Conclusions	127
Acknowledgements	130
References	131

## ABSTRACT

When surface water waves propagate over undulating seabed topography, the resulting interaction may modify both the seabed, if the orbital velocities near the bed are sufficient to cause sediment motion, and also the waves, possibly causing a proportion of the energy of an incident wave to be reflected. Linear perturbation theory is used here to examine this interaction for the case of two dimensional oscillatory uniplanar nonseparating flow, in which the surface wave crests are parallel to the crests of the bottom undulations. Initially, a method is developed for calculating the velocity field over the undulations, and examples are given for the cases of ripples and sandwaves. Then the reflection of incident surface waves is considered in detail.

The report is written in two parts. In Part I, a steady state perturbation solution is developed for the interaction of first order incident progressive surface waves with small sinusoidal bottom undulations of infinite horizontal extent. This interaction produces two new waves, whose wavenumbers are the sum and difference of those of the surface waves and the undulations. The sum wave is always onwards transmitted while, for sufficiently small surface wavenumbers, the difference wave is reflected. In fact, there is a singularity in the solution for the difference wave, which indicates strong reflection when the bed wavenumber is twice the surface wavenumber. The consequences of this for possible dune growth on an erodible bed are discussed.

In Part II, the problem of the reflection of incident surface waves by bottom undulations is studied in more detail. The undulations are now assumed to be of limited horizontal extent, enabling results for the reflected and transmitted waves to be obtained in the perturbation solution by Fourier transform methods. The same general results are produced by steady state and initial value problem formulations, and these are applied to the case of a patch of sinusoidal undulations on the seabed. The principal conclusions are that the reflection coefficient is both highly oscillatory in the ratio of the length of the patch to the surface wavelength, and also critically dependent on the ratio of the surface to bed wavenumbers. In addition, the transmitted wave may experience a small phase shift, even in cases of zero reflection. Examples are presented which indicate that relatively few bottom undulations, with wavenumber equal to approximately twice the surface wavenumber, may give rise to a very substantial reflected wave. A possible consequence of this is a coupling between dune growth and wave reflection, which may be important in problems of coastal protection.

## GENERAL INTRODUCTION

### § 1. SUMMARY

There have been many studies of surface wave propagation in water of variable depth, ranging from the scattering of planetary waves by topographic variations, to the reflection of short incident gravity waves by obstacles, such as engineering works, on the bed. Since the implications of these results for workers in the field of sediment transport do not seem to be widely known, it is the purpose of this report to consider the problem in this context. In particular, a linearized analysis of surface wave propagation over an undulating bed of ripples and dunes is presented with a view to predicting details of both the flow field over the bed-forms and the amount of incident wave energy reflection which occurs as a result of the presence of the bedforms. Certain quantitative conclusions can be drawn from the results relating to sediment motion on an instantaneous (wave by wave) basis on an undulating bed. Also, qualitative conclusions can be drawn concerning the possible formation of dunes on an erodible bed by a process of resonant interaction between the free water surface and the seabed.

The report is written in two parts, though the underlying theoretical basis is the same in each. In Part I, the well established two-dimensional linearized theory for the propagation of water waves above a flat horizontal bed is extended to study the case in which the bed comprises small undulations, with crests parallel to the surface wave crests. The findings presented complement the results of Davies (1979), which were to do with the "deep" flow of a perfect fluid over ripples of finite amplitude. The aim here is to use linearized equations to predict the flow pattern above a prescribed bed structure, knowing the surface wave parameters and the water depth. What is of interest in connection with sediment transport is the near-bed velocity field, and, in particular, the enhancement of flow velocity above ripple crests and the reduction above troughs, compared with the unperturbed flat bed velocity.

The method adopted in Part I is to take the familiar velocity potential for a flat bed as the lowest order term in a small parameter expansion scheme, and to deduce higher order solutions containing perturbations due to the bed features. Initially, the analysis is confined to a bed of purely sinusoidal ripples. It is then extended, by the addition of harmonics of the fundamental sinusoid, to account for the shapes of symmetrical wave-generated sand ripples, and also for the shapes of asymmetrical sandwaves. The role of the free surface in the problem is established by comparison of the present results with equivalent deep flow results. This enables a distinction to be drawn between the cases of "ripples" in deep flow

and "dunes" in shallow flow. The linearized analysis is valid only if certain conditions on the wave and bedform dimensions are satisfied. Furthermore, the flow is assumed to be nonseparating above the lee slopes of the bedforms, which restricts the range of application of the results. However, despite these limitations, the results obtained are found to be valid over physically interesting ranges of surface wave and bedform parameters.

It is assumed in Part I that the bed is composed of an infinite number of undulations in the direction of wave travel, and no conditions are imposed at infinity except that the solutions are bounded there. It is suggested that results obtained on this basis may be used with confidence to predict the flow field over a particular ripple or dune of interest, provided its profile is representative of the profiles of the neighbouring ripples or dunes on the bed, and provided also that its wavelength is much smaller than the surface wavelength. In other words, it is suggested that the method of Part I may be used in many practical cases, despite the fact that an infinitely long region of bedforms is physically unrealistic. However, care must be taken in using the results in cases in which the bed wavelength is comparable to the surface wavelength, since the solution is not uniformly valid in the ratio of these wavelengths. In particular, for a purely sinusoidal bed perturbation and an assumed sinusoidal surface wave in the first-order solution, an infinite resonance arises in the (second-order) perturbation solution if the surface wavelength is twice the bed wavelength. Close to this critical condition, the solution is invalid.

An examination of the perturbation solution in the neighbourhood of the critical ratio of wavelengths reveals the prediction of a strong reflection of incident wave energy. In fact, the solution in Part I predicts a reflected wave of infinite amplitude, which is physically unrealistic and is due to the assumption of an infinite number of undulations on the bed. It is the purpose of Part II of this report to extend the analysis of Part I to the case in which there is a finite number of bedforms upon an otherwise flat bed. In other words, surface waves are now assumed to be incident upon a region of bedforms of limited horizontal extent, and the question which arises is how much of the incident wave energy is reflected and how much is transmitted. This is a physically well posed problem, and one in which the radiation condition can be properly applied to ensure that the only waves in the perturbation solution are outgoing waves from the region of disturbance on the bed. We do not evaluate the solution obtained in the immediate vicinity of the bedforms, assuming that the solution in Part I will suffice in this respect for most practical purposes. Instead, we are concerned

only with the asymptotic solutions well away from the bedforms, and with the prediction of an approximate reflection coefficient.

It is found that, for the case of sinusoidal surface waves incident upon a patch of purely sinusoidal bedforms, the reflection coefficient may be characterized by two properties. In the first place, it is oscillatory in the ratio of the surface wavelength to the overall length of the region of bedforms. Secondly, it has a pronounced, but finite, resonance when the surface wavelength is approximately twice the bed wavelength. In this critical situation, the amplitude of the reflected wave is proportional to the number of bedforms in the patch. It follows that, as in Part I, an infinite number of bedforms leads to the prediction of a reflected wave of infinite amplitude. In the more realistic situation in Part II, the amplitude of the reflected wave depends not only upon the two ratios mentioned above, but also upon the ratios of both ripple amplitude and mean water depth to the surface wavelength.

The ability of an undulating bed to reflect incident wave energy is important in respect both of coastal protection, and of possible dune growth if the bed is erodible. This latter possibility arises where the combination of incident progressive waves and reflected waves leads to a partially standing wave structure, with all that this implies for preferred regions of deposition and erosion on the bed. In fact, there is good reason to postulate a direct coupling between the processes of dune generation and wave reflection.

## § 2. LITERATURE REVIEW

The principal qualitative conclusions of the present report, such as for example the oscillatory nature of the reflection coefficient, have been referred to in the existing literature in other applications. In addition, the present analysis methods are well known. However, as far as the author is aware, there has been no previous treatment of the undulating bed problem along the lines described here in Parts I and II.

The existing literature can be discussed under various headings, some more closely related to the present work than others. Firstly, there have been both rigorous and approximate studies of wave propagation over topography, based on the classical linear equations of surface waves in two dimensions. Secondly, under the usual approximations, the problem has been studied for long waves, and also for small bottom slopes. Thirdly, there have been studies of the effects of topographic variations on long barotropic coastal waves, the types of waves considered including Kelvin and Poincaré waves, continental shelf waves and edge

waves. Fourthly, there have been various treatments of the scattering of internal tidal waves and planetary waves by topography. All the above mentioned topics incorporate a description of the depth variations, or of the coastline. However, further comments having a relevance to the present report can be made on the basis of studies of the interaction of surface waves with internal waves. It has been thought worth reviewing the existing literature under each of the above headings in order, firstly, to place the present work in its proper general context and, secondly, to show how the various specific conclusions which arise here tie in with the qualitative conclusions of previous studies. Strictly, however, it is only work under the first two of the above headings which has any immediate quantitative relevance to the present study.

Under the first two of the above headings, problems involving the propagation of water waves in fluid of variable depth can be divided into three categories: 'beach' problems, where the depth tends to zero; 'obstacle' problems, where the depth is constant except for variations extending over a finite interval in space; and 'changing depth' problems, where the depth changes from one limiting (non-zero) value to a second limiting (non-zero) value. We shall be concerned here principally with 'obstacle' problems, to a lesser extent with 'changing depth' problems, and hardly at all with 'beach' problems.

## 2.1 Solutions of the classical wave equations

Solutions of the classical equations for wave propagation in water of variable depth have been obtained in several ways. Usually, these have restricted the solutions to the particular simple topographies examined, for instance by the need for a knowledge of the conformal mapping of the fluid domain into some simpler domain, usually a strip, for which the potential problem can be solved. Such mappings are not available for general topographic variations, though approximate mappings may sometimes be found. When approximate solutions of the boundary value problem have been sought on a different basis, these solutions have been generally quite complicated and again restricted to simple topographic variations, such as step changes in the depth.

Kreisel (1949) set out to determine the reflected and transmitted wave system for surface waves of general wavelength incident upon low (cylindrical) obstacles lying in a finite part of the bed. His method requires a knowledge of the conformal mapping which takes the fluid domain to a uniform strip, and he has thus reduced the mixed boundary value problem to an integral equation which can be solved iteratively. Kreisel's solution shows that, at a few depths from the

obstacle, the potential is very nearly a superposition of simple wave trains, the error falling off exponentially with distance. Another important result is a symmetry relation between the reflection coefficients of waves incident on the obstacle from either direction. In particular, it is shown that the reflection coefficient is the same for waves incident from either the deep or shallow end, provided that the approach to uniform depth at both ends is exponential. Strictly, Kreisel's asymptotic results enable bounds to be placed on the reflection coefficient only if the mapping of the fluid domain into a strip is known. However, if the exact mapping is not known, but an approximate mapping can be obtained, it is still possible to place bounds on the reflection coefficient by use of certain theorems which are proved. It should be noted also that, since Kreisel's approach is aimed primarily at reflection by obstacles of scale comparable to the wavelength, it does not result in close bounds for reflection by long topographic features. In addition, estimates obtained for the reflection coefficient grow more precise in the limit as the wavelength grows large with respect to the depth (ie in shallow water). Kreisel has considered in detail only the case of a thin barrier on the seabed, of height less than the water depth. He quotes also, though without giving any derivation, a result for reflection by a horizontal "reef" on an otherwise flat bed. Interestingly, the reflection coefficient in this case has an oscillatory nature in respect of the ratio of the width of the reef to the surface wavelength. Although Kreisel has presented an analysis which is in some respects very general, it is not one which can be adapted readily to cases of interest in the present report, due to the fact that suitable mapping functions are not known. The method of Kreisel has been extended by Ogilvie (1960) who has used a mapping method to study the propagation of long surface waves over an obstacle. He too has considered the case of reflection by a thin vertical barrier on the seabed.

Roseau (1952) has found an exact solution for a depth profile which varies continuously between two different asymptotic limits, by mapping the flow domain into a uniform strip and solving the transformed boundary value problem. Compared with results for an equivalent abrupt change in depth, the reduction of the reflection coefficient for a continuous profile is considerable (though Roseau's theory itself does not yield the reflection coefficient for the case of the abrupt change).

More recently, a mapping method has been developed by Fitz-Gerald (1977) to study the reflection of an incident surface gravity wave that travels over a region of varying depth. Here the existence of a unique velocity potential is



proved for general bottom profiles in the limiting cases when the surface wavelength is either small compared with the depth, or large compared with a suitably defined "transition width" (between the limiting deep and shallow ends). A general numerical procedure is described for wavelengths of the order of the depth. Essentially, Fitz-Gerald's rigorous approach involves reformulating the basic equations as a boundary value problem in a parallel strip. Then Fourier transform techniques are applied, and two integro-differential equations are obtained for the wave amplitude. The key to obtaining the results in the paper lies in choosing particular linear combinations of the two integro-differential equations for which convergent iteration schemes can be developed. The mappings used by Fitz-Gerald are adaptations of an appropriate Schwarz-Christoffel mapping, and contain a parameter related to the horizontal length scale of the depth variations. The particular topographies examined are mounds superimposed on steps and plateaus; as limiting cases of these, steps, symmetrical mounds and "reefs" are considered. In the case of plateaus it is found that the reflection coefficient is oscillatory, whether the plateaus are defined with smooth bottom profiles or as reefs (with discontinuous changes in depth). For wave propagation over a step, the value of the reflection coefficient corresponds, in the long wave limit, to the formula of Lamb (1932), about which more is written later.

While Fitz-Gerald's work has extended the class of bottom profiles for which numerical results can be achieved, it calls again for a knowledge of an appropriate mapping of the fluid domain. There have been several studies carried out on a different basis however. Biesel and Le Méhauté (1955) have considered wave propagation over a pair of short, individually symmetrical obstacles. These authors have not concerned themselves with local perturbations in the vicinity of the obstacles but, having restated Kreisel's (1949) symmetry principle, have identified resonance conditions which depend upon the obstacle spacing. Obstacles with a long elevated horizontal surface, such as submerged rectangular parallelepipeds, have been treated experimentally and theoretically by Jolas (1960) and Takano (1960). Jolas has proposed a linear treatment, and concentrated some attention on the wave field above the obstacle itself. In particular, he has noted that, when the depth of water above the obstacle is relatively small, very short transmitted waves may be generated by nonlinear effects.

A more complete treatment of the above problem has been given by Newman (1965 a, b). Firstly, he has considered (Newman, 1965a) waves normally incident on a step, the depth on one side of the step being infinite, and has given numerical results for the reflection and transmission coefficients over the

complete range of wavelengths of practical interest. Newman's approach has been to reduce the linear two dimensional boundary value problem for the velocity potential to an integral equation and, following the transformation of this equation into an infinite set of linear algebraic equations, has developed a numerical solution for the reflection and transmission coefficients. The complete solution comprises solutions for the individual domains in the problem (ie above the step and in deep water), and these involve summations providing the local effects at the step, which decay exponentially with distance from the step. In the long wave limit, the results obtained are consistent with those of Lamb (1932) (see later). However, it is found that, for practical purposes, the long wave limit gives a poor approximation for the reflection and transmission coefficients even for quite small values of the depth and that, even for relatively long waves entering quite shallow water, frequency effects are important. Secondly, Newman (1965b) has extended the above results for the infinite step to the problem of the propagation of waves past very long symmetrical obstacles, by considering separately the effects of reflection and transmission at each end. It is envisaged that the incident wave is partially reflected at the first obstacle (ie depth discontinuity) and partially transmitted to the second, where a smaller part is transmitted on and another part is reflected back to the first, and so on. Kreisel's (1949) symmetry relations are used in an extended form, and it is established that, for suitably chosen values of obstacle length, there is complete transmission due to interference between the two ends. In other words, the reflection coefficient is a highly oscillatory function of the obstacle length for waves of given frequency.<sup>d</sup>

Newman's (1965a) numerical results were based on the solution of as many as eighty simultaneous equations. A more economical, but still powerful, method of solution has been proposed by Miles (1967) for the case of a step discontinuity between two finite depths. A "scattering matrix" is defined and the problem reduced to the solution of integral equations. The elements of the scattering matrix are determined by means of variational integrals, and the results obtained are found to be in good agreement with those of Newman (1965a) in the appropriate limit for the infinite step. The variational formulation of Miles has been used by Mei and Black (1969) to study the scattering of waves by a rectangular obstacle in a channel of finite depth. Radiation conditions are imposed, and the potentials for the different regions are expressed as infinite eigenfunction expansions. For explicitness, the propagating modes are separated from the non-propagating modes which describe the flow in the immediate vicinity of the obstacle, and the solution depends ultimately on the numerical evaluation of

various determinants. The theory predicts a reflection coefficient having an oscillatory nature, and is in good agreement with Newman's (1965b) results, at least for long and very short wavelengths. Also it is in good agreement with Ogilvie's (1960) long wave theory approximation, and with Jolas' (1960) experiment.

Finally, under the present heading, we note the recent work of Shinbrot (1980) who has studied three dimensional irrotational free-surface flow over a periodic bottom. Surface tension effects are included in this analysis, specifically to ensure a well posed problem. With surface tension, flows having the same periodicity as the bottom are calculated. The main results in the paper are for doubly-periodic flows in three dimensions. Again, a mapping of the fluid domain into some fixed domain is called for, but this is achieved non-conformally.

## 2.2 Solutions for long waves and small bottom slopes

We turn next to studies of the propagation of long surface waves over obstacles. The best known and most often quoted result of this type is due to Lamb (Art 176, 1932), who has treated the case of long waves passing over a finite step, from one constant depth to another. Continuity of mass and surface elevation lead to expressions for the reflection and transmission coefficients, though no information is sought or obtained about the detailed nature of the flow in the vicinity of the step. Lamb's results have been generalized in the previously mentioned studies of Newman (1965a), Miles (1967) and Fitz-Gerald (1977). In addition, Bartholomeusz (1958) has given a complete analysis of the boundary value problem for the potential. He has formulated the integral equation that governs the motion, and has solved this equation, a Fredholm integral equation of the second kind, in the limiting case of long waves to obtain reflection and transmission coefficients that are identical with those of Lamb.

The result of Lamb has been extended by Jeffreys (1944) to the case of two sudden changes in depth. This leads to a transmission coefficient which is periodic in the ratio of the surface wavelength to the obstacle width. For certain values of this ratio the reflected wave is zero, while for intermediate values reflection is maximized. Jeffreys has pointed out that the minima for transmission thus predicted are equal to the result for transmission across a single jump of the same height (on Lamb's argument) and, therefore, that the second discontinuity helps the transmission of energy, where it affects it at all. Jeffrey's result is quoted, perhaps slightly inappropriately, in the United States Army's (1973) Shore Protection Manual as being applicable to wave transmission over an offshore bar. It is not pointed out there that his result is probably best regarded as providing

an upper bound for the reflection of long waves by a bar.

A study having considerable relevance, at least as far as technique is concerned, to the initial value formulation in § 3, Part II, of this report is that of Harband (1975). In his study, asymptotic expressions are developed for the refraction, reflection and modulation of long waves progressing in water of variable depth, when the rate of depth variation is small compared with the surface wavelength. The approach adopted by Harband has been to start with an initial value problem for the potential in which the bottom boundary condition is linearized, to solve the resulting approximate linear problem and only finally, in the steady state solution, to make the shallow water approximation. As we shall argue later in Part II, this procedure does away with the need to prescribe radiation conditions on an a-priori unknown steady state solution. The nature of the initial value problem is as follows. The bed is taken initially to be flat, but quickly assumes its final varying shape such that, for large time, the transient effect due to the "creation" of the variable bottom decays and the steady state solution is obtained. This technique has been discussed fully by Lighthill (1965). In Harband's study, after the shallow water limit has been taken in the steady state solution, an expression for the surface elevation is obtained which is independent of depth, but dependent on the rate of variation of the bottom elevation. Wave reflection is investigated when derivatives of the bottom elevation are piecewise continuous, and it is suggested (misleadingly according to Meyer (1979) - see later) that the reflection tends to zero with increasing bottom smoothness.

A further study having relevance to the present report, as far as technique of solution is concerned, is that of Carrier (1960). This work comprises an initial value formulation which is used to generate transient wave motions, in particular tsunamis. In contrast to the work of Harband, the transient wave motions are themselves the prime objects of study. Carrier has used linear theory to describe the propagation of these waves in the deep ocean, and nonlinear shallow water theory as the waves approach the shore. In the former considerations, Carrier has both Laplace and Fourier transformed the governing equation and boundary conditions, and has thus obtained the solution for the potential in the form of an integral. This has then been evaluated by residues in such a way that the radiation condition is satisfied. Carrier neglects the non-propagating modes in the solution which describe the flow in the immediate vicinity of the initial bed disturbance. In several of the above respects, the approach in Part II of the present report is similar to that of Carrier, though no Laplace transform is applied in the present work and the bottom disturbance is prescribed in a different region

of the bed. Ultimately Carrier's analysis is applied to the specific case of wave propagation over seabed topography which is slowly varying. As has been pointed out by Fitz-Gerald (1977) and Meyer (1979), this analysis is deficient in providing no description of the effects of reflections, though what amounts to an ad hoc correction procedure is proposed to allow for reflection by topographic features like underwater ridges. In Carrier's approach, the local value of the wavelength is determined from the local value of the depth. In practice, however, the wavelength is determined by global features of the bottom profile (eg Harband (1975), see above).

Long wave reflection by seabed topography has been considered also by Kajiura (1963) and Hamilton (1977). Kajiura has discussed the manner in which reflections can be calculated for bottom profiles which do not possess abrupt changes in depth. He notes, in particular, that the reflection coefficient associated with a given depth transition is very small except in that part of the spectrum for which the wavelength is very large compared with the "transition width" of the depth change; and even in that part of the spectrum, for which the reflection coefficient is similar to that for a discontinuous change of depth (Lamb (1932)), the reflection is small unless the depth ratio associated with the transition differs greatly from unity. The reflection coefficient is found to oscillate as the ratio of transition width to surface wavelength varies. However, for cases in which the depth varies continuously (ie the transition width is infinite), there is no periodic fluctuation in the reflection coefficient. This latter case is studied in relation to symmetric ridges or valleys on the bed, the bed level taking different values on opposite sides of the ridge or valley. For the case of a finite transition, it is argued that the fluctuation of the reflection coefficient with respect to the wavelength is a result of the interference of reflected waves (see Newman (1965b) above) and, for the case of a continuous infinite transition, that the interference of reflected waves extends over the whole region so that the resultant reflection coefficient at infinity shows no periodic fluctuation, though the value of the coefficient itself may be greatly reduced. Hamilton (1977) has also studied the reflection of long waves by topography. The equations which he has used are based on an initial conformal mapping of the fluid domain onto a uniform strip, his aim being to study the effects of bottom topography without recourse to the rather more difficult short wave theory. The 'reformulated equations' are found to be accurate for abrupt bottom topographies, and reflection coefficients have been calculated for long period waves incident upon a step change in depth and a half-depth barrier. Lamb's (1932) result for the reflection coefficient at a step is recovered.

The difficulty experienced by Carrier (1966) in arriving at an estimate of long wave reflection by "slowly varying" topography has been considered by Meyer (1979). He has discussed the problem on the basis of both linear long wave theory and "refraction" theory, and has pointed out that, while estimates of reflection are readily obtained when the seabed topography is not smooth (eg Harband (1979) - see above), these indicate misleadingly that wave reflection tends to zero with increasing smoothness. In fact, Mahony (1967) and Fitz-Gerald (1977) have conjectured, and Meyer (1979) has established, that the reflection coefficient becomes transcendental in some measure of the ratio of the surface wavelength to the transition width. However, Meyer's approach gives no more than an estimate of the small reflection effect, and even this is obtained on the basis of an approximate theory.

In discussing "refraction" theory, Meyer refers to the simplifications which arise from the assumptions of small wave amplitude and slowness of variation in water depth: in other words, with the assumptions of the linearization of the surface condition, and of the vertical structure of the motion being dependent on the local depth, but not on its gradient. The equations obtained on these assumptions have been used by Berkhoff (1973) and Jonsson et al (1976) to estimate the slow cumulative effects on waves caused by gradual changes in the water depth, without restriction to shallow water. Berkhoff has studied the propagation of short waves (short with respect to the size of the disturbance of the bottom) over a shoal with a parabolic bottom profile. Jonsson et al have compared results obtained on the basis of simple refraction theory with those emerging from the complete solution of the reduced wave equation (ie diffraction theory, or "refraction" theory in Meyer's terminology). The problem is studied with reference to an idealized island of circular cylindrical shape situated on a paraboloidal shoal, and the solution is evaluated for tsunami periods.

Finally, under this heading, we note the work of McGoldrick (1968) who has used linearized shallow water theory to study the propagation of long waves over bottoms having sinusoidal undulations. Unlike most of the studies cited above, the region of bedforms is here assumed to be of infinite horizontal extent and not to be confined to some limited part of the bed. Periodic solutions of the long wave equation are sought and, for the prescribed sinusoidal bedforms, the governing equation is cast into the form of Mathieu's equation. Regions of stability and instability are thus identifiable in the solution. Generally, it is found that the bottom undulations impede the propagation speed of the surface wave. However, there is a range of ratios of surface wavelength to bed wavelength, namely ( $\sqrt{3}, 2$ ), for which the waves are not retarded but, in fact, travel

faster than the phase speed based on the average depth. This result is related to a subharmonic resonance between the surface waves and the bed. Furthermore, because of the instability of the solution it is found that progressive wave type solutions cannot be formed for the following wavelength ratios:  $2$ ,  $2/3$ ,  $2/5$ ,  $2/7$  ..... and so on. The subharmonic resonance is interpreted by McGoldrick as implying that the amplitude of the surface wave will grow exponentially as the wave progresses, until either the shallow water approximation or the linearized equation are no longer reasonable approximations. Rhines (1970), in a footnote, has pointed out that this conclusion of unstable growth of a wave as it proceeds away from its source is in error. McGoldrick does not appear to consider the possibility of wave reflection, which is curious since this would seem to be a physically more sensible conclusion. In fact, in more recent (but as yet unpublished) work on this subject, Dr W G Pritchard\* has argued that the solution of Mathieu's equation suggests a reflection of wave energy, particularly when the ratio of the surface to the bed wavelength is two. In the present report, this ratio of wavelengths is shown to be associated with a resonance in the (perturbation) solution, the resonance becoming infinite as the number of sinusoidal ripples becomes infinite.

### 2.3 Solutions for long barotropic coastal waves

The papers cited above are those which are most directly relevant to the present study. In what follows, we concentrate attention on more distantly related topics, and we are highly selective in referring only to studies in which the interaction between surface waves and seabed topography leads to a conclusion which bears some qualitative similarity to the conclusions in the present report. Further discussion on the majority of these papers has been given by LeBlond and Mysak (1978). We start with studies of the effects of longshore variations, in either the depth or the coastline, on the propagation of long barotropic coastal waves in a rotating ocean. These may be Kelvin and Poincaré waves (eg Pinsent (1972), Howe and Mysak (1973), Mysak and Tang (1974)), continental shelf waves (eg Allen (1976), Hsueh (1980), Brink (1980)) or edge waves (Fuller and Mysak (1977)).

Pinsent (1972) has studied the problem of Poincaré waves incident upon a coastline which is nearly straight, in an ocean of nearly uniform depth. His results are based on a second order expansion in powers of a small parameter describing the relative magnitude of the coastal irregularities. In particular, solutions of the long gravity wave (shallow water wave) equation are obtained to first and second order by Fourier transform methods, and the radiation condition is

\*Fluid Mechanics Research Institute, University of Essex

satisfied at infinity. Initially, Pinsent considers a system of waves incident on the coastline and finds, in addition to reflected waves, a Kelvin wave which travels along the coast. First order linearized theory is used to obtain the details of the Kelvin wave for arbitrary perturbations in the coastline and depth. Interestingly, certain combinations of coastline and depth variations are found which produce no Kelvin wave. A condition for this to happen, at a particular wave period, is expressed in terms of the transforms of the coastline and depth changes. Conversely, resonance effects are produced at other periods. Next, the deduced Kelvin wave is treated as the incident wave, the theory is extended to second order in the perturbations and the amount of energy scattered away from the coastline as Poincaré waves is determined. It is found that this energy is maximized for a coastline perturbation of length comparable to the incident wavelength. Conversely, some other combinations of coastal and depth perturbations cause no Poincaré waves to be set up.

Pinsent's approach gives a uniformly valid solution only for irregularities that occur in a finite segment of the coast (ie that have "compact support"), or which tend to zero sufficiently rapidly away from the centre of the irregular region. To deal with extensive irregular coastlines, other techniques have been suggested. One such approach involves treating an infinitely long coast as straight, except for small deviations which are represented by a stationary, random zero-mean function. The two problems considered by Pinsent (Kelvin wave generation and attenuation) have been treated in this manner by Howe and Mysak (1973) and Mysak and Tang (1974) respectively. Howe and Mysak have found that Poincaré waves are always generated by coastal irregularities, but that a Kelvin wave is only generated when a certain 'resonant interaction condition' is satisfied by the incident wave and the Fourier components of the coastal irregularities. It is found that on a relatively smooth coast, Kelvin waves are preferentially generated by incident waves propagating in the same direction as the Kelvin modes ('forward scattering'). However, more irregular coastlines result in Kelvin waves propagating in the opposite direction ('back-scatter'), and in such cases the waves are more sharply tuned in the sense that only waves incident in progressively narrower bands of direction of propagation actually contribute to the power flux in the Kelvin waves. It is found that Kelvin waves are scattered in preference to Poincaré waves when the frequency of the incident wave is rather small, the reverse being the case at higher frequencies. Mysak and Tang (1974) have found both that the propagation speed of a Kelvin wave is decreased, and that the wave is damped, by coastal irregularities. The size of the decrease in phase velocity, and in wave amplitude, is determined by an



integral involving the power spectrum of the coastline.

The scattering of barotropic continental shelf waves has been studied by Allen (1976), Brink (1980) and Hsueh (1980). Allen has considered the effects of small amplitude alongshore deviations from a "classical" shelf topography (ie topography varying only in a coordinate perpendicular to the coast and varying exponentially). The problem solved is one of forced motion in which the perturbation flow is governed by a first order wave equation, in which terms from the interaction of the basic (lowest order) flow with the bottom and coastline topography act as the forcing function. The perturbation flow adjusts to the alongshore variations in topography through the propagation of disturbances as free continental shelf waves. A result of Allen's that is of particular interest is that, for certain forms of shelf deviation, scattering does not occur. This suggests the existence of a class of shelf topography that is variable in the alongshore direction (and not necessarily with an amplitude which is small), yet is regular in the sense that it does not give rise to the scattering of long shelf waves. It is expected, however, that the incident wave will be modified by the bottom variations. In Allen's study, the relevant alongshore topographic scales are assumed to be greater than the shelf slope width, and the resulting motion is treated in the long wave non-dispersive limit. Phase velocity changes and the damping of free continental shelf waves caused by random bottom topography have been studied by Brink (1980). He has found that damping peaks occur at frequencies where scattering takes place into modes which have a zero group velocity and, therefore, do not transport energy. The existence of damping maxima is proposed as a valid result though, in practice, the peaks may not accumulate because of the presence of a mean flow. Hsueh (1980) has found that the scattering of long shelf wave energy does not occur for 'shelf-similar' depth changes, for which distances of isobaths to the shore remain a fixed fraction of the local shelf width. Forward scattering occurs only when a wave is incident upon topographic irregularities that are not shelf-similar. Hsueh has studied this phenomenon by carrying out a perturbation analysis to investigate the effects of small deviations from a shelf-similar depth change; in particular, given an incident long shelf wave, he has constructed long wave solutions at points far downstream from topographic irregularities. One conclusion of the study is that, at a fixed alongshore position, forward scattering gives rise to a difference in phase between the occurrence of flow events at different points across the continental shelf.

A study of shorter period edge waves in the presence of small alongshore coastal variations has been carried out by Fuller and Mysak (1977). They have

modelled the continental shelf as a flat shelf that gives way abruptly to a deep ocean of uniform depth, and have studied two problems. Firstly, they have considered incident waves originating in the deep ocean, and have calculated the reflection coefficient and the fraction of the energy scattered into various "trapped" and "leaky" edge wave modes. Secondly, they have looked at the effects of coastal irregularities on the propagation of a coherent trapped edge wave. The results obtained are valid for wave periods much shorter than the period associated with the Coriolis parameter, and for wavelengths much greater than the average size of the coastal irregularities.

#### 2.4 Solutions for internal tidal waves and planetary waves

The papers discussed above, under the heading coastal waves, indicate the variety of interactions which may arise between ocean waves and both seabed topography and the coastline. Of particular interest in the present context are the various resonant interactions which have been discovered, and conversely the conditions of zero interaction, which, taken together, are qualitatively similar to the oscillatory reflection coefficients described earlier. The remaining class of studies discussed here is that which involves the scattering of planetary waves and internal tides by the deep sea topography, well away from the continental margins.

The problem of the propagation of barotropic planetary waves over a sinusoidally varying bottom has been studied by Rhines and Bretherton (1973). Using a linearized depth-averaged equation which describes the changes in relative vorticity due to fluid motion northwards or up a (very slight) slope, they have derived a solution for free waves of low frequency in a homogeneous  $\beta$ -plane ocean. The special case of long waves over small sinusoidal undulations is described by an equation which is nearly Mathieu's equation, and the resulting solution is dominated by waves with the scale of the topography. Very slight three-dimensional topographic features are shown to provide weak, resonant interactions between Rossby waves of the same frequency, such that the waves trade energy back and forth via a "catalytic Fourier component of the depth". In general, the results of Rhines and Bretherton indicate that severe topographic roughness reduces both the scale of the waves and their associated energy propagation. Thomson (1975) has considered further the energy loss from barotropic planetary waves due to scattering from rough random topography. His study is concerned particularly with changes, caused by topographic variations, in the phase speed of planetary waves in an ocean having an exponentially varying mean depth. The propagation of planetary waves over short scale

topographic variations has been considered, in the baroclinic case, by McWilliams (1974) in a study which has concentrated on forced transient flow. Various forms for both the forcing and the topography have been employed, the main emphasis of the work being on low frequency motions containing horizontal scales large compared with those of the sinusoidal topography. Free modes are considered and are found to be significantly influenced by the topography only for frequencies small compared with the inertial frequency. The forced response is studied with reference to the free modes, and the possibility of resonant forcing is examined. Although the theory predicts a resonant response which is infinite, in practice the response will be finite since the forcing must be confined to only a part of the ocean.

The coupling of barotropic surface tides and baroclinic internal tides in the ocean has been studied in various ways, and it is an important effect since the transferred energy is lost to the surface tide and effectively represents its dissipation. Cox and Sandstrom (1962) have used a normal mode approach to determine the internal tidal wave field generated in the open ocean by tidal flow over small arbitrary topographic variations. In particular, for water of arbitrary stratification, they have developed perturbation equations to study the coupling of infinitesimal internal waves of all modes, both to one another and to surface waves, with a view to determining the energy flow between modes. They have found that, at particular wavelengths of the depth variations, a resonant transfer of energy occurs to the higher order solutions from the zero order solution (which governs the motion of both surface and internal waves in water of constant depth). For the case of a limited patch of roughness on the sea floor, incident waves are partially converted into a sum of internal wave modes which propagate radially away from the rough patch. The transfer of energy depends upon the existence of orbital currents at the seabed - clearly, there can be no coupling unless orbital currents of both modes reach the bed - and also of bottom undulations with a wavenumber equal to the difference between the wavenumbers of the two coupled modes. In this respect, the results of Cox and Sandstrom have a qualitative similarity to the perturbation solution in Part I of the present report.

Sandstrom (1976) has suggested that the above approach underestimates the contribution to the energy transfer from high modes, and has studied the problem further using ray theory. In particular, he has exploited the hyperbolic nature of the two-dimensional wave equation to develop solutions in the presence of localized topographic variations, and has achieved an overall energy balance such that the total baroclinic energy flux radiating away from a source area is

equal to the total rate of work done by the barotropic motion as it interacts with the bottom. Interestingly, he has identified cases of total transmission, one such being associated with a hump on the bed. Results are obtained also for a cosine-ridge topography and a vertical partial barrier, and it is found that the main factor in energy conversion is the roughness amplitude. Furthermore, a comparison of various solutions suggests that it is the blocking action of an obstacle, be it a slope, a shelf or a knife-edge barrier, that determines the gross features (low modes) of the solution, while the high modes are sensitive to the obstacle's shape.

A different approach to the surface-internal tide problem is that of Baines (1971, 1973 and 1974) who has exploited characteristic theory to cast the problem in the form of integral equations. These are solved numerically. Baines (1971) has assumed that the bed is "smooth" and, further, that it is of "flat-bump" type; that is the incident internal wave "lights" or "sees" the entire bed surface, so that wave characteristics all reflect off in the same direction. The equation which governs the wave field and which satisfies the radiation condition is a Fredholm equation of the second kind, with a non-singular kernel which depends upon the bottom topography. Bumps and troughs are considered, as well as a smooth change in depth from one horizontal plane to another. When a plane wave is incident upon a small amplitude sinusoidal bottom it is found that, in addition to the basic reflected wave, two new waves are produced whose wavenumbers are the sum and difference of those of the incident wave and the bottom topography. The sum wave is always in the onwards transmitted direction, whereas the difference wave is back reflected if the incident wavelength is sufficiently long. Baines (1973) has studied the case of a cosine ridge and has found that the energy flux and energy density of the internal wave motion generally increase rapidly as the height of the topography is increased. However, if a characteristic, continued by reflections from the boundaries, spans the topography exactly, the energy fluxes and densities may be rather small. In fact, in the case of a cosine ridge, they may vanish. Baines (1974) has extended the theory to (almost) arbitrary topography and density stratifications.

Finally, it is appropriate to note here the work of Larsen (1969). Although his study does not fall strictly under the present heading, it is concerned with the effect of a knife-edge barrier on the propagation of an internal wave. The wave is confined in a channel and, in the absence of the barrier, propagates as a single mode. A solution is found, satisfying the radiation criteria, for all the modes passing over, and reflected by, the barrier.

## 2.5 Interactions between surface waves and internal waves

In the above review, we have concentrated exclusively on the interaction between free surface waves and undulating seabed topography. We close with a brief comment on the interaction between surface waves and internal waves, in the absence of any topographic variations. Lewis et al (1974) have studied the perturbation to a pre-existing surface gravity wave, caused by an internal wave propagating in the same direction. The internal wave enters their analysis by way of the perturbations to the surface currents which it causes, and the problem is to determine the consequent changes in the surface wave characteristics, as functions of both position and time. Characteristic theory is used in the solution, and a perturbation solution of the governing equations is obtained in closed form, on the assumption that the magnitude of the surface current is small compared with the group velocity of the surface waves. Solutions are derived on this basis for first order changes in the surface wavenumber and the surface wave amplitude. Interestingly, a resonance, though not an infinite resonance, occurs in the solution when the phase speed of the internal wave and the group velocity of the surface wave are matched. Furthermore, for the resonant case, the linearized solution predicts a monotonic increase of certain "effects" with interaction distance, these effects being internal wave-induced modulations of surface wave amplitude and slope. Also, as the interaction distance increases, the variations become increasingly 'narrow band', with maximum effects concentrated within a progressively narrower range of relative wave speeds centred on the 'resonant condition'. Experimental results are here in good agreement with the theoretical predictions. Although the problem considered by Lewis et al is rather distantly related to that which is considered in the present report, it again leads to conclusions of a qualitatively similar kind to those arrived at later, in particular with the structure of the response curves of § 4, Part II.

## 2.6 Conclusions

Several of the qualitative conclusions, which have been identified separately in the above literature review, are drawn together in the study discussed in Parts I and II. This is not to say that the detailed results obtained in the present report may be found elsewhere, but rather that the principal conclusions reached have parallels in a variety of previous studies. For example, in Part I, it is shown that the interaction of incident surface waves with an infinite number of sinusoidal undulations on the bed produces two new

waves, whose wave numbers are the sum and difference of those of the incident waves and the bed. A very similar conclusion to this has been reached by Baines (1971), but in a rather different context. Again, in Part II, the reflection of surface waves by a limited patch of undulations on the bed is found to depend upon the ratio of the surface wavelength to both the bottom wavelength, and also the length of the patch. The importance of the first of these ratios has been identified by, for example, McGoldrick (1968), and the second by Jeffreys (1944), Newman (1965b) and Mei and Black (1969), but in none of these studies have the combined effects of patch length and bottom wavelength been explored. In the context of the implications of the results for sediment transport studies, such combined effects have a clear physical relevance, and it is one of the aims of this report to indicate their possible importance in relation to the growth or destruction of undulations on the bed.

## PART I THE WAVE-INDUCED FLOW OVER SEABED TOPOGRAPHY

### §1. INTRODUCTION

The aim of Part I is to use linear theory to calculate the wave-induced flow over prescribed seabed topography. The general approach adopted has been described earlier. Briefly, we assume that the water is of constant mean depth, but that the bed is rippled indefinitely in the direction of surface wave travel. The surface wave crests are assumed to be parallel to the ripple crests, enabling a two-dimensional problem to be solved for the velocity potential, and the steady state results obtained are based on a perturbation expansion in powers of a small parameter which is identified with ratios of the various length scales in the problem. In this approach, bottom topography variations are regarded as small perturbations on a plane surface, and the boundary condition is linearized in the usual way. Hence, from the condition that the component of fluid velocity normal to the bed must vanish on the boundary, the interaction between the (first order) flow, which would be present without the boundary perturbations, and the perturbations themselves, is treated as a new source of (second order) fluid motion situated on the plane surface. Although the problem tackled in Part I is physically unrealistic in the sense that the number of ripples on the bed is infinite, and improperly posed mathematically from the point of view of satisfying the radiation condition, it is suggested that the solution obtained provides a simple way of calculating the flow field over a variety of ripples and dunes, given the water depth, and surface wave period and amplitude, and provided that the bed wavelength is rather less than half the surface wavelength. If this restriction is not complied with, the solution in Part I is not uniformly valid in the ratio of the two wavelengths. However in Part II, where the problem is well posed mathematically, this restriction is relaxed.

The solution given is important in considering sediment transport on erodible beds (Davies and Wilkinson (1979)), and may be important also in providing an understanding of the mechanism of formation of certain features of relatively long wavelength on the bed. It is suggested that such features may arise from a resonant interaction between the undulating bed and the water surface. However this report is not concerned with the detailed sediment transport processes involved in the formation of such bed features.

In § 2. the use of linear theory is justified by reference to previously published results concerning the flow over ripples of finite amplitude. In § 3. the formulation is described, and first and second order solutions are presented

for a sinusoidally rippled bed. The limitations on these solutions are discussed, and examples are given which display the velocity field in the interior of the fluid and at the bed surface. These results are then compared both with equivalent "deep flow" results in order to assess the influence of the presence of the free water surface, and with results based on the local water depth (assuming an otherwise flat bed) in order to evaluate the importance of ripple steepness and shape, in association with depth, in determining seabed velocity amplitudes. In § 4. wave energy fluxes are examined for the first two terms of the small parameter expansion, and the resonant interaction between the water surface and the seabed is considered. In § 5. the third order term of the solution is presented, mainly with a view to determining the limitations on the second order solution. In § 6. the second order solutions are applied in two limiting practical cases, namely sand ripples on the seabed in "deep flow" and sandwaves in "shallow flow". In each case the bed surface is represented in Fourier series form, and surface velocity amplitudes are calculated over the simulated profiles. Finally, in § 7. the implications of the resonant interaction between the water surface and the bed are discussed in the event of the bed surface being erodible.

## § 2. JUSTIFICATION FOR THE USE OF THE LINEARIZED EQUATIONS

The model which has been proposed by Davies (1979) enables the exact prediction of the "deep flow" above prescribed bottom undulations of finite amplitude. In this approach, a uniform flow is perturbed by the introduction of a repeated pattern of discrete singularities, having strengths chosen such that one of the stream lines of the resulting motion takes the shape of the prescribed profile. The solution then enables the prediction of the velocity field close to the bed, in relation to the unperturbed free stream flow. It was thought important to establish, at the outset of the present study, whether similar results are obtained from an analysis in which the bed is assumed to be of small amplitude. Milne-Thomson (1968, Section 15.40) has given a solution for deep steady flow, bounded by a sinusoidal surface along the  $x$  - axis, having velocity potential

$$\phi = -Ux - bU e^{-\ell y} \sin(\ell x) \quad (1)$$

where the coordinate axes are as defined in Fig 2,  $U$  is the unperturbed free stream velocity,  $b$  is the ripple amplitude and  $\ell = 2\pi / \{\text{ripple wavelength}\}$ . The velocity components are taken as  $(-\phi_x, -\phi_y)$ , and so the unperturbed



flow is in the positive direction of  $x$ . To the order of approximation adopted, the bed surface  $y = y_b$  is given by

$$y_b = b \cos(\ell x) \quad (2)$$

The solution is based on a linearized kinematical boundary condition which is applied at the mean bed level  $y = 0$ , and the approximation involved in obtaining (1) on this basis can be illustrated by noting that the horizontal surface velocities at the ripple crest ( $u_{cr}$ ) and trough ( $u_{tr}$ ) positions, where the horizontal velocity takes its extreme values in the flow, are

$$u_{cr/tr} = U (1 \pm b\ell) \quad (3)$$

In Fig 1,  $u_{cr}/U$  and  $u_{tr}/U$  from (3) are plotted against the ripple steepness ( $b\ell$ ), together with exact results from Davies (1979) for a sinusoidal bed of finite amplitude. It can be seen that, at both crest and trough positions, good agreement exists between the solutions at small ( $b\ell$ ). Differences arise at larger values of ( $b\ell$ ), the linearized solution slightly overestimating departures from the unperturbed stream speed at both crest and trough positions. However the agreement is quite good enough to justify proceeding with a linearized analysis in the present free surface problem, since the upper bound of natural ripple steepness is about  $0.2\pi$ .

Although the flow given by (1) is steady, it is permissible to regard  $U$  as the velocity amplitude in the context of a deep oscillatory flow, since time may be introduced as a parameter in the deep flow solution. Thereby, a basis is secured for comparisons with the theory to follow and, in fact, Eq (3) is used later as a means of determining the influence of water depth on velocity close to the seabed.

### § 3. STATEMENT OF THE PROBLEM

The seabed is assumed to be composed of periodic two-dimensional ripples extending indefinitely in the positive and negative  $x$ -directions, as shown in the definition sketch in Fig 2. It is assumed that the mean water depth is  $h$  and that the flow is irrotational, so that Laplace's equation is satisfied in  $\mathcal{D}$  by the velocity potential  $\phi$ :

$$\nabla^2 \phi = 0 \quad \text{in} \quad \mathcal{D} \quad (4)$$

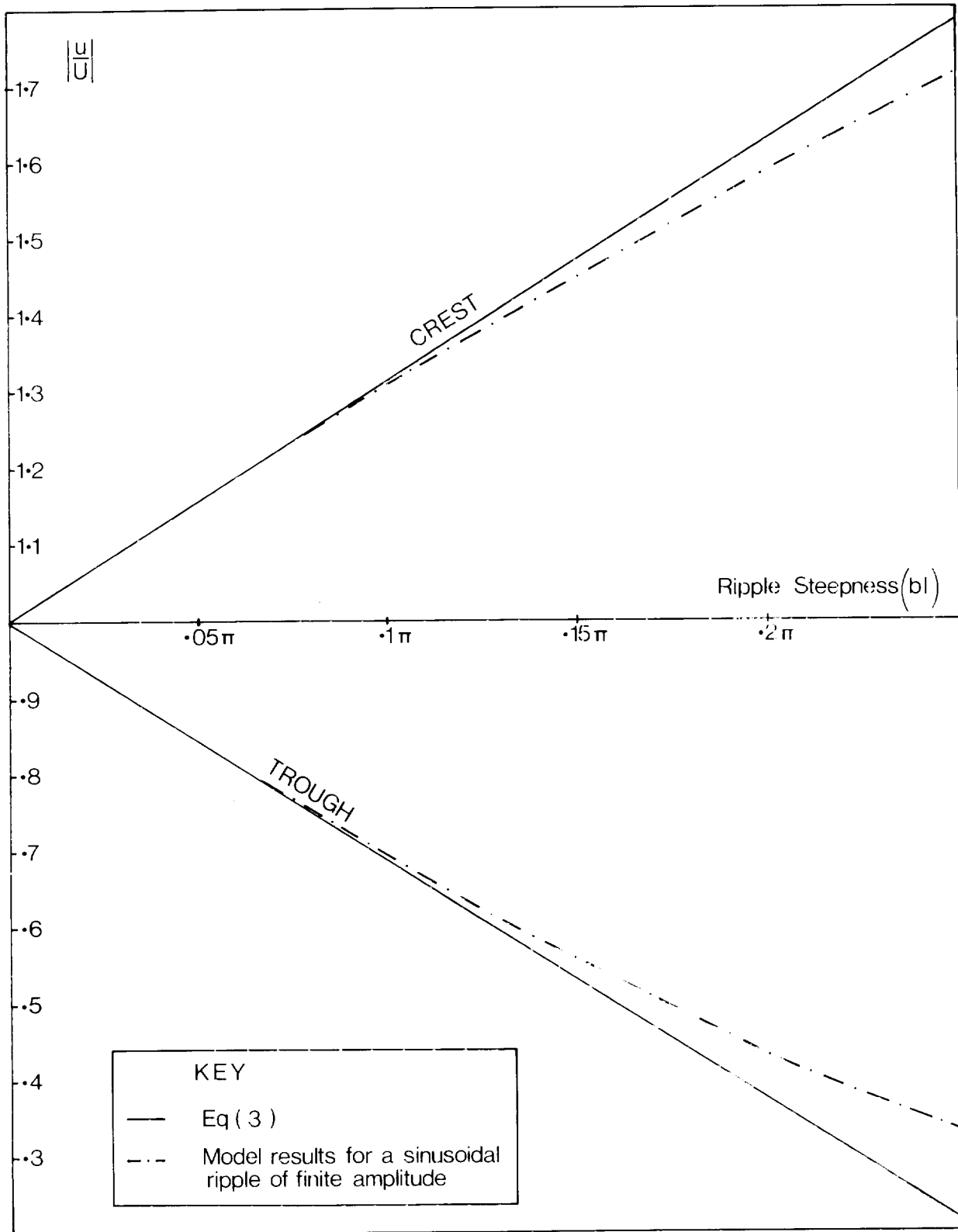


Fig 1 Surface velocities at the crest and trough of a purely sinusoidal ripple in deep flow plotted against ripple steepness ( $bl$ ). Results from small amplitude theory (Eq (3)) are compared with results from the finite ripple amplitude model of Davies (1979).

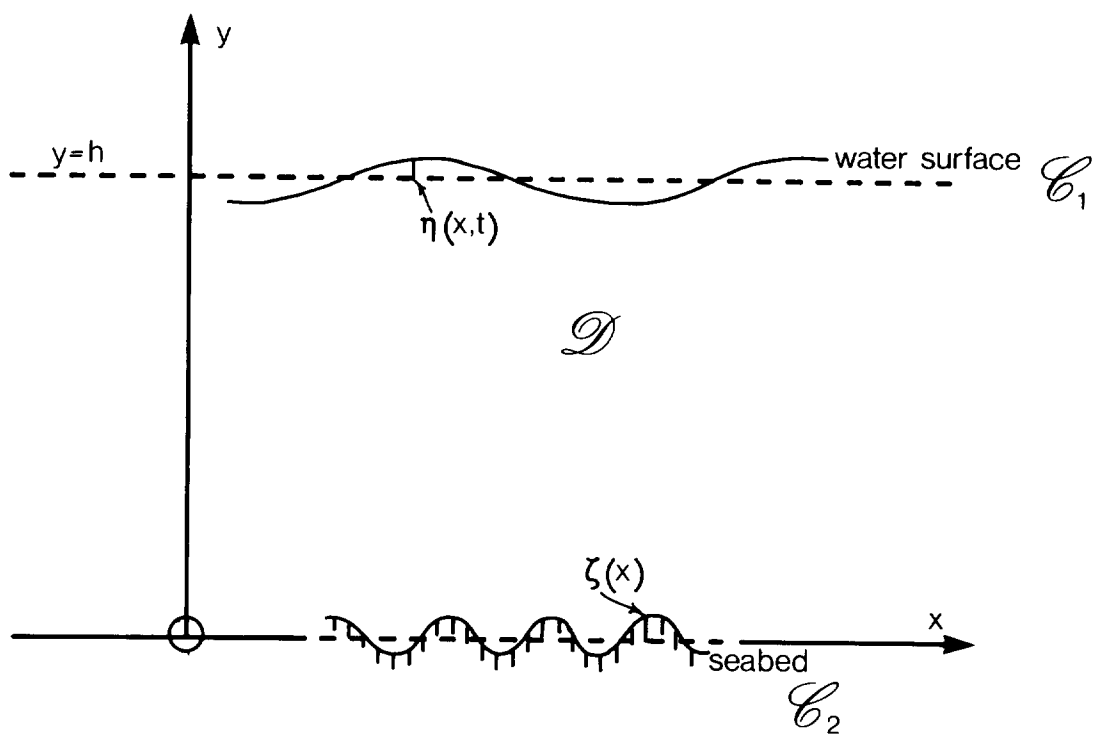


Fig 2 Definition sketch

The departure of the water surface from its mean position is taken as  $\eta(x,t)$  and that of the bed surface from its mean level as  $\zeta(x)$ .

The method of solution adopted is a small parameter expansion, which enables a basic hierarchy to be established in each of  $\phi$ ,  $\eta$  and  $\zeta$ , as follows:

$$\phi = \alpha \phi_1 + \alpha^2 \phi_2 + \alpha^3 \phi_3 + \dots \quad (5)$$

$$\eta = \alpha \eta_1 + \alpha^2 \eta_2 + \alpha^3 \eta_3 + \dots \quad (6)$$

$$\zeta = \alpha \zeta_1 + \alpha^2 \zeta_2 + \alpha^3 \zeta_3 + \dots \quad (7)$$

The use of the same small parameter  $\alpha$  in each of the above equations is not too restrictive, nor, as will be seen later, is it unreasonable to take the highest term in each expansion <sup>1</sup> to be  $O(\alpha)$ . The small parameter  $\alpha$  is identified with the physical parameters in the problem later.

The boundary conditions are

$$-\phi_x \eta_x + \phi_y + \eta_t = 0 \quad \text{on } G_1 \quad (\text{kinematical condition}) \quad (8)$$

$$g\eta - \phi_t + \frac{1}{2}(\phi_x^2 + \phi_y^2) = 0 \quad \text{on } G_1 \quad (\text{pressure condition}) \quad (9)$$

and 
$$-\phi_x \zeta_x + \phi_y = 0 \quad \text{on } G_2 \quad (\text{kinematical condition}) \quad (10)$$

In practice these conditions are satisfied at the mean water surface and bed levels,  $y = h$  and  $y = 0$  respectively, by way of the introduction of the following Taylor expansions

$$\begin{aligned} \phi \Big|_{y=h+\eta} &= \phi \Big|_h + \eta \frac{\partial \phi}{\partial y} \Big|_h + \frac{\eta^2}{2!} \frac{\partial^2 \phi}{\partial y^2} \Big|_h + \dots \\ \phi \Big|_{y=\zeta} &= \phi \Big|_0 + \zeta \frac{\partial \phi}{\partial y} \Big|_0 + \frac{\zeta^2}{2!} \frac{\partial^2 \phi}{\partial y^2} \Big|_0 + \dots \end{aligned}$$

Use of (5)-(7) permits their further expansion in powers of  $\alpha$ , for example

$$\phi \Big|_{y=h+\eta} = \alpha \phi_1 \Big|_h + \alpha^2 \left( \phi_2 + \eta_1 \frac{\partial \phi_1}{\partial y} \right) \Big|_h + \alpha^3 \left( \phi_3 + \eta_1 \frac{\partial \phi_2}{\partial y} + \eta_2 \frac{\partial \phi_1}{\partial y} + \frac{1}{2} \eta_1^2 \frac{\partial^2 \phi_1}{\partial y^2} \right) \Big|_h + \dots$$

---

<sup>1</sup>For a discussion of the small parameter expansion method in surface wave problems see Stoker (1957), Chapter 2.

By substituting this and the similar expansion for  $\phi|_{y=\zeta}$ , together with (5), (6) and (7), into Eqs (4), (8), (9) and (10), the original problem can be broken down into a series of problems, the first to order  $\alpha$ , the second to order  $\alpha^2$ , and so on.

Since this study is concerned with the interaction of progressing surface waves with a rippled seabed, it is assumed that

$$\eta_1 = a \sin(kx - \sigma t) \quad (11)$$

corresponding to waves of amplitude  $a$ , frequency  $\sigma$  and wavenumber  $k$ , travelling in the positive direction of  $x$ , and that

$$\zeta_1 = b \cos(\ell x + \delta) \quad (12)$$

where  $\ell$  is the wavenumber of sinusoidal bedforms,  $b$  is their amplitude and  $\delta$  is an arbitrary phase angle. This completes the statement of the problem.

### 3.1 Solution of the first order problem

If Eq (5) is substituted into (4), then to order  $\alpha$

$$\nabla^2 \phi_1 = 0 \quad \text{in} \quad 0 < y < h \quad (13)$$

Similarly the boundary conditions  $O(\alpha)$  at the free surface ( $y = h$ ) are

$$\frac{\partial \phi_1}{\partial y} + \frac{\partial \eta_1}{\partial t} = 0 \quad \text{from (8)}$$

$$g\eta_1 - \frac{\partial \phi_1}{\partial t} = 0 \quad \text{from (9)}$$

$$\text{and so} \quad g \frac{\partial \phi_1}{\partial y} + \frac{\partial^2 \phi_1}{\partial t^2} = 0 \quad \text{on } y = h \quad (14)$$

At the bed, from (10),

$$\frac{\partial \phi_1}{\partial y} = 0 \quad \text{on } y = 0 \quad (15)$$

It will be noted that no terms of (7) appear in the problem  $O(\alpha)$  and that the solution corresponding to (11) is

$$\phi_1 = \frac{a\sigma}{k \sinh kh} \cosh(ky) \cos(kx - \sigma t) \quad (16)$$

where  $\sigma$  is related to  $\omega$  and  $k$  by the dispersion relation

$$\sigma^2 = gk \tanh(kh) \quad (17)$$

The limitations on (16) are discussed later.

### 3.2 The second order problem

The governing equation to order  $\alpha^2$  is

$$\nabla^2 \phi_2 = 0 \quad \text{in} \quad 0 < y < h \quad (18)$$

and from (8)-(10) the boundary conditions are

$$-\frac{\partial \phi_1}{\partial x} \frac{\partial \eta_1}{\partial x} + \frac{\partial \phi_2}{\partial y} + \eta_1 \frac{\partial^2 \phi_1}{\partial y^2} + \frac{\partial \eta_2}{\partial t} = 0 \quad \text{on} \quad y = h \quad (19)$$

$$g\eta_2 - \frac{\partial \phi_2}{\partial t} - \eta_1 \frac{\partial^2 \phi_1}{\partial t \partial y} + \frac{1}{2} \left\{ \left( \frac{\partial \phi_1}{\partial x} \right)^2 + \left( \frac{\partial \phi_1}{\partial y} \right)^2 \right\} = 0 \quad \text{on} \quad y = h \quad (20)$$

$$-\frac{\partial \phi_1}{\partial x} \frac{\partial \xi_1}{\partial x} + \frac{\partial \phi_2}{\partial y} + \xi_1 \frac{\partial^2 \phi_1}{\partial y^2} = 0 \quad \text{on} \quad y = 0 \quad (21)$$

If the bed is flat the solution of the problem  $O(k^2)$  (Stokes' theory at the second order of approximation) is well known (see, for example, Peregrine (1972)). It is convenient, therefore, to subdivide the present problem into this well known one, which will be denoted by a superscript (1), and a complementary problem, which is of main interest in the present report and which will be denoted by a superscript (2). So writing

$$\phi_2 = \phi_2^{(1)} + \phi_2^{(2)}$$

and

$$\eta_2 = \eta_2^{(1)} + \eta_2^{(2)}$$

Problem 1 is taken as

$$\nabla^2 \phi_2^{(1)} = 0 \quad \text{in} \quad 0 < y < h \quad (18a)$$

$$\frac{\partial \eta_2^{(1)}}{\partial t} - \frac{\partial \phi_1}{\partial x} \frac{\partial \eta_1}{\partial x} + \frac{\partial \phi_2^{(1)}}{\partial y} + \eta_1 \frac{\partial^2 \phi_1}{\partial y^2} = 0 \quad \text{on} \quad y = h \quad (19a)$$

$$g \zeta_2^{(1)} - \frac{\partial \phi_2^{(1)}}{\partial t} - \zeta_1 \frac{\partial^2 \phi_1}{\partial t \partial y} + \frac{1}{2} \left\{ \left( \frac{\partial \phi_1}{\partial x} \right)^2 + \left( \frac{\partial \phi_1}{\partial y} \right)^2 \right\} = 0 \quad \text{on } y = h \quad (20a)$$

$$\frac{\partial \phi_2^{(1)}}{\partial y} = 0 \quad \text{on } y = 0 \quad (21a)$$

This problem is to do with the steepening of waves at the free surface, above a bed which is flat. It is important to note that the dispersion relation (17) is still valid here, but that in the equivalent "surface problem"  $O(\kappa^3)$  this is no longer the case.

Problem 2 is then as follows:

$$\nabla^2 \phi_2^{(2)} = 0 \quad \text{in } 0 < y < h \quad (18b)$$

$$\frac{\partial \zeta_2^{(2)}}{\partial t} + \frac{\partial \phi_2^{(2)}}{\partial y} = 0 \quad \text{on } y = h \quad (19b)$$

$$g \zeta_2^{(2)} - \frac{\partial \phi_2^{(2)}}{\partial t} = 0 \quad \text{on } y = h \quad (20b)$$

$$-\frac{\partial \phi_1}{\partial x} \frac{\partial \zeta_1}{\partial x} + \frac{\partial \phi_2^{(2)}}{\partial y} + \zeta_1 \frac{\partial^2 \phi_1}{\partial y^2} = 0 \quad \text{on } y = 0 \quad (21b)$$

This second problem has the same boundary conditions at the free surface as the problem  $O(\kappa)$ , while in (21b) the effect of the rippled bed comes through for the first time; that is, Eqs (18b)-(21b) for the perturbation potential  $\phi_2^{(2)}$  contain the interaction of the first order solution  $\phi_1$ , given by (16), with the prescribed bedforms  $O(\kappa)$  given by  $\zeta_1$ .

### 3.3 Solution of Problem 1

This well known solution can be quoted without derivation as

$$\phi_2^{(1)} = \frac{3a^2\sigma}{8 \sinh^4 kh} \cosh(2ky) \sin 2(kx - \sigma t) \quad (22)$$

The vertical attenuation of  $\phi_2^{(1)}$  is more pronounced than that of  $\phi_1$ , but the phase speed of the wave is the same as that of  $\phi_1$ . The surface elevation corresponding to (22), and given by (20a), is

$$\zeta_2^{(1)} = -\frac{a^2 k}{4} \frac{\cosh(kh) (\cosh(2kh) + 2)}{\sinh^3(kh)} \cos 2(kx - \sigma t) \quad (23)$$

which, in combination with (11), can be seen to lead to a steepening of the wave crests and a flattening of the troughs.

### 3.4 Solution of Problem 2

From the substitution of Eqs (11) and (16) in (21b), it can be seen that the solution for  $\phi_2^{(2)}$  must contain periodic terms

$$\sim \cos((\ell+k)x - \sigma t + \delta) \quad \text{and} \quad \sim \cos((\ell-k)x + \sigma t + \delta)$$

The governing equation (18b) is then satisfied if each of these terms is multiplied by an appropriate attenuation expression. The remaining arbitrary constants can be determined from the surface boundary conditions (19b) and (20b). The resulting solution is

$$\phi_2^{(2)} = \frac{ba\sigma}{2\sinh(kh)} \left\{ -A(\ell+k, \sigma, y) \cos((\ell+k)x - \sigma t + \delta) + A(\ell-k, \sigma, y) \cos((\ell-k)x + \sigma t + \delta) \right\} \quad (24)$$

in which the attenuation term is

$$A(r, s, y) = \frac{g + \cosh(+ (y - \ell)) + s^2 \sinh(+ (y - \ell))}{s^2 \cosh(+ \ell) - g + \sinh(+ \ell)}$$

Like (22), the velocity potential (24) is associated with a deformation of the free surface, which is given from (20b) by

$$\eta_2^{(2)} = -\frac{ba\sigma^2}{2g\sinh(kh)} \left\{ A(\ell+k, \sigma, \ell) \sin((\ell+k)x - \sigma t + \delta) + A(\ell-k, \sigma, \ell) \sin((\ell-k)x + \sigma t + \delta) \right\} \quad (25)$$

Since the velocity potential (24) is attenuated upwards from the bed,  $\eta_2^{(2)}$  will generally make a very small contribution to the surface elevation.

For  $\ell \gg k$  the attenuation terms in (24) can be seen to reduce to  $\sim \cosh \ell(y - \ell) / \sinh(\ell h)$ , which may be contrasted directly with the downward attenuation terms in  $\phi_1$  and  $\phi_2^{(1)}$ .

In general, the solution (24) can be seen to comprise two new waves with wavenumbers which are the sum and difference of those of the incident wave and the bottom undulations. The sum wave is always in the onwards transmitted direction, whereas the difference wave may travel in either direction and is back reflected if the incident wavelength is sufficiently long (see § 4.). At the changeover point ( $\ell = k$ ), the difference wave has infinite wavelength and the energy flux associated with it vanishes (ie the second terms on the right hand sides of both (24) and (25) are zero). The difference wave tends to be long, and is always longer than the wavelength of the sinusoidal bed. In all these respects, the



present result is qualitatively similar to that of Baines (1971). It may be noted also that both (24) and (25) are singular when

$$\sigma^2 \cosh(\ell \pm k) \ell = g(\ell \pm k) \sinh(\ell \pm k) \ell$$

that is when  $\ell = \pm 2k$ . The physically admissible case is  $\ell = 2k$ , in the neighbourhood of which the solution  $\phi_2^{(2)}$  must break down. This is discussed later.

### 3.5 Limitations on the first order solution

It is well known that, if the bed is flat, the solution  $O(\kappa)$ , ie Eq (16), is valid if  $ak \ll 1$  and  $a/h \ll 1$  (see Peregrine (1972)). These restrictions arise on account of the terms which are dropped in linearizing the boundary conditions. However, if  $kh \ll 1$ , there is a further restriction on the solution  $O(\kappa)$ . This follows from the clear requirement of the present method that  $|\phi_2^{(1)}/\phi_1| \ll 1$  and, using (16) and (22), can be expressed

$$\frac{a}{k^2 \ell^3} \ll \frac{8}{3} \quad (26)$$

The term on the left hand side of (26) is called the Ursell parameter, after its importance was first noted by Ursell (1953).

Similar conditions arise in the present problem as a result of the undulations on the bottom boundary. In the first approximation  $O(\kappa)$  certain terms were dropped in writing condition (15). In particular, it was assumed that

$$\left| \frac{\partial \phi_1}{\partial y} \right| \gg \left| \frac{\partial \phi_1}{\partial x} \frac{\partial \zeta_1}{\partial x} \right| \quad \text{and} \quad \left| \zeta_1 \frac{\partial^2 \phi_1}{\partial y^2} \right|$$

which imply that

$$b\ell \ll 1 \quad \text{and} \quad bk \ll 1 \quad (27)$$

The first of these is a condition on the ripple steepness, into which we can gain further insight by recalling Figure 1. Here it was shown that, for deep flow, the effect on the results of linearizing the boundary condition is small if  $b\ell \lesssim 0.1\pi$ . The second condition is perhaps less expected in that it concerns the ratio of ripple amplitude to surface wavelength. In fact, a more stringent condition on  $b\ell$  arises as a result of a further Ursell-type condition, namely  $\left| \phi_2^{(2)} / \phi_1 \right| \ll 1$ . From Eqs (16) and (24) this condition is that

$$\left| \frac{bk}{2} A(\ell \pm k, \sigma, y) \right| \ll 1 \quad \text{in} \quad 0 < y < \ell \quad (28)$$

in which the plus and minus signs relate to the first and second terms on the right hand side of (24) respectively. It should be noted that, whereas the condition leading to (26) is valid at all phase angles of the wave cycle, this is not strictly true of the condition  $\left| \phi_2^{(2)} / \phi_1 \right| \ll 1$ . When  $\phi_1 = 0$  at  $(kx - \sigma t) = \pm \pi/2, \pm 3\pi/2, \dots$ , it can be seen from (24) that  $\phi_2^{(2)}$  takes a non-zero value unless  $(\ell x + \delta) = 0, \pm \pi, \pm 2\pi, \dots$ , implying a position in the flow above either a ripple crest or a trough. In this respect, condition (28) is not as all-embracing as (26). At phase angles other than those corresponding to  $\phi_1 \approx 0$ , it is possible to ensure that condition (28) is satisfied, however. In the limiting case  $\ell \gg k$  condition (28) reduces to

$$\frac{bk}{2} \ll \tanh(\ell h) \quad (29)$$

while, in the case  $k \gg \ell$ , the denominators of the terms  $A(\ell \pm k, \sigma, y)$  are small (and, ultimately, zero as  $\ell/k \rightarrow 0$ ). It follows that the analysis is not valid if  $k \gg \ell$ .

Condition (28) and, more obviously, condition (29) can be viewed as providing a restriction on the ratio of ripple amplitude to water depth (in other words, a condition comparable with  $a/h \ll 1$  above). For small  $\ell h$ , (29) gives  $b/h \ll 2\ell/k$  which is a weak restriction in view of the fact that  $\ell \gg k$  in this limiting case. The full condition (28) must be used to cover this aspect, therefore, and intuition suggests that  $b/h$  must be small in practice. For large  $b/h$ , the waves behave nonlinearly (see § 6.2, Part II, and also Jolas (1960) and Longuet-Higgins (1977)).

In conclusion, it has been shown here that in addition to three conditions relating  $a$ ,  $k$  and  $\ell$ , there are two further conditions given by (27) and (28) which arise upon the introduction of a sinusoidally rippled bed defined by the parameters  $b$  and  $\ell$ .

### 3.6 Results to second order for the Velocity Field

The velocity components  $(u, v)$  are given by  $(-\phi_x, -\phi_y)$ , and the horizontal velocity components corresponding to (16), (22) and (24) are as follows

$$u_1 = U_{\max} \frac{\cosh(ky)}{\cosh(kh)} \sin(kx - \sigma t) \quad (30)$$

$$u_2^{(1)} = U_{\max} \left( \frac{-3ak}{2 \sinh^2(kh)} \right) \frac{\cosh(2ky)}{\sinh(2kh)} \cos 2(kx - \sigma t) \quad (31)$$

$$u_2^{(2)} = U_{\max} \left( \frac{b}{2 \cosh(kh)} \right) \left\{ -(\ell+k) A(\ell+k, \sigma, y) \sin((\ell+k)x - \sigma t + \delta) \right. \\ \left. + (\ell-k) A(\ell-k, \sigma, y) \sin((\ell-k)x + \sigma t + \delta) \right\} \quad (32)$$

where  $U_{\max} = gak/\sigma$  is the amplitude of the horizontal velocity at the water surface in the solution  $O(u)$ . The vertical attenuation of  $u_1/U_{\max}$  is fixed if  $(kh)$  is known, but to compare the vertical profiles of horizontal velocity given by (30)–(32), it is necessary to further specify  $\ell$ ,  $ak$ ,  $b\ell$  and  $\ell h$ . The vertical profiles in Fig 3 show the amplitudes of  $u_1/U_{\max}$ ,  $u_2^{(1)}/U_{\max}$  and  $u_2^{(2)}/U_{\max}$ , for the case  $\ell = 10$  m,  $ak = 0.1$ ,  $kh = 1.0$ ,  $b\ell = \pi/10$  and  $\ell h = 2\pi$ . These bedforms have the height and wavelength of typical megaripples on the seabed (Langhorne (1978)). The downward attenuation of  $u_1/U_{\max}$  is accompanied by an even more pronounced downward

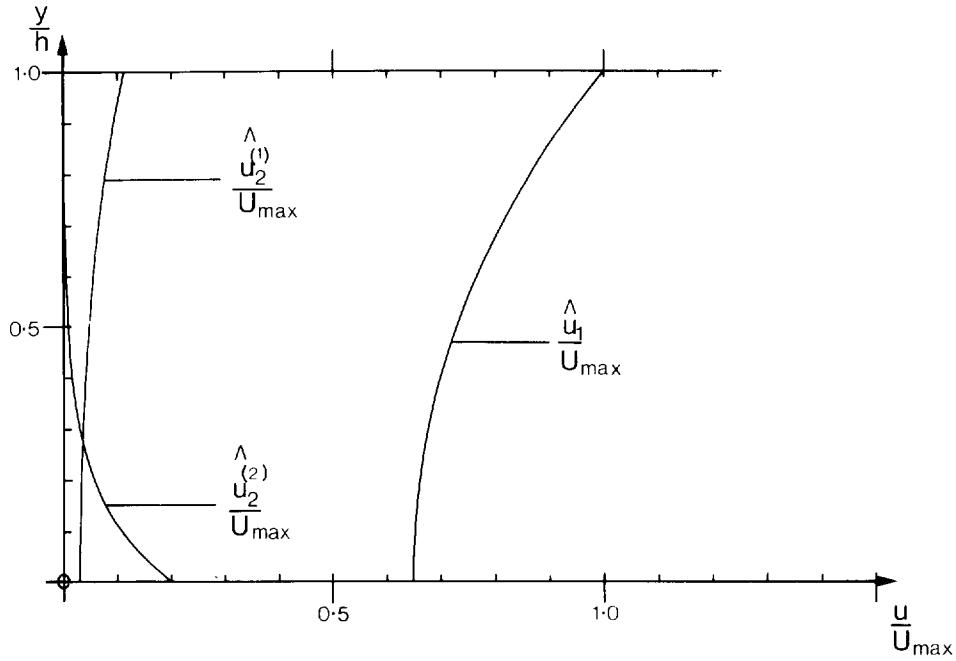


Fig 3 Vertical profiles of horizontal velocity amplitude corresponding to the solutions  $u_1, u_2^{(1)}$  and  $u_2^{(2)}$  for the case  $\lambda = 10\text{m}$ ,  $kh = 1.0$ ,  $ak = 0.1$ ,  $bl = 0.1\pi$  and  $ch = 2\pi$ . Each solution has been normalised by  $U_{\max}$ .

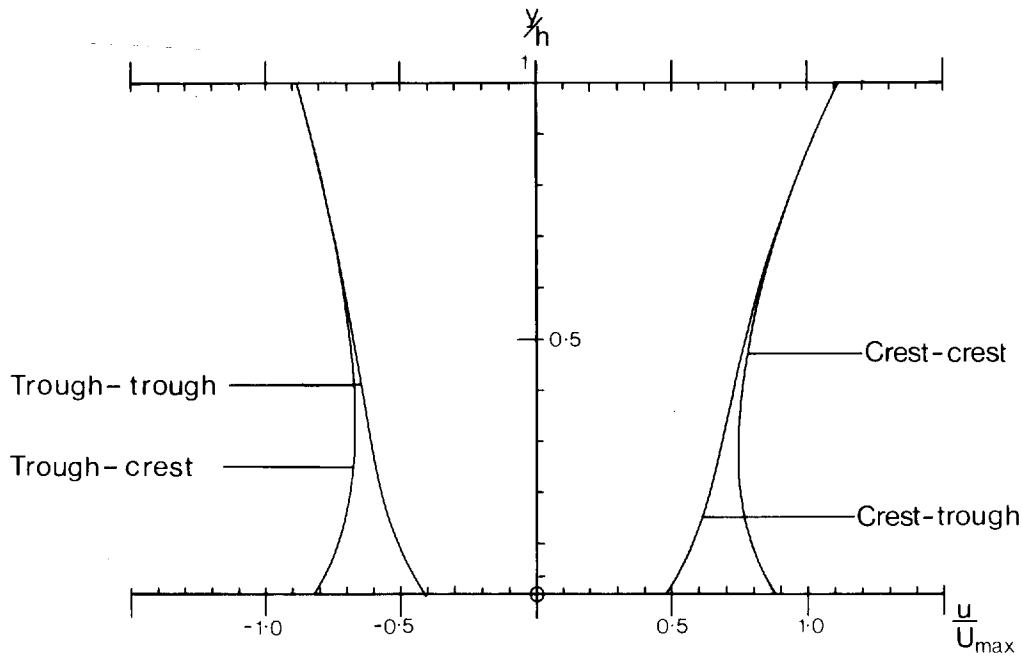


Fig 4 Linear combinations of the profiles shown in Fig 3 for four extreme cases designated (i) 'crest - crest' at the instant when a surface wave crest is above the ripple crest; (ii) 'crest - trough' when a surface crest is above a ripple trough; (iii) 'trough - crest' when a surface trough is above a ripple crest; and (iv) 'trough - trough' when a surface trough is above a ripple trough.

attenuation of the small term  $u_2^{(1)}/U_{max}$ . The term  $u_2^{(2)}/U_{max}$  is attenuated upwards, and its effect can be seen to extend almost to the free surface. The linear combinations of these curves corresponding to the flows beneath the crests and troughs of the surface waves, and above both crest and trough positions on the bed, are of particular interest. The three curves shown in Fig 3 lead to the four extreme velocity profiles shown in Fig 4. Clearly, the presence of the ripples has a major influence on the flow velocities near the bed. In Fig 5, the velocity at the bed surface itself is shown as a function of phase angle in the wave cycle, firstly at a ripple crest position (Fig 5(i)), secondly at a mean level position (Fig 5(ii)), and thirdly at a ripple trough position (Fig 5(iii)). Although the bed velocity is dominated by the solution  $O(\kappa)$ , the solution of problem 2,  $O(\kappa^2)$ , provides an important perturbing influence in the final result in cases (i) and (iii). The difference between the horizontal surface velocity, shown in Fig 5(i-iii), and the tangential surface velocity is generally small. In Fig 5(iv) curves are shown of the horizontal, vertical and tangential velocity for a point on the bed surface at its mean level (c.f. Fig 5(ii)). Here the vertical velocity is at its greatest, but its influence on the total velocity is very small.

### 3.7 The Influence of the Free Surface

From results of the type shown in Figs 3-5 it is possible to assess the effect of flow depth on the horizontal velocity at the bed surface. In particular, it is possible to assess the accuracy of the use of deep flow results of the type shown in Fig 1, when there is a free water surface at  $y = \zeta$ .

The problem of determining the height of influence of undulations above the bed surface has been examined by Davies (1979) for bedforms of finite amplitude. This height of influence  $\hat{y}$ , defined as the height above the bed at which the perturbation to the free stream velocity drops to 1% of the perturbation at the bed surface, has been found to be about  $0.6 \bar{L}$  above a crest and  $0.8 \bar{L}$  above a trough, where  $\bar{L}$  is the wavelength of the bedforms. In other words, the effects of the bedforms are confined to a layer which is of thickness less than one wavelength above the bed surface. This result was found to be essentially the same for sinusoidal bedforms and for profiles of real sand ripples having strongly peaked crests, and longer and flatter troughs, than a sine wave. In terms of the linearized analysis for deep flow based on the velocity potential (1), the thickness  $\hat{y}$  can be shown on the above definition to be given by  $e^{-\epsilon \hat{y}} = 0.01$  or  $\hat{y} = 0.733 \bar{L}$ .

As a general rule it might be expected that deep flow results are accurate if

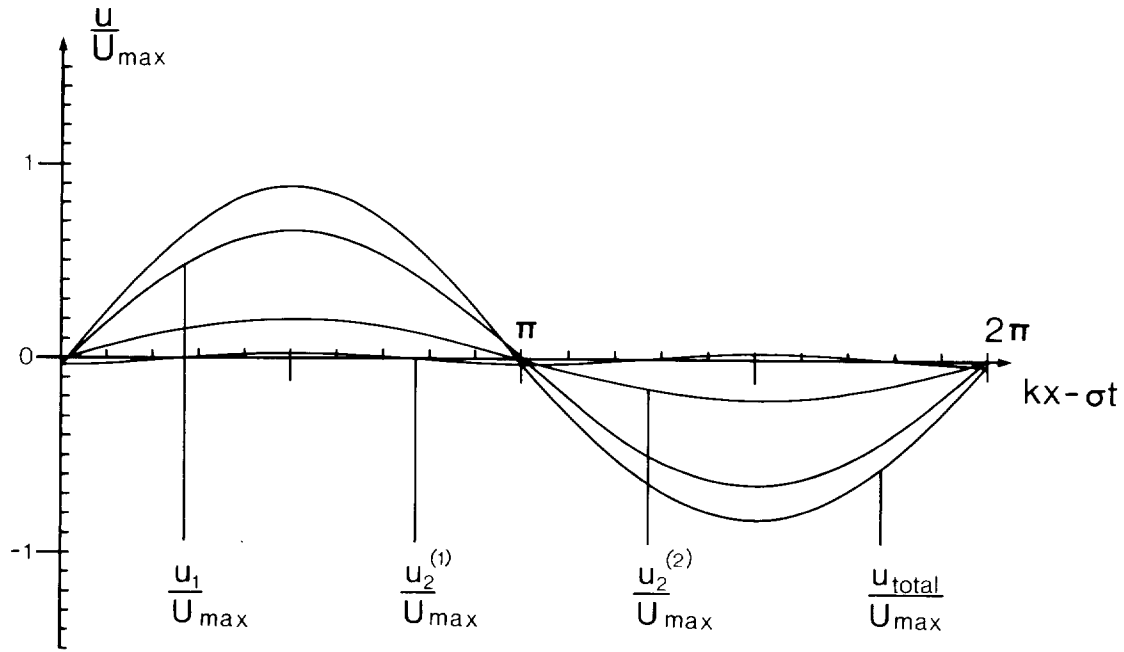


Fig 5 Normalized bed velocities during a complete surface wave cycle for the case  $\lambda = 10\text{m}$ ,  $kh = 1.0$ ,  $ak = 0.1$ ,  $bl = 0.1\pi$  and  $lh = 2\pi$ . Fig 5 (i) shows the horizontal velocity, together with its constituent parts, at a ripple crest ( $lx + \delta = 0$ ); Fig 5 (ii) shows corresponding results at a mean level position ( $lx + \delta = \pi/2$ ); and Fig 5 (iii) shows corresponding results at a trough position ( $lx + \delta = \pi$ ). Fig 5 (iv) shows both the horizontal and vertical components, and the total tangential velocity at a point on the bed surface where  $lx + \delta = \pi/2$ .

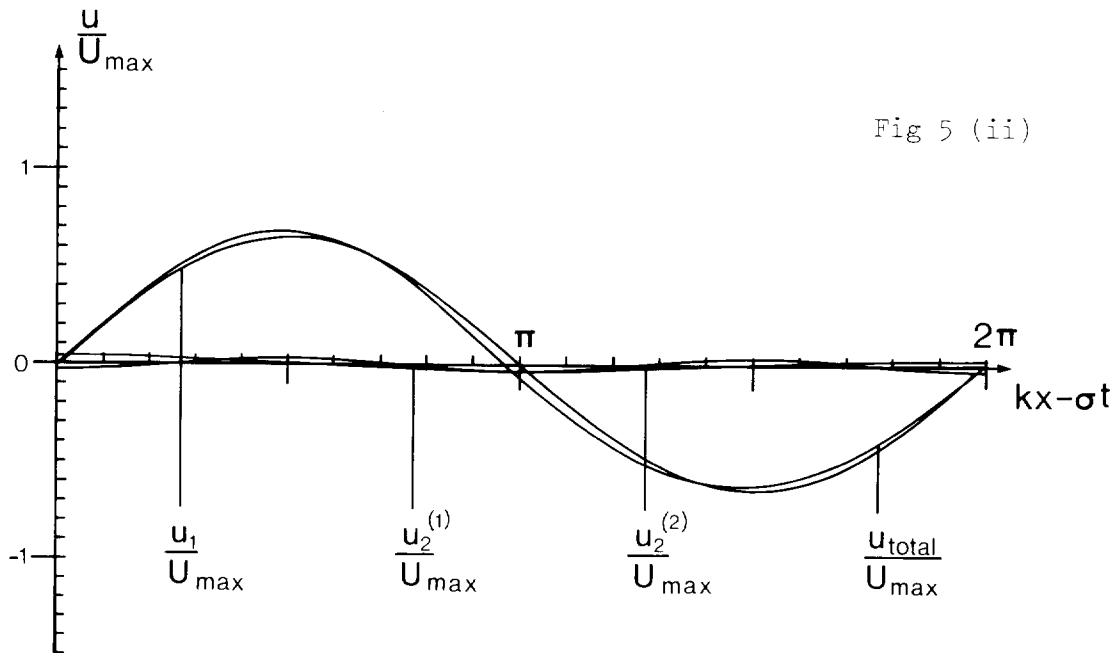
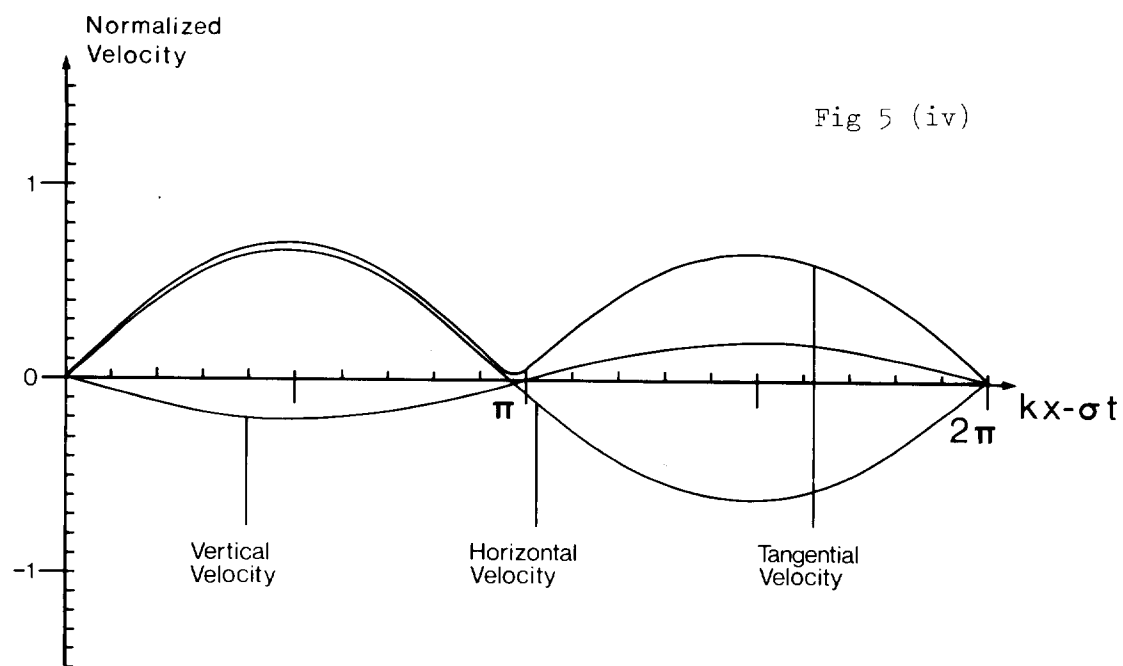
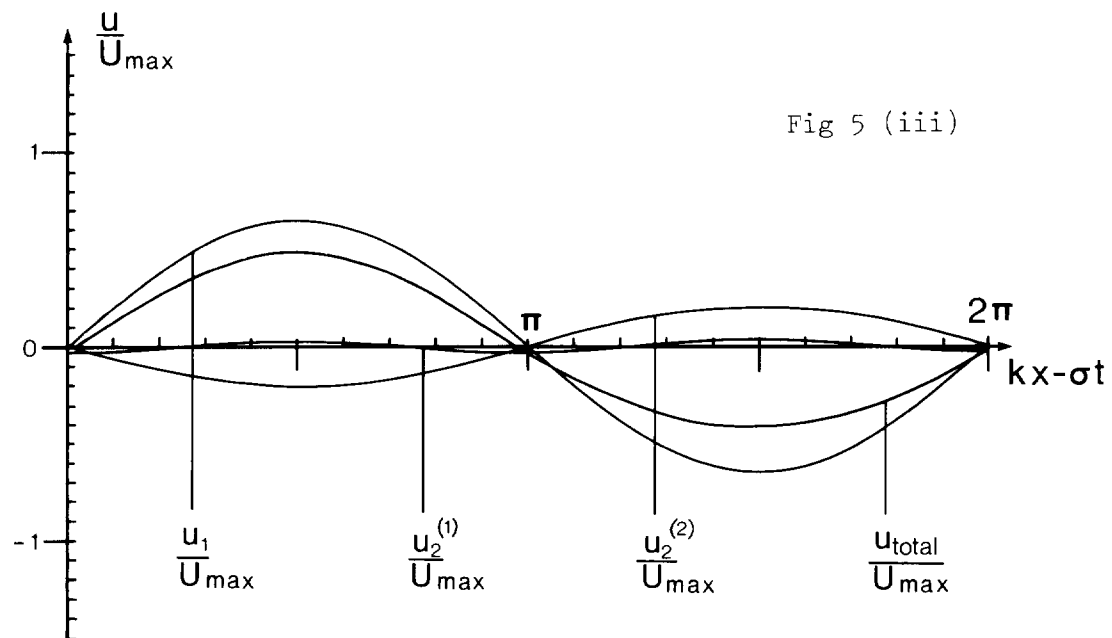


Fig 5 (ii)



$\hat{y} < h$ , and this can be shown to be so as follows. For deep flow, the ratio  $r_1 \equiv u_{cr}/U$  ( $= (1 + bl)$  from (3)) has been compared with the corresponding ratio  $r_2$  for the free surface problem at the same bedform steepness, namely

$$r_2 = \frac{\text{Amplitude } (u_1 + u_2^{(2)})_{\text{surface crest}}}{\text{Amplitude } (u_1)_{\text{surface crest}}}$$

(It is not relevant to include a contribution from  $u_2^{(1)}$  in the numerator of  $r_2$  since the interaction of the solution  $O(\kappa)$  with the bed is contained entirely within problem 2,  $O(\kappa^2)$ . Nor is it necessary to consider the troughs rather than the crests in calculating  $r_1$  and  $r_2$ , since the same results are obtained.)

The procedure adopted has been to examine the quotient  $R = r_2/r_1$ , over full ranges of the parameters in the problem, significant departures of  $R$  from unity indicating the inapplicability of the deep flow result. Generally, the departures which arise are such that  $R > 1$ , showing that the deep flow result underestimates the velocity at the bed. For  $\bar{L}/h < 2$ ,  $1 < R < 1.01$ , unless  $\ell \approx 2h$ , and so the bed velocities on the two calculations are in agreement to within 1%, thus confirming  $\hat{y} < h$ . However, for  $\bar{L}/h > 2$  quite large differences start to arise. This is illustrated in Fig 6 in which contours of  $R$  are plotted for the special case of  $h = 4$  m and  $bl = \pi/20$ , on a graph having axes  $(\bar{L}/h, \lambda_s/h)$ , where  $\lambda_s = 2\pi/k$ ; these axes are used rather than  $(\ell h, kh)$  in order to emphasise the present point of discussion. Although the assumptions underpinning the theory start to break down in various ways where the contours are dashed, it can be seen that without extrapolating too unreasonably into the dashed region, the deep flow results can underestimate the actual bed velocity by 10% if  $\bar{L}/h$  is of the order 7. This substantial discrepancy lends emphasis to the importance of checking  $\bar{L}/h$  before using a deep flow result. The condition of resonance  $\ell = 2h$  causes  $R$  to be singular on the straight line shown in Fig 6; this aspect of the solution is discussed in detail later.

### 3.8 The Accuracy of a quasi-uniform flow assumption

In considering the propagation of surface waves above sandwaves, that is bedforms having wavelength much greater than the water depth ( $\bar{L}/h \gg 1$ ), it is tempting to make calculations of the velocity field based upon the local water depth. It is useful to know, therefore, whether adopting the local depth, from



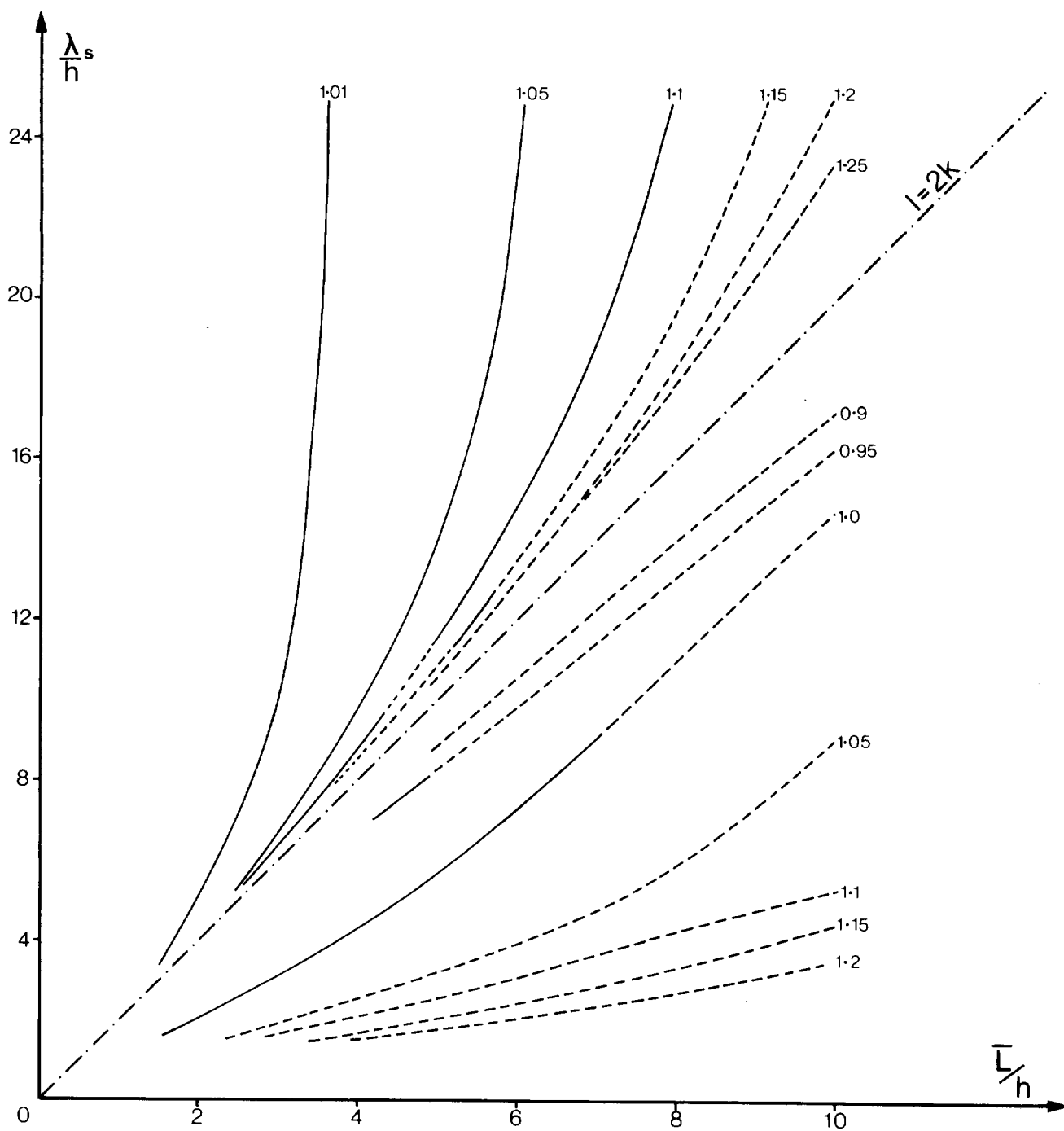


Fig 6 Contours of the ratio  $R$  for the case  $\lambda = 4m$  and  $b\ell = 0.05\pi$ .  
Where the contours are dashed either  $|b k A| > 0.2$  or  $b/\lambda > 0.2$ .

the mean water level to the bed surface, in the solution  $O(\kappa)$  gives approximately the same result as the full analysis  $O(\kappa^2)$ . For deep flow ( $\bar{L}/\lambda < 1$ ) there will be large differences between the two cases, the quasi-uniform solution predicting a minimal variation in the bed velocity over a ripple wavelength, and the full analysis predicting substantial variations of the type shown in Figs 3-5. However, for shallow flow with  $\bar{L}/\lambda \gg 1$ , the picture is rather different in that calculations based on a quasi-uniform assumption will be in much closer agreement with the solution  $O(\kappa^2)$ . This can be illustrated by defining a ratio  $S$  of the differences between the horizontal velocities at crest and trough positions on the bed surface given by the two arguments, namely

$$S = \frac{[\text{Amplitude} (u_{cr}) - \text{Amplitude} (u_{tr})]_{O(\kappa^2)}}{[\text{Amplitude} (u_{cr}) - \text{Amplitude} (u_{tr})]_{\text{quasi-uniform}}}$$

If  $\ell \neq 2k$ , this ratio is generally greater than unity for sinusoidal ripples, as can be seen in Fig 7(i) where contours of  $S$  are plotted for the particular case of  $\lambda = 16$  m and  $b\ell = \pi/20$ . For small  $\bar{L}/\lambda$ , the values of  $S$  are quite large, as anticipated, indicating that the quasi-uniform assumption is not at all adequate. As  $\bar{L}/\lambda$  increases the value of  $S$  steadily falls at any given value of  $\lambda_s/\lambda$ , apart from in the neighbourhood of the singularity  $\ell = 2k$ . For large  $\bar{L}/\lambda$ ,  $S$  tends to unity indicating that the quasi-uniform assumption provides a reasonable first approximation for the velocities at the seabed. (The contours in Fig 7 are once again dashed where the assumptions upon which the theory is based start to become questionable.) In view of the rather complicated nature of the curves shown in Fig 7(i), it is not possible to state a single value of  $\bar{L}/\lambda$  above which the quasi-uniform assumption is valid. Each case must be treated on its merits.

This point is reinforced by the curves of  $S$  shown in Fig 7(ii) for three particular values of  $\lambda_s/\lambda$  corresponding to waves of period 6, 10 and 14 sec. In the first case ( $T=6$  sec),  $S$  tends to its terminal value unity, interrupted only in the neighbourhood of the point of resonance at  $\bar{L}/\lambda = 1.675$ . The remaining curves show similar tendencies, although the effects of the resonance are relatively more widespread in  $\bar{L}/\lambda$  on either side of the respective critical values  $\bar{L}/\lambda = 3.493$  ( $T=10$  sec) and  $\bar{L}/\lambda = 5.180$  ( $T=14$  sec).

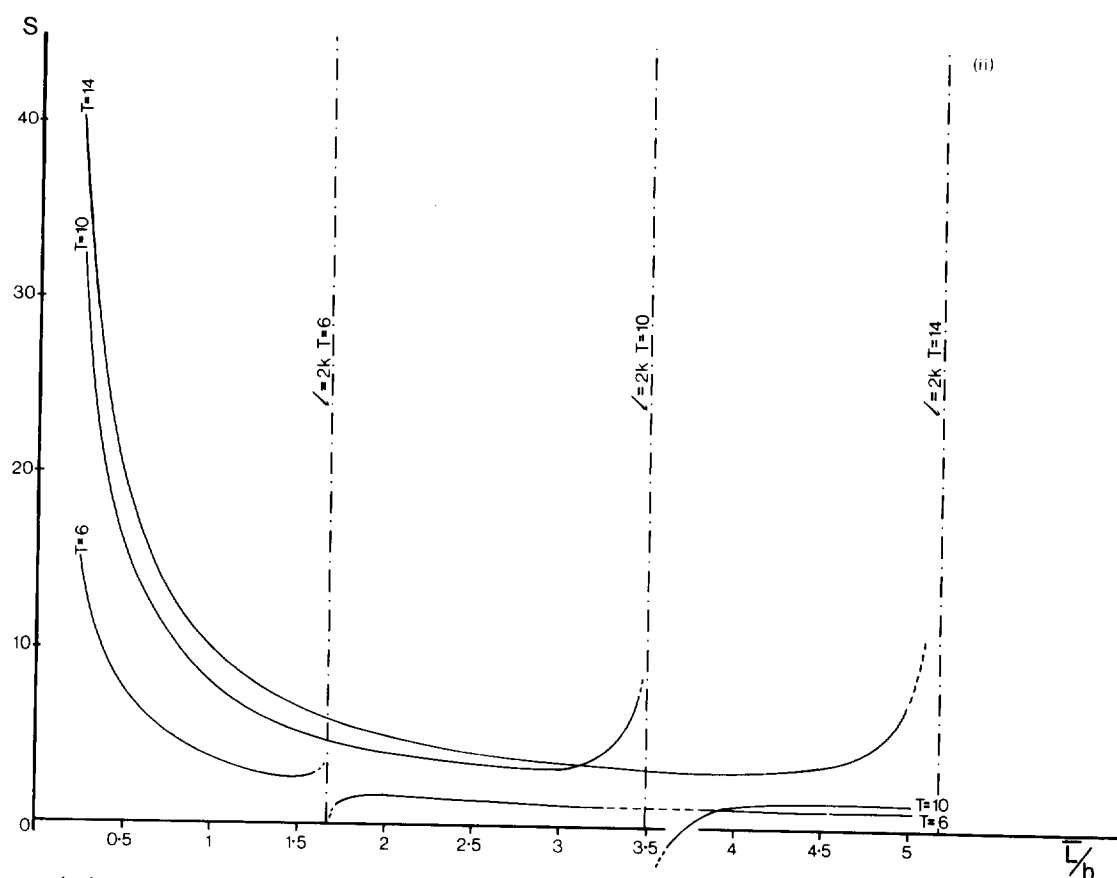
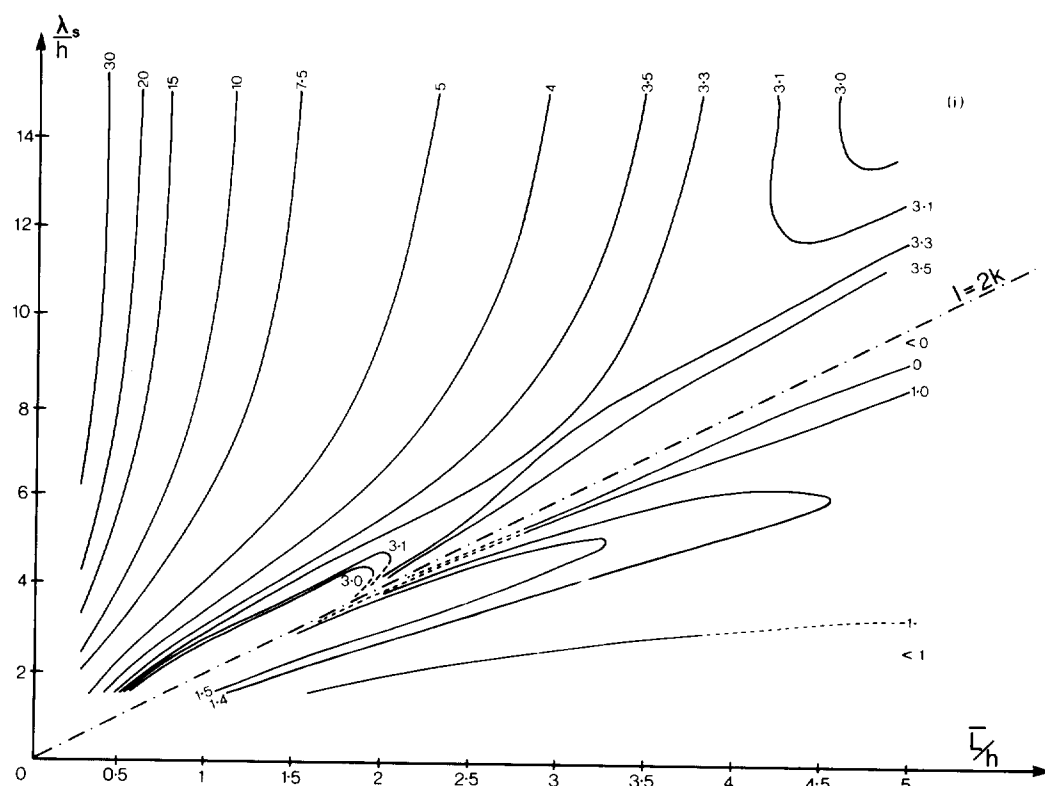


Fig 7 (i) Contours of the ratio  $S$  for the case  $\lambda = 16m$  and  $bl = 0.05\pi$ . Where the contours are dashed either  $|bkA| > 0.2$  or  $b/\lambda > 0.2$ .  
(ii) Values of  $S$  plotted against  $L/h$  for three fixed values of  $\lambda_s/\lambda$  corresponding to  $T = 6, 10$  and  $14$  sec. ( $\lambda = 16m, bl = 0.05\pi$ ) Contours are dashed on the same criteria as in Fig 7 (i).

#### § 4. ENERGY FLUXES

Each of the velocity potential terms  $\phi_1$ ,  $\phi_2^{(1)}$  and  $\phi_2^{(2)}$  is associated with a deformation of the free surface and with particle motions in the interior of the fluid. Hence the potential ( $V_E$ ) and the kinetic ( $T_E$ ) energies can be calculated for each term. The energy flux can also be calculated and hence the propagation velocity of the energy can be deduced. The average potential ( $\overline{V_E}$ ) and kinetic ( $\overline{T_E}$ ) energy densities per unit area of the water surface are given by

$$\overline{V_E} = \overline{\int \frac{1}{2} \rho_w g \eta^2 d(\text{area})} \quad \text{and} \quad \overline{T_E} = \overline{\int \frac{1}{2} \rho_w (u^2 + v^2) d(\text{volume})}$$

where  $\rho_w$  is the water density. These integrals have been evaluated per unit width of the wave front, the overbar denoting spatial averaging in the direction of wave propagation. The total energy density per unit area is given by  $\overline{E} = \overline{V_E} + \overline{T_E}$ .

The energy flux, or rate of doing work by the wavetrain, per unit width of wave front, is expressed

$$\frac{dW}{dt} = \int p u dy$$

where  $p$  is the subsurface water pressure and where the integration is made from the bed to the water surface. Hence the speed of energy propagation is given by

$$C_g = \frac{\overline{dW/dt}}{\overline{E}}$$

Preserving the earlier suffix notation, the results are as follows:

for  $\phi_1$

$$\overline{E_1} = \frac{1}{2} \rho_w g a^2 \quad (33)$$

$$\frac{dW_1}{dt} = \frac{1}{2} \rho_w g a^2 \cdot \frac{\sigma}{\sinh(2kh)} \cdot B(2k, L) \quad (34)$$

for  $\phi_2^{(1)}$

$$\overline{E_2^{(1)}} = \frac{1}{4} \rho_w g \left( \frac{a^2 k}{4 \sinh^3 kh} \right)^2 \left\{ 4 \cosh^6(kh) + 4 \cosh^4(kh) + 19 \cosh^2(kh) - 9 \right\} \quad (35)$$

$$\frac{dW_2^{(1)}}{dt} = \frac{9}{16} \rho_w g a^4 k^2 \cdot \frac{\sigma}{\sinh^4(kh)} \cdot \left\{ \frac{B(4k, L)}{2 \sinh^2(kh) \sinh(2kh)} - \frac{1}{6} \right\} \quad (36)$$

where

$$B(r, s) = \left\{ \frac{\sinh(+L)}{+} + s \right\}$$

and for  $\phi_2^{(2)}$

$$\overline{E_2^{(2)}} = \frac{1}{4} \rho_w g \left[ \{D(\ell+k)\}^2 + \{D(\ell-k)\}^2 \right] + \frac{1}{8} \rho_w \left[ \{D(\ell+k)\}^2 F(\ell+k) + \{D(\ell-k)\}^2 F(\ell-k) \right] \quad (37)$$

$$\frac{dW_2^{(2)}}{dt} = \rho_w \{D(\ell+k)\}^2 G(\ell+k) - \rho_w \{D(\ell-k)\}^2 G(\ell-k) \quad (38)$$

where

$$D(+)=\frac{b a k}{2 \cosh (k h)}\left(\frac{g+}{\sigma^2 \cosh (+h)-g+\sinh (+h)}\right)$$

and

$$F(+)=\left(\frac{g^2+\sigma^2}{\sigma^2}\right) \sinh (2+h)+2 g(1-\cosh (2+h))$$

$$G(+)=\frac{1}{2 \sigma^2}\left\{\frac{(g+)^2}{2} B(2+, h)-g \sigma^2 \sinh ^2(+h)+\frac{\sigma^2}{2} B(2+,-h)\right\}$$

In the calculation of  $\overline{E_2^{(1)}}$ , Eqs (22) and (23) have been used, and the subsurface pressure  $p_2^{(1)}$  in the expression for  $\frac{dW_2^{(1)}}{dt}$  has been given by

$$\frac{p_2^{(1)}}{\rho_w} = \frac{\partial \phi_2^{(1)}}{\partial t} - \frac{1}{2} \left( \left( \frac{\partial \phi_1}{\partial x} \right)^2 + \left( \frac{\partial \phi_1}{\partial y} \right)^2 \right)$$

Similarly, in the calculation of  $\overline{E_2^{(2)}}$ , Eqs (24) and (25) have been used, with the subsurface pressure  $p_2^{(2)}$  in the expression for  $\frac{dW_2^{(2)}}{dt}$  given by

$$\frac{p_2^{(2)}}{\rho_w} = \frac{\partial \phi_2^{(2)}}{\partial t}$$

It might be noted that, from Eqs (33) and (34), the familiar expression for the group velocity of waves in water of intermediate depth can be obtained.

The wave energy fluxes have been contrasted by comparing (34), (36) and (38), and a typical example of the results is shown in Fig 8. Here a logarithmic scale has been used for energy flux on account of the large differences in magnitude between the terms plotted. It can be seen that  $\frac{dW_1}{dt} \gg \frac{dW_2^{(1)}}{dt}$ , and this is generally so for all acceptably small values of steepness ( $ak$ ).

Both of these fluxes are in the direction of wave travel and both are independent of ripple wave number  $\ell$ , which is plotted on the abscissa. The feature of interest is clearly the energy flux  $\frac{dW_2^{(2)}}{dt}$  which, while being small and in the opposite direction to that of the other terms for  $\ell > k$ , has a singular behaviour at  $\ell = 2k$ . This singularity was discussed earlier in relation to Eq (25) and its physical interpretation is discussed in the next section.

Clearly, in the neighbourhood of the singularity, the analysis must break down, with the waves steepening and possibly breaking. However, where  $\left| \frac{dW_2^{(2)}}{dt} \right| \approx \left| \frac{dW_1}{dt} \right|$

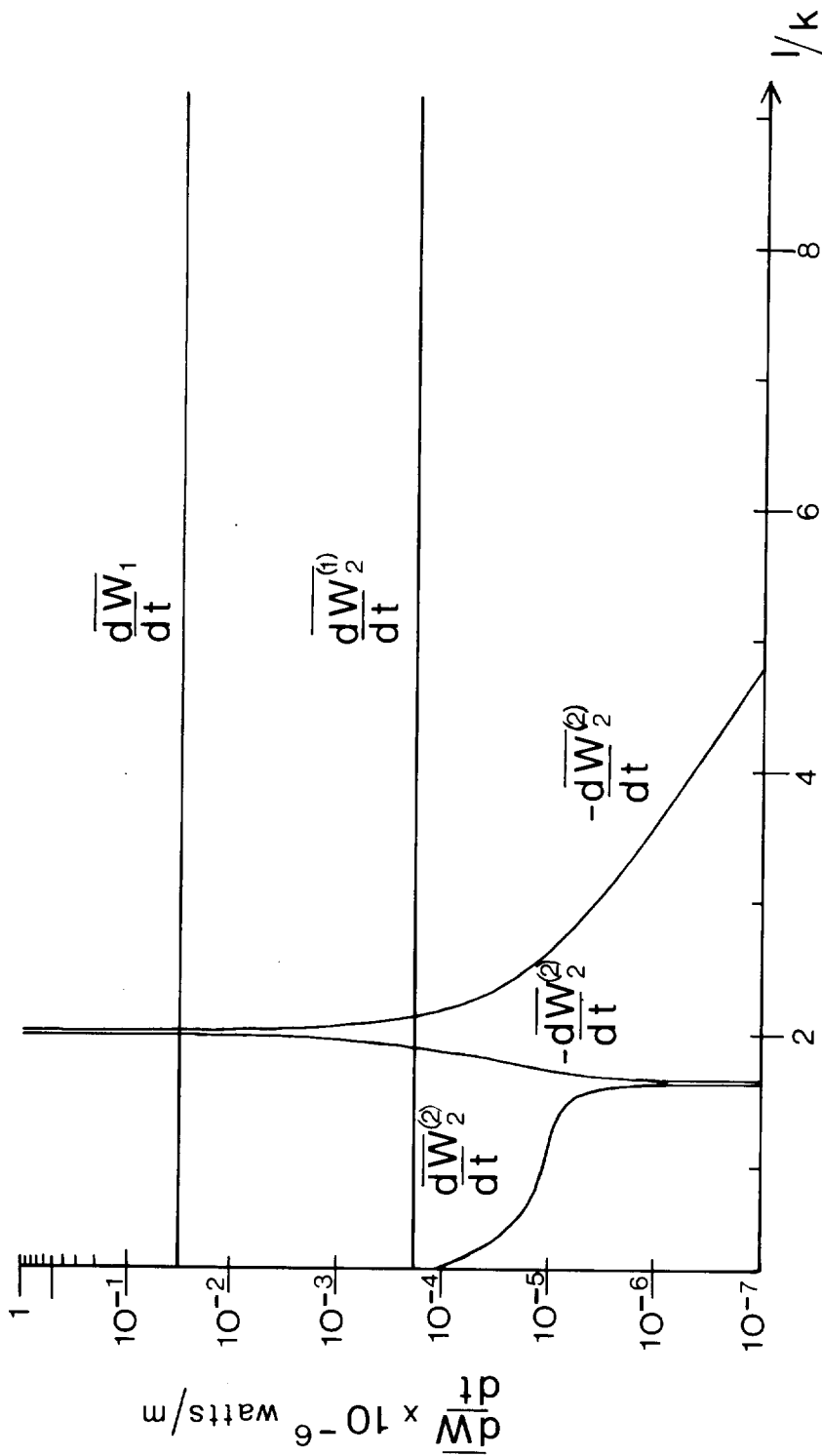


Fig 8 The behaviour of the wave energy flux  $\frac{dW_2}{dt}$  is shown in relation to  $\frac{dW}{dt}$  and  $\frac{dW_2}{dt}$  as  $\ell$  is varied, for the case  $\ell = 10m$ ,  $kh = 1.0$ ,  $ak = 0.1$  and  $b/\ell = 0.05$ . The resonance ( $\ell = 2k$ ) occurs at  $\ell = 0.2 m^{-1}$ .

much of the incident wave energy might be expected to be reflected by the bedforms, and although the present analysis is unrealistic in that the bed is assumed to be of infinite horizontal extent, there are possible implications in this for coastal protection.

#### 4.1 The resonant interaction at $\ell = 2k$

It was pointed out earlier that  $\gamma_2^{(2)}$ , given by Eq (25), is singular when  $\ell = \pm 2k$ . In particular, the first term of this solution achieves a resonance when  $\ell = -2k$ , at which

$$\sin((\ell+k)x - \sigma t + \delta) \longrightarrow \sin(-kx - \sigma t + \delta)$$

and the second term is resonant when  $\ell = +2k$ , at which

$$\sin((\ell-k)x + \sigma t + \delta) \longrightarrow \sin(kx + \sigma t + \delta)$$

Although it is only the latter case which is physically admissible, it can be seen that both conditions of resonance correspond to waves progressing in the negative  $x$ -direction, as expected from the conclusion of the previous section concerning the energy flux  $\frac{dW_2^{(2)}}{dt}$ . Close to the point of resonance (ie  $|\ell - 2k| < \epsilon$ ,  $\epsilon$  small), the superimposition of  $\gamma_2^{(2)}$  and the primary oscillation  $\gamma_1 = a \sin(kx - \sigma t)$  produces a partially progressing and partially standing wave structure in the surface elevation. In fact, for a suitable choice of wave and ripple parameters, a predominantly standing wave structure can result at the free surface. It might be expected on the basis of the earlier arguments that, in the interior of the fluid, the particle motions would not be those of a standing wave in the usual sense, on account of the downward and upward attenuations of the respective solutions  $\phi_1$  and  $\phi_2^{(2)}$ . However, the attenuation expression in the numerator of the second term of Eq (24) reduces for  $\ell = +2k$  to  $\sim \cosh(ky)$  upon using the dispersion relation. Thus the attenuation of  $\phi_2^{(2)}$  is the same as that of  $\phi_1$ , namely a downward attenuation from the free surface, rather than the upward attenuation found generally for  $\phi_2^{(2)}$ . Close to the resonance point this behaviour is still evident.

Depending upon whether  $\ell \leq 2k$  or  $\ell > 2k$ , distinct differences arise in the velocity field throughout the flow. Although the theory is liable to inaccuracy in the examples now taken to illustrate this, since  $|\phi_1| \approx |\phi_2|$ , it is instructive to examine cases in which  $|\frac{dW_1}{dt}| \approx |\frac{dW_2^{(2)}}{dt}|$ . For example, if  $\lambda = 10$  m,  $k\lambda = 1.0$ ,  $ak = 0.1$ ,  $bl \approx 0.2$  and  $\ell\lambda \approx 2.0$  the above condition is satisfied approximately by  $\ell/k = 1.984$  and  $2.016$  and, to illuminate some of the

later discussion, results are now presented of the horizontal velocities at the bed surface (cf Figs 5(i) and (iii)). Firstly, in Figs 9(i) and 9(ii), the horizontal surface velocities are shown as functions of time through a wave cycle for  $\ell/k = 1.984$  at (i) the crest and (ii) the trough positions on the bed surface. At the crest, the total horizontal velocity can be seen to be small at all phase angles due to the cancellation of  $u_1$  and  $u_2^{(2)}$ . At the trough, these two components reinforce one another to produce a much enhanced total bed velocity. For  $\ell/k = 2.016$  the picture is rather different as a result of the  $\pi$  - phase shift in  $\phi_2^{(2)}$ . Now, in Figs 9(iii) and 9(iv), it can be seen that the superimposition of  $u_1$  and  $u_2^{(2)}$  produces a much enhanced velocity at the crest position, and a much reduced velocity at the trough position. So, close to the point of resonance, the general picture to emerge is of a weak horizontal velocity fluctuation above the ripple crest if  $\ell \lesssim 2k$  and a strong fluctuation if  $\ell \gtrsim 2k$ . Conversely, at the trough, there is a strong horizontal fluctuation if  $\ell \lesssim 2k$  and a weak fluctuation if  $\ell \gtrsim 2k$ . The possible sedimentological consequences of this, for cases in which the bed is erodible, are discussed later.

The type of resonant interaction described above is found quite commonly in related fields. For example, Rhines and Bretherton (1973) have found such a resonance in their study of planetary waves over a sinusoidally undulating ocean floor. In particular, they have shown how two Rossby waves of the same frequency trade energy back and forth "via a catalytic Fourier component of the depth". Rhines and Bretherton also describe briefly an analogy in solid state physics, concerning the vibration of regular atomic lattices. In this case the scattering of projected high energy particles is strongest when resonance between the incident wave function and the lattice periodicity is satisfied. A special case of this is Bragg reflection of X-rays from a crystal plane.

## § 5. THE THIRD ORDER PROBLEM

The formulation of the problem and the solution  $O(\alpha^3)$  are discussed now mainly with a view to establishing further conditions of Ursell-type, based on the terms of  $\phi_2$  and  $\phi_3$ . The only part of the solution which is stated here is to do with the interaction  $O(\alpha^3)$  between the lower order solutions for velocity potential,  $\phi_1$  and  $\phi_2$ , and the bed surface given by  $\zeta_1$  and  $\zeta_2$ . In other words, this is the extension to third order of Problem 2,  $O(\alpha^2)$ . The remaining part of the solution, which provides the next approximation at the free surface and which is the extension of Problem 1,  $O(\alpha^2)$ , is not discussed here



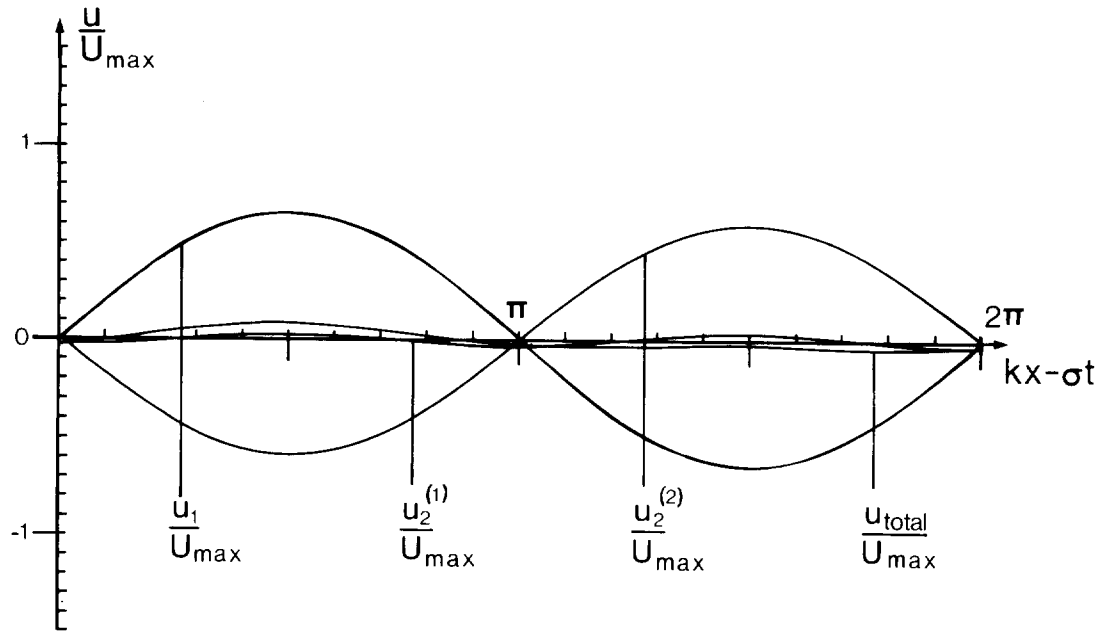


Fig 9 Normalized horizontal bed surface velocities during a complete surface wave cycle for the case  $h = 10\text{m}$ ,  $kh = 1.0$  and  $ak = 0.1$ , and close to the resonance at  $\ell = 2k$ . Fig 9 (i) is for a crest position ( $\ell x + \delta = 0$ ) and Fig 9 (ii) for a trough position ( $\ell x + \delta = \pi$ ) with  $bl = 0.1984$  and  $\ell h = 1.984$ . The equivalent Figures 9 (iii) and (iv) are for  $bl = 0.2016$  and  $\ell h = 2.016$ .

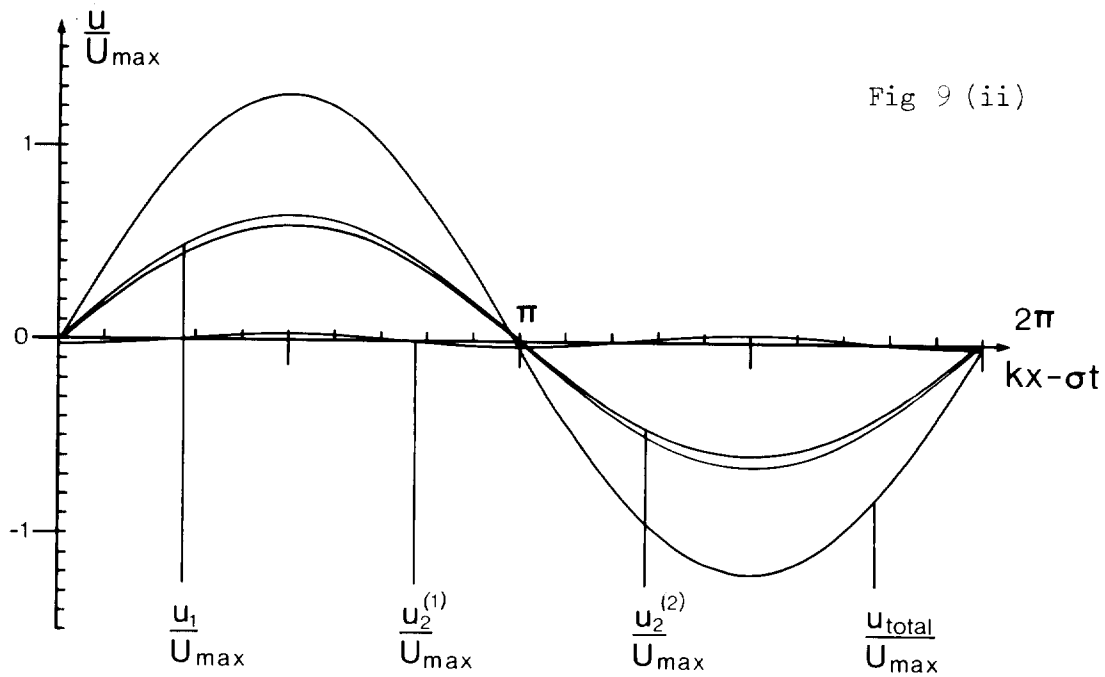
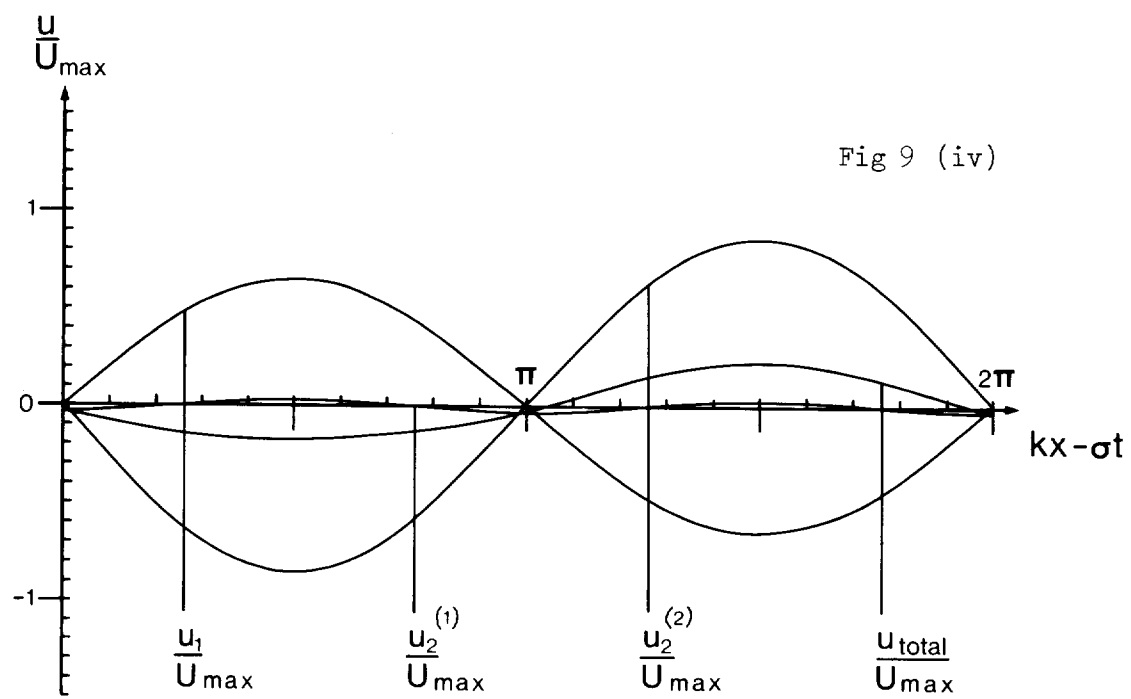
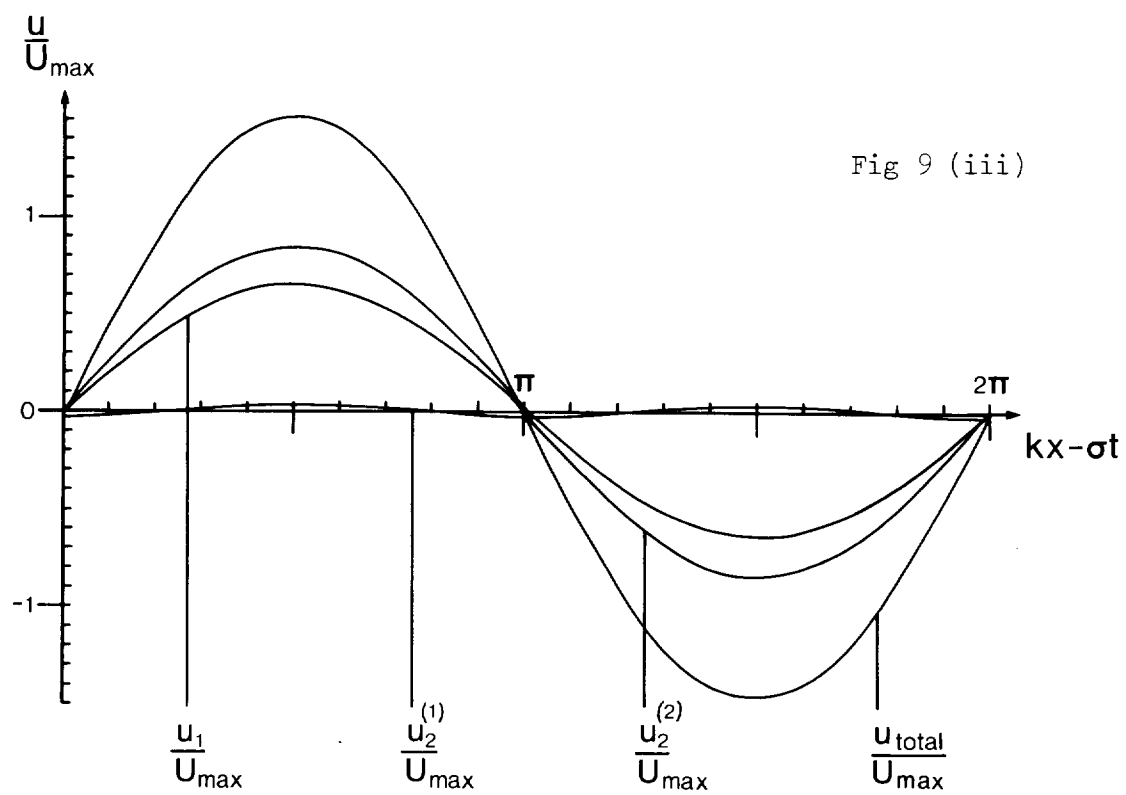


Fig 9 (ii)



since the dispersion relation (17) is valid in the present surface wave analysis only to  $O(\kappa^3)$ .

Although two main points of interest about the solution  $O(\kappa^3)$  are highlighted here, the practical usefulness of the velocity potential  $\phi_3^{(2)}$  is in some doubt, as can be illustrated by considering the solution  $O(\kappa^3)$  for steady deep flow over sinusoidal bedforms. By a simple extension of the earlier argument, the peak surface velocities in the horizontal direction are given (cf Eq (3)) by

$$u_{cr} = U(1 \pm b\ell \pm (b\ell)^2) \quad (39)$$

If Eq (39) is compared with the finite amplitude model results of Davies (1979) shown in Fig 1, there is rather poor agreement at both crest and trough positions. In fact, the agreement between Eq (3), which is plotted in Fig 1, and the model results is much better than the agreement between Eq (39) and the model results at all but very small values of  $(b\ell)$ . This suggests that, while the solution  $O(\kappa^3)$  can be used to clarify the limitations on the earlier analysis, an improvement in accuracy is not likely to be achieved by the inclusion of the small terms given in Eqs (43)-(46).

Using the superscript (2) in the sense in which it was used in Eqs (18b)-(21b), the problem  $O(\kappa^3)$  can be stated as follows:

$$\nabla^2 \phi_3^{(2)} = 0 \quad \text{in} \quad 0 < y < h \quad (40)$$

$$y \frac{\partial \phi_3^{(2)}}{\partial y} + \frac{\partial^2 \phi_3^{(2)}}{\partial t^2} = 0 \quad \text{on} \quad y = h \quad (41)$$

$$-\frac{\partial \phi_1}{\partial x} \frac{\partial \zeta_1}{\partial x} - \left\{ \frac{\partial \phi_2}{\partial x} + \zeta_1 \frac{\partial^2 \phi_1}{\partial x \partial y} \right\} \frac{\partial \zeta_1}{\partial x} + \left\{ \frac{\partial \phi_3^{(2)}}{\partial y} + \zeta_1 \frac{\partial^2 \phi_2}{\partial y^2} + \zeta_2 \frac{\partial^2 \phi_1}{\partial y^2} + \frac{1}{2} \zeta_1^2 \frac{\partial^3 \phi_1}{\partial y^3} \right\} = 0 \quad (42)$$

on  $y = 0$

While the same boundary condition is satisfied at the free surface as in Eq (14), the interaction of both  $\phi_1$  and  $\phi_2$  with the rippled bed represented by  $\zeta_1$  and  $\zeta_2$  can be seen in Eq (42). The solution for  $\phi_3^{(2)}$  comprises the sum of the following terms

$$\phi_{31}^{(2)} = - \frac{3 a^2 b k \sigma}{8 \sinh^4(kh)} \left[ A(\ell + 2k, 2\sigma, y) \sin\{(\ell + 2k)x - 2\sigma t + \delta\} + A(\ell - 2k, 2\sigma, y) \sin\{(\ell - 2k)x - 2\sigma t + \delta\} \right] \quad (43)$$

which expresses the interaction of  $\phi_2^{(0)}$  with  $\zeta_1$ , and

$$\phi_{32}^{(2)} = \frac{ab^2\sigma}{4 \sinh(kh)} \{H(\ell+k) + H(\ell-k)\} A(k, \sigma, y) \cos(kx - \sigma t) \quad (44)$$

$$\phi_{33}^{(2)} = \frac{ab^2\sigma}{4 \sinh(kh)} \left[ H(\ell+k) A(2\ell+k, \sigma, y) \cos\{(2\ell+k)x - \sigma t + 2\delta\} \right. \\ \left. - H(\ell-k) A(2\ell-k, \sigma, y) \cos\{(2\ell-k)x + \sigma t + 2\delta\} \right] \quad (45)$$

which express the interaction of  $\phi_2^{(2)}$  with  $\zeta_1$ , where

$$H(\ell) = \frac{g + \cosh(\ell) - \sigma^2 \sinh(\ell)}{\sigma^2 \cosh(\ell) - g + \sinh(\ell)}$$

The remaining interaction is between  $\phi_1$  and  $\zeta_2$ . If  $\zeta_2 = b_* \cos(2\ell x + \delta_*)$ , which for  $\delta_* = 2\delta$  corresponds to a ripple profile  $(\zeta_1 + \zeta_2)$  with a more peaked crest and a longer flatter trough than  $\zeta_1$  alone, the solution is completed by the addition of

$$\phi_{34}^{(2)} = -\frac{b_* a \sigma}{2 \sinh(kh)} \left[ A(2\ell+k, \sigma, y) \cos\{(2\ell+k)x - \sigma t + \delta_*\} \right. \\ \left. - A(2\ell-k, \sigma, y) \cos\{(2\ell-k)x + \sigma t + \delta_*\} \right] \quad (46)$$

The terms  $\phi_{3i}^{(2)}$ ,  $i = 1, 4$ , provide small contributions compared with the terms in the solution  $O(\kappa^2)$ . Despite this, it is worth identifying where the terms are singular and denoting these as points of weak resonance. Equation (43) is singular if

$$(\ell \pm 2k) \tanh(\ell \pm 2k) \ell = 4k \tanh(kh) \quad (47)$$

For  $k\ell \tanh(k\ell) \gg 0.7$ , a reasonable approximate solution of this equation is  $\ell = \pm 2k \pm 4k \tanh(kh)$  and so, for example, if  $\ell = 10$  m and  $k = 0.1 \text{ m}^{-1}$  solutions of Eq (47) are given by  $\ell/k = \pm 1.06$  and  $\pm 5.06$ . The term  $\phi_{32}^{(2)}$  has a weak resonance if  $\ell = \pm 2k$ , but, by virtue of the dispersion relation Eq (17), is also resonant for all  $k$  on account of the term  $(gk \sinh(kh) - \sigma^2 \cosh(kh))$  in its denominator. This term can be viewed, therefore, as providing a feedback of energy into the main motion given by  $\phi_1 \sim \cos(kx - \sigma t)$ . The term  $\phi_{33}^{(2)}$  is resonant if  $\ell = \pm k$  or  $\pm 2k$ , the former case corresponding to a direct match between the surface wavelength and the ripple wavelength.

The only term of the  $\phi_{3i}^{(2)}$  which is used in the practical examples later in this report is  $\phi_{34}^{(2)}$ , which can be seen also to be resonant if  $\ell = \pm k$ . From a comparison of Eqs (24) and (46), it is apparent that the terms  $\phi_2^{(2)}$  and

$\phi_{34}^{(2)}$  are of a similar type, and this similarity is utilized later in writing down solutions for the interaction of the main motion  $\phi_i$  with any harmonic constituent of the bed surface.

### 5.1 Limitations on the second order solution

Further conditions of Ursell-type can be obtained based on the fundamental requirement of the analysis that  $|\phi_3/\phi_2| \ll 1$  and, hence, more can be understood about the nature of the small parameter  $\alpha$  used at the outset to establish the hierarchy of terms in the solution.

Firstly the term  $\phi_{31}^{(2)}$  must be small compared with  $\phi_2^{(1)}$  from which it is derived and this leads to the condition, which is stated here for the limiting case  $\ell \gg k$ ,

$$bk \ll \tanh(\ell k) \quad (\ell \gg k) \quad (48)$$

This is slightly more restrictive than condition (29). Although it is not strictly necessary to establish a similar condition in relation to  $\phi_2^{(2)}$ , it is worth noting that such a condition is

$$\frac{\alpha}{k^2 \ell^3} \ll \frac{4}{3} \quad (k\ell \text{ small}) \quad (49)$$

This differs from (26) by a factor of two on the right hand side of the inequality. The terms  $\phi_{32}^{(2)}$  and  $\phi_{33}^{(2)}$  express the interaction of  $\phi_2^{(2)}$  and  $\zeta_1$ , and they must therefore be small in comparison with  $\phi_2^{(2)}$ . This leads to the requirement

$$\frac{b\ell}{2} \cosh(\ell k) \ll 1 \quad (\ell \gg k) \quad (50)$$

(which has been derived for  $\phi_{32}^{(2)}$  by omitting the singular term on the right hand side of Eq (44)).

The term  $\phi_{34}^{(2)}$  expresses the interaction of  $\phi_i$  and  $\zeta_2$ . As such, it could have been obtained in the solution  $O(\kappa^2)$  quite as readily as in the present order of approximation, and this fact lies at the heart of the discussion in the next section. For the present purpose, it is noted that it is not entirely logical to require that  $|\phi_{34}^{(2)}| \ll |\phi_2^{(2)}|$  and, instead, we state as our basic requirement only that  $|\phi_{34}^{(2)}/\phi_i| \ll 1$ . By the same reasoning as led to Eq (28), this produces a fairly complicated condition but, in the limiting case  $2\ell \gg k$  a simpler form (cf (29)) is obtained, namely

$$\frac{b_* k}{2} \ll \tanh(2\ell h) \quad (51)$$

It is now possible to see that the small parameter  $\alpha$ , which was introduced in Eqs (5)-(7) to set up a basic hierarchy of terms in the solution, is connected with the smallness of  $(a/k^2 h^2)$ ,  $b\ell$ ,  $b k$  (and  $b_* k$ ). This was evident earlier in considering the solution  $O(\alpha^2)$  and is confirmed by the results of the present section. It may be concluded, therefore, that the basic hierarchy in the solution is established, at least for  $\ell \gg k$ , if conditions (48)-(51) are satisfied. (These are generally rather stronger conditions than those determined earlier in comparing  $\phi_2$  with  $\phi_1$ .) For  $\ell = O(k)$ , full conditions of the type (28) are needed. It is not necessary or possible to identify  $\alpha$  with any one of the above parameters, and it is not a requirement of the method of analysis that this be done.

## § 6. APPLICATION OF THE METHOD TO NATURALLY OCCURRING SEABED TOPOGRAPHY

Sinusoidal variations for the bed profile of the type  $\zeta_1 = b \cos(\ell x + \delta)$  provide a rather inadequate description of natural sand ripples on the seabed. The addition of  $\zeta_2 = b_* \cos(2\ell x + \delta_*)$ , containing a contribution from the second harmonic, improves matters in the way described earlier. In general, however, it is necessary to provide a more accurate description of the ripple profile than is possible with these two terms and, in this section, a simple extension of the earlier results is described which is based on a Fourier series representation for the ripple profile. Even though the coefficients in the series (ie constituent ripple amplitudes) at the higher harmonics may be small, their effect on the flow near the bed may be large since, as seen earlier, the effect of ripples depends not on their amplitudes, but upon their steepnesses.

The earlier results can be generalised by taking at the outset

$$\bar{\zeta}_1 = \sum_{m=1}^N b_m \cos(m\ell x + \delta_m) \quad (52)$$

Following the comments in the previous section it is assumed here that the only interactions of importance are those between  $\bar{\zeta}_1$  and  $\phi_1$ . Therefore, by extension of Eqs (24) and (46), the solution  $\phi_2^{(2)}$  corresponding to  $\bar{\zeta}_1$  is taken as

$$\phi_2^{(2)} = \sum_{m=1}^N \frac{b_m a \sigma}{2 \sinh(kh)} \left[ -A(m\ell + k, \sigma, y) \cos\{(m\ell + k)x - \sigma t + \delta_m\} + A(m\ell - k, \sigma, y) \cos\{(m\ell - k)x + \sigma t + \delta_m\} \right] \quad (53)$$

The choice of  $N$  in Eq (52) must be governed by the steepnesses of the harmonic constituents, such that the steepnesses of the  $N$ th and all higher harmonics are small compared with the steepnesses of the lower harmonics. All the harmonic constituents of importance are then retained in  $\overline{\zeta}$ . The solution (53) is used in two practical applications, namely sand ripples in deep flow and sandwaves in shallow flow.

## 6.1 Results for sand ripples in deep flow

The flow velocities above nine natural sand ripples are discussed here. These were first examined by Davies (1979) in the context of a model of deep nonseparating potential flow over ripples of finite amplitude. The profiles in question were obtained in water of depth which was an order of magnitude greater than the ripple wavelength ( $L/\lambda \approx 0.2$ ) and were evidently wave-generated, being almost symmetrical about their crests. The ripple profiles were drawn out on thin rigid sheets inserted into the seabed by divers, and were subsequently digitized in the laboratory. For the finite amplitude model, each profile was reduced to sixteen points ( $N = 8$  in Eq (52)) per ripple wavelength, and the model then assumed the profiles to be repeated indefinitely in the positive and negative directions of  $x$ . In this section, comparisons with these earlier independent results are made using the velocity potential in Eq (53). The choice  $N = 8$  is thought to give a good compromise between the preservation of the important features of the ripple profiles, and the avoidance of concentrating on fine details of little general interest. Such details have been partly eliminated in the following examples by a smoothing procedure.

In the first place, each of the ripple profiles in Fig 10 has been represented by thirty two equally spaced points per ripple wavelength, and any slight asymmetry about each crest has been removed by a simple averaging (ie  $\delta_m = 0$ ,  $m = 1, N$  in Eq (52)). Next, each profile has been Fourier analyzed using a Fast Fourier Transform routine, resulting in sixteen coefficients ( $N = 16$ ) for each ripple. The smoothing procedure has then merely involved truncating each series at the eighth harmonic, resulting in the coefficients  $b_m$  ( $m = 1, 8$ ) in Table 1. In Fig 10, these coefficients can be seen to correspond to simulated profiles which represent each ripple quite adequately. For each ripple, the fundamental ( $m = 1$ ) makes the major contribution, as expected. The contribution from the second harmonic ( $m = 2$ ) is also substantial in most cases, and particularly where a 'secondary ripple crest' occurs in the 'primary trough' (Ripples 1, 3, 4 and 6). The contributions from  $b_m$ ,  $m = 3$  to 8, appear less important, until

TABLE 1

Ripple Number	1	2	3	4	5	6	7	8	9
Wavelength $\lambda$ cm	112.5	112.5	109	73.5	54.6	81.6	66.4	81.1	79.6
Harmonic $m$	Fourier coefficients $b_m$ (scaled to $\lambda = 100$ )								
1	4.33	5.17	4.51	5.98	8.36	6.04	8.71	6.55	6.91
2	2.57	1.89	1.67	1.94	-0.23	2.63	1.01	2.07	1.66
3	-0.26	0.19	-0.14	-0.43	0.52	0.34	0.09	0.52	0.37
4	0.24	0.01	0.14	0.18	-0.10	0.17	0.31	-0.12	-0.19
5	-0.02	0.04	-0.10	0.27	0.14	0.22	0.06	0.14	0.05
6	0.01	0.04	0.05	0.11	-0.02	0.19	0.04	-0.05	-0.06
7	0.07	0.02	0.08	0.00	0.03	-0.02	0.10	0.14	0.05
8	-0.03	0.00	0.06	0.09	0.14	0.02	-0.01	-0.03	-0.05
	Steepness $mb_m\ell$								
1	0.272	0.325	0.283	0.376	0.525	0.379	0.547	0.412	0.434
2	0.323	0.238	0.210	0.243	-0.029	0.330	0.126	0.260	0.208
3	-0.049	0.036	-0.026	-0.081	0.099	0.063	0.018	0.098	0.070
4	0.060	0.003	0.035	0.047	-0.026	0.042	0.078	-0.030	-0.046
5	-0.008	0.012	-0.031	0.084	0.045	0.070	0.020	0.043	0.015
6	0.003	0.015	0.017	0.040	-0.008	0.072	0.016	-0.019	-0.024
7	0.030	0.007	0.035	0.0	0.015	-0.008	0.045	0.060	0.022
8	-0.016	0.000	0.031	0.047	0.069	0.012	-0.005	-0.016	-0.027
$\sum mb_m\ell$	0.615	0.634	0.554	0.756	0.690	0.960	0.845	0.808	0.652



the steepnesses of all the constituents ( $m b_m \ell$ ,  $m = 1, N$ ) are compared (see Table 1). Although, in general, the values of steepness diminish as  $m$  increases, the steepnesses for  $m = 7$  and  $8$  are by no means always negligible compared with values for  $m = 1$  and  $2$ . The significance of this is that, by extension of the argument leading to Eq (3) for a deep flow,

$$u_{cr} = U \left( 1 + \sum_{m=1}^N m b_m \ell \right) \quad (54)$$

In other words, if  $\delta_m = 0$  ( $m = 1, N$ ) the sum of the steepnesses of the constituent harmonics enables the departure of the surface velocity at the crest ( $x = 0$ ) to be calculated in relation to the unperturbed velocity  $U$  which would exist at  $y = 0$  in the absence of the bedforms. In Table 2, the values of  $u_{cr}$  calculated from Eq (54) are compared with the equivalent values obtained by the method of Davies (1979) for the flow over finite amplitude ripples. The small discrepancies between the results are due, most likely, to variations of the simulated ripple profiles in the immediate vicinity of the ripple crests by the two methods. In most cases, the present method gives a slightly lower value for  $u_{cr}/U$ , indicating a rather less peaked simulated crest than in the earlier method. This emphasizes the importance of the peakedness of ripple crests in the determination of surface velocities. It should be recalled also that the linearization involved in the present method is expected to lead to variations in  $u_{cr}/U$  of the type shown in Fig 1. But it is not possible to make any simple assessment of the likely overall error in the result due to linearization, since discrepancies such as are shown in Fig 1 are not additive harmonic by harmonic.

In Fig 10, the peak horizontal velocity occurring during a wave cycle at each point on the bed surface is plotted for Ripples # 1-9. The normalized values of velocity amplitude shown have been obtained by forming the quotient

$$U_n = \frac{\text{Amplitude} (u_2^{(2)} + u_1)}{\text{Amplitude} (u_1)}$$

for each point on the bed surface. The small term  $u_2^{(1)}$  has not been included in the calculation in order to enable direct comparisons to be made with equivalent deep flow results, and the horizontal velocity has been considered rather than the tangential on the grounds that the two results are very similar for all  $x$ , and are identical at the crest and trough positions where the extreme values of surface velocity are attained. The horizontal velocity amplitudes take the

TABLE 2

Ripple Number	1	2	3	4	5	6	7	8	9
$u_{cr}/U$ Eq. (54)	1.62	1.63	1.55	1.76	1.69	1.96	1.85	1.81	1.65
$u_{cr}/U$ From Davies (1979)	1.63	1.65	1.61	1.80	1.68	2.05	1.90	1.89	1.65
% difference	- 0.6	- 1.2	- 3.7	- 2.2	0.6	- 4.4	- 2.6	- 4.2	0.0

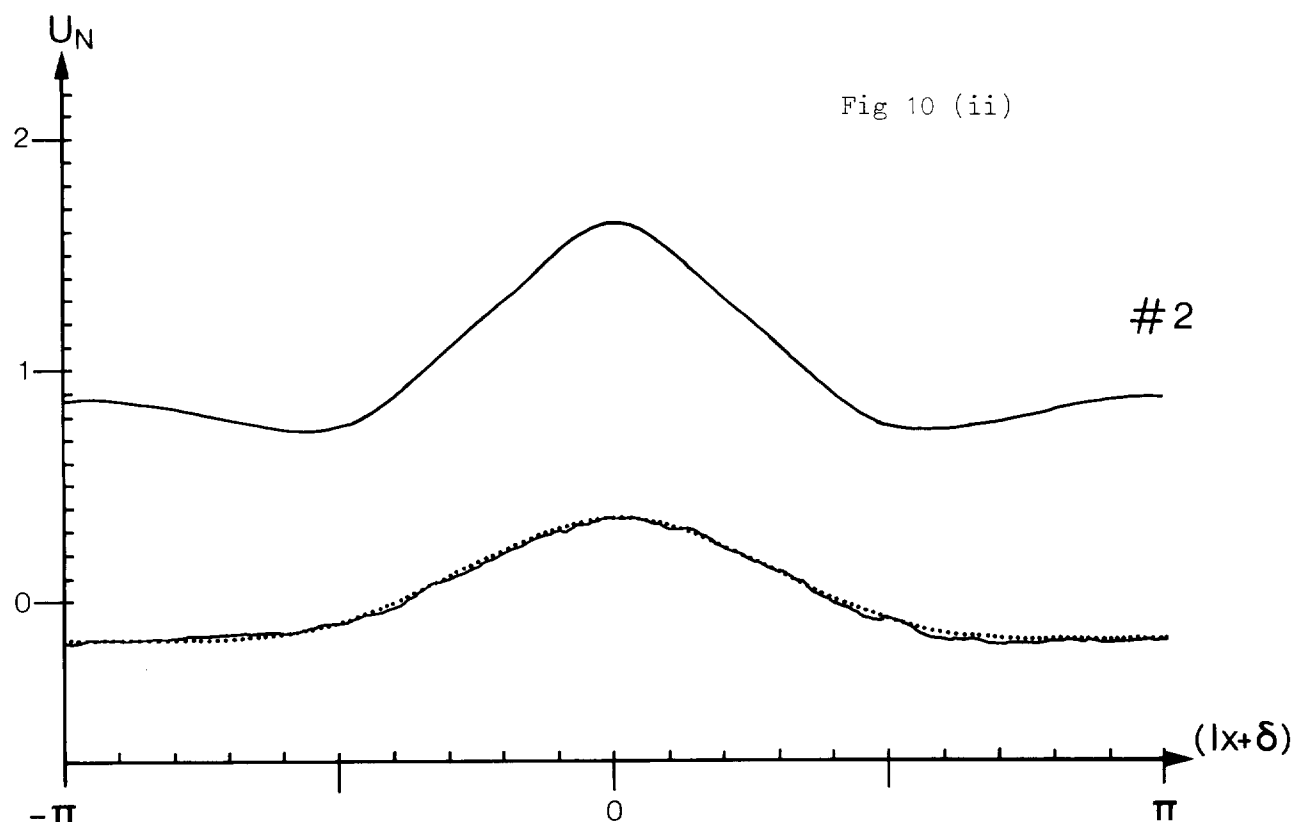
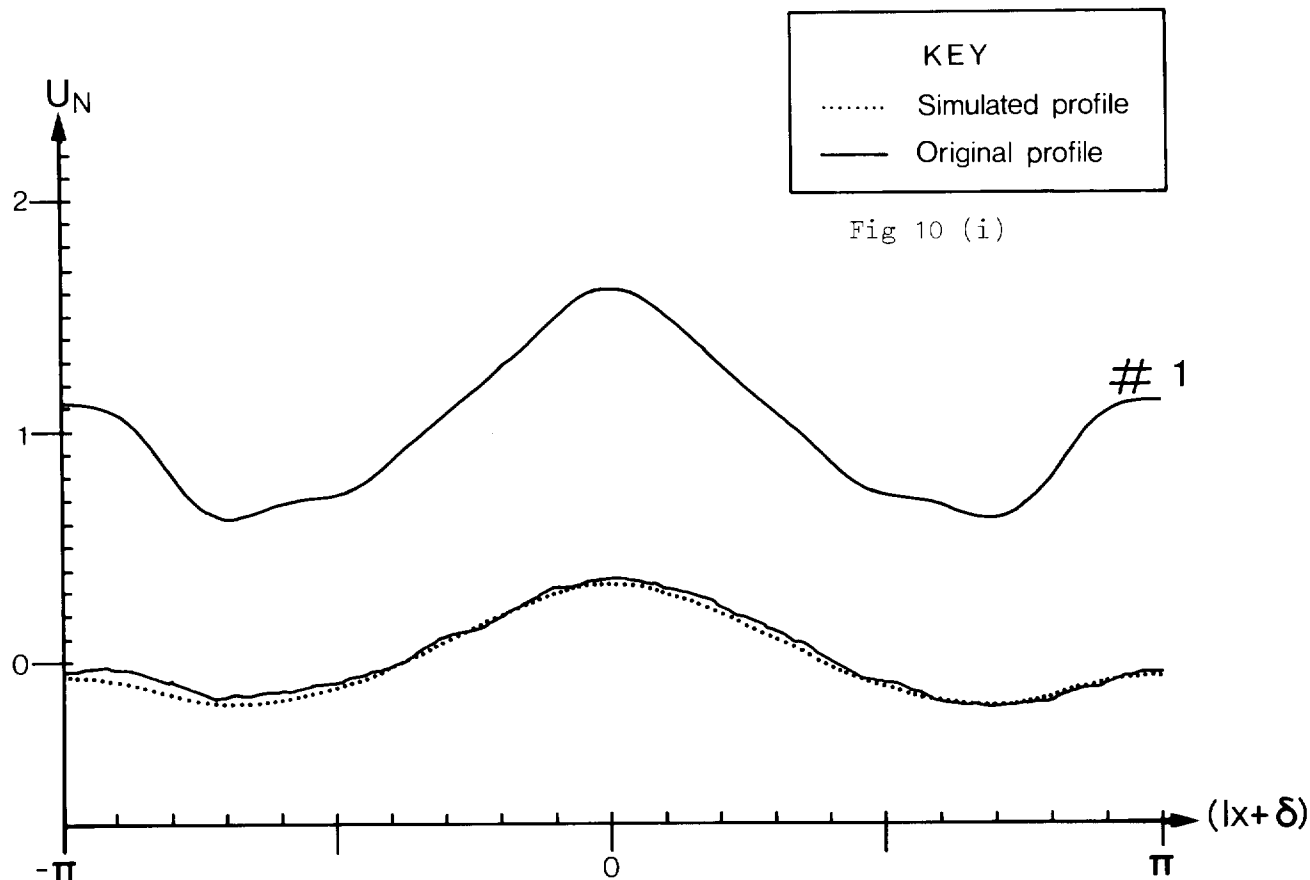
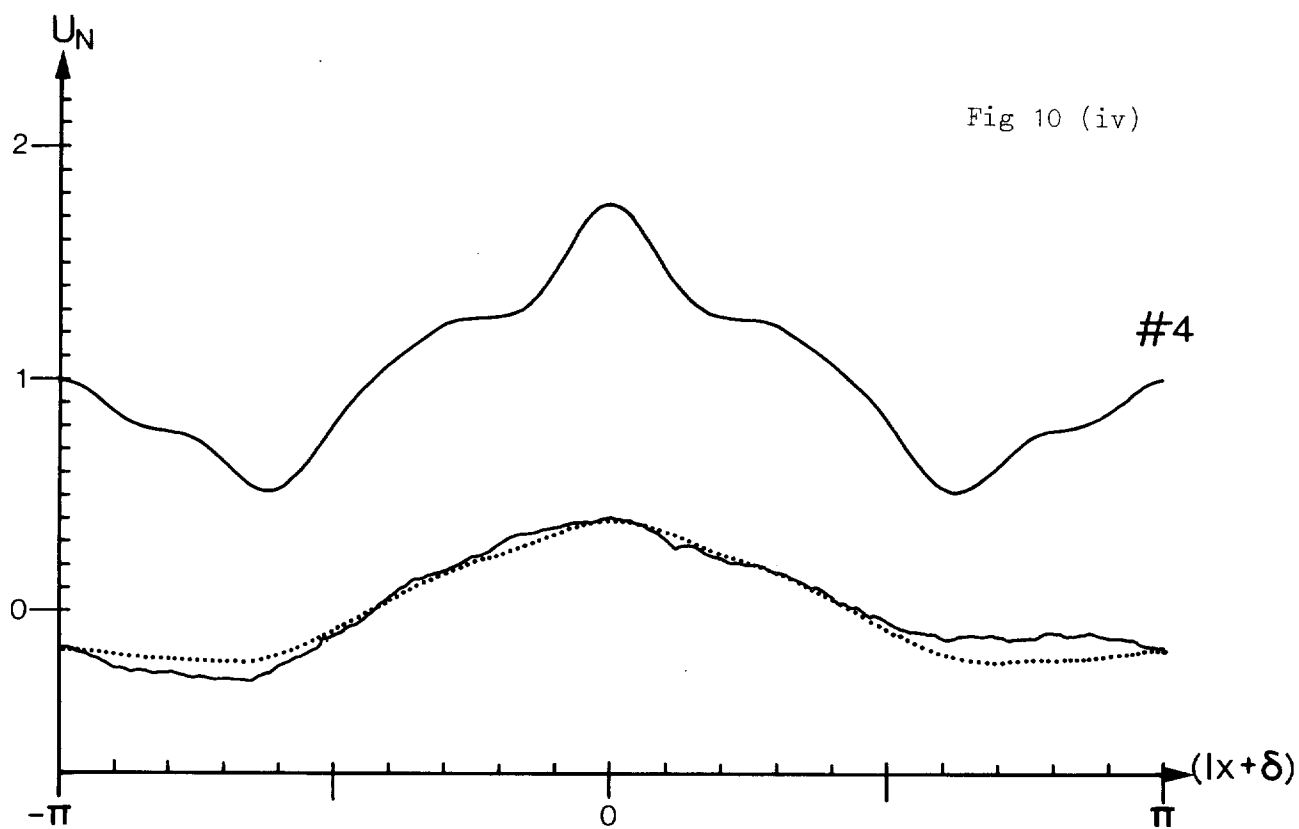
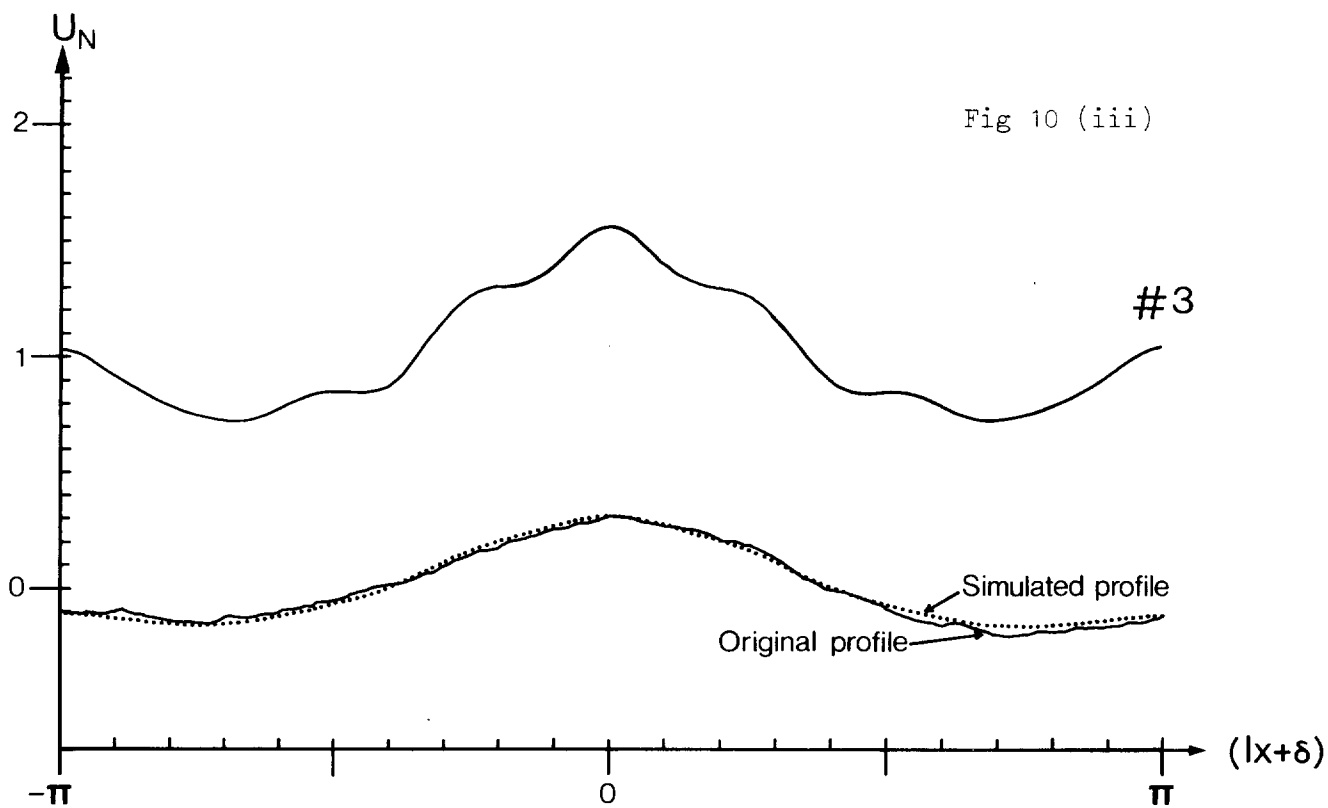


Fig 10 In each of Figs 10 (i) to 10 (ix) the upper curve shows the normalized peak value of velocity amplitude at the bed surface over a complete wavelength of the rippled bed. The original ripple profile is shown in the lower part of each diagram together with the simulated ripple shape, assumed symmetrical and obtained taking  $N = 8$ . The profile is drawn without vertical exaggeration.



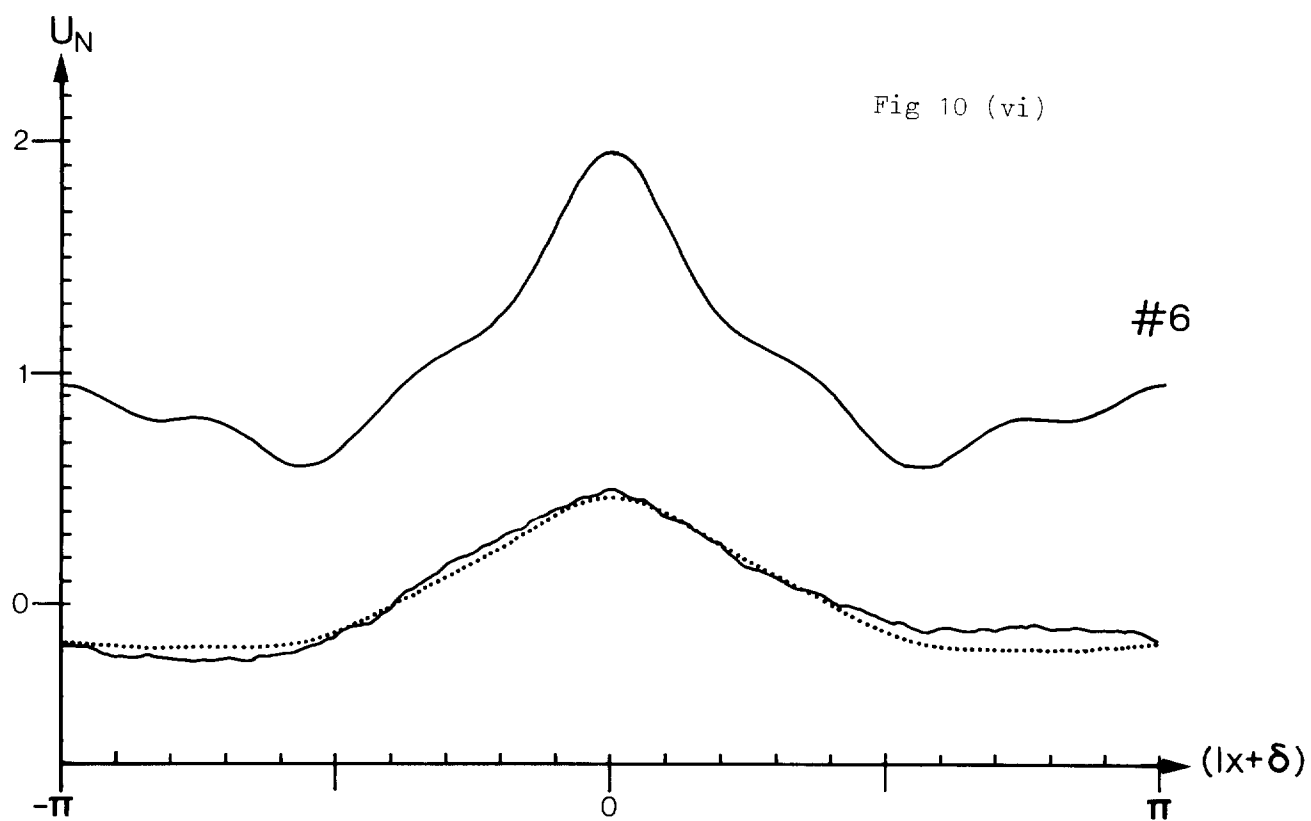
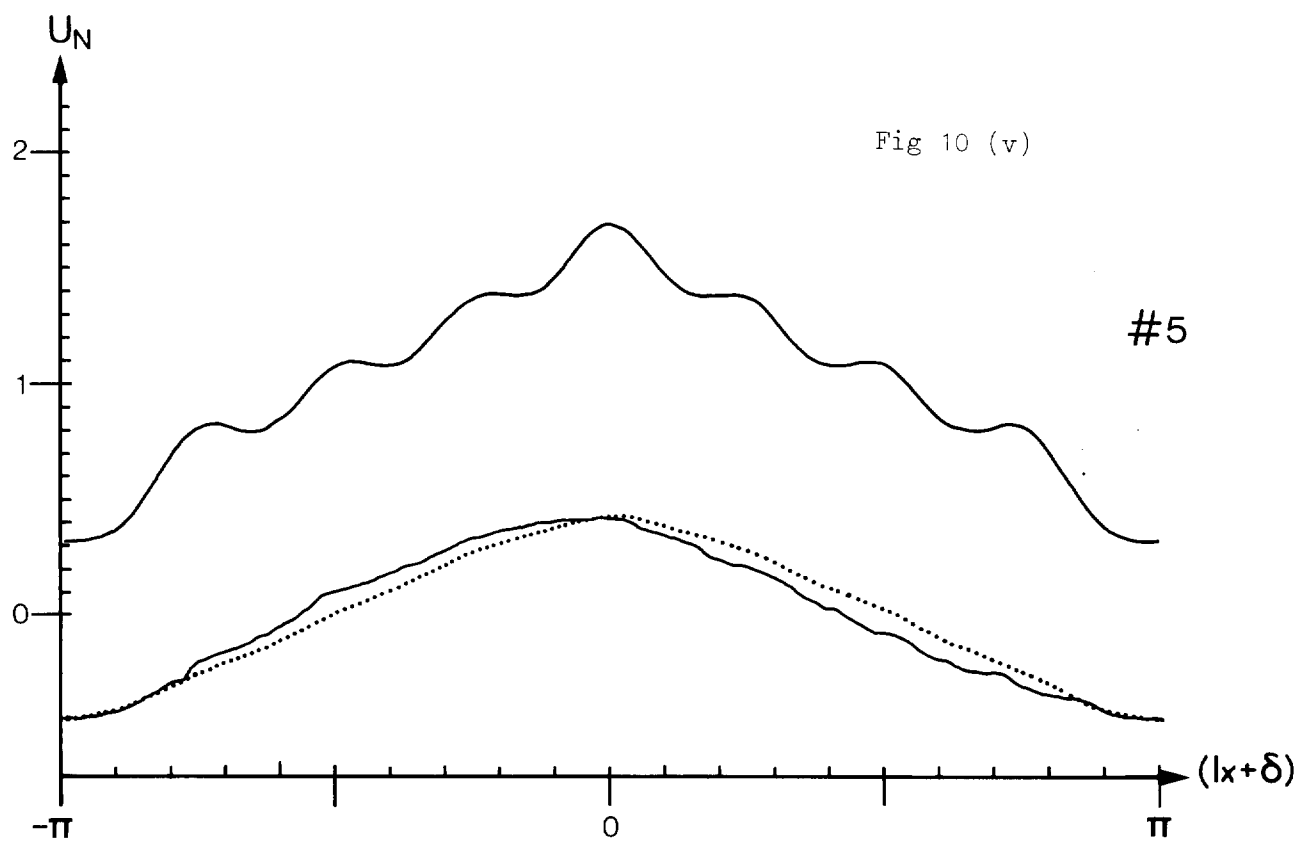


Fig 10 (vii)

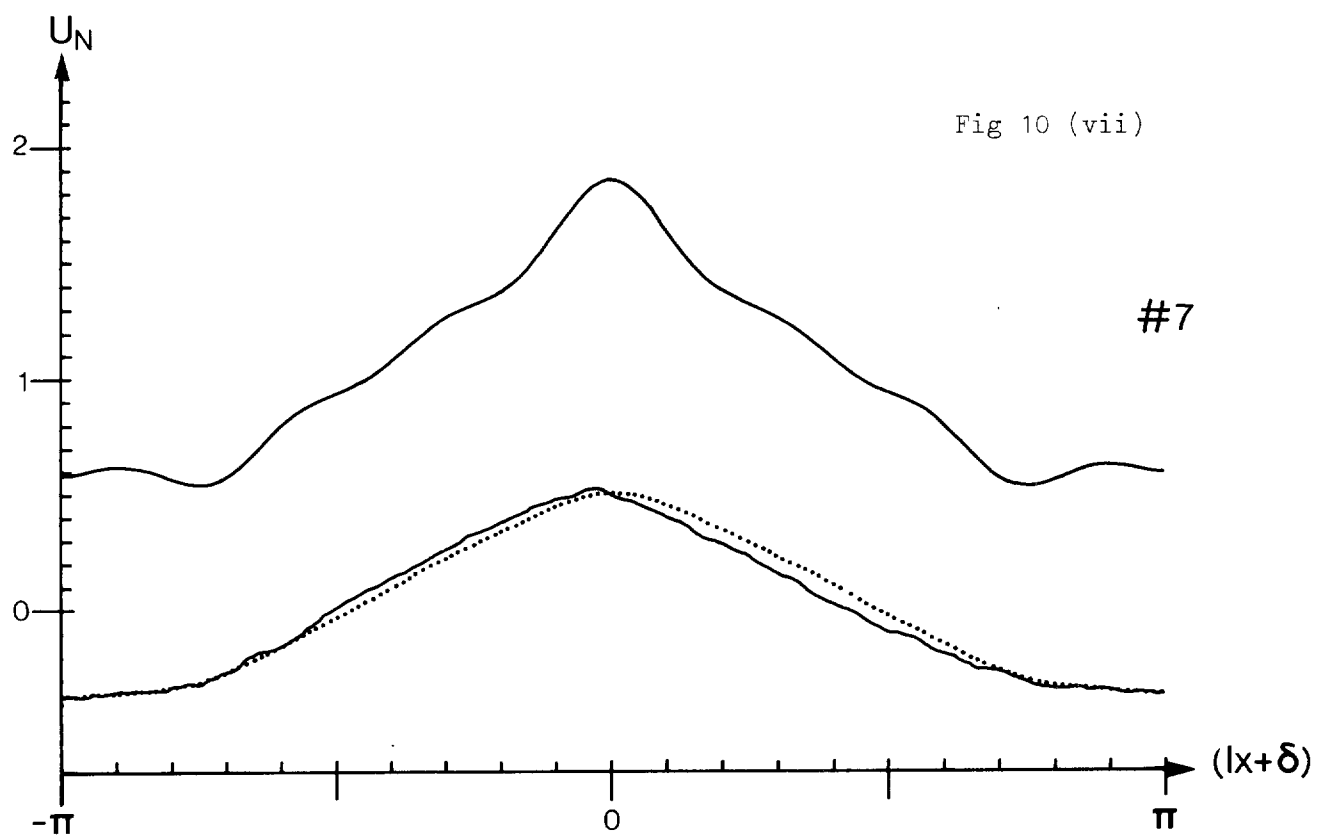
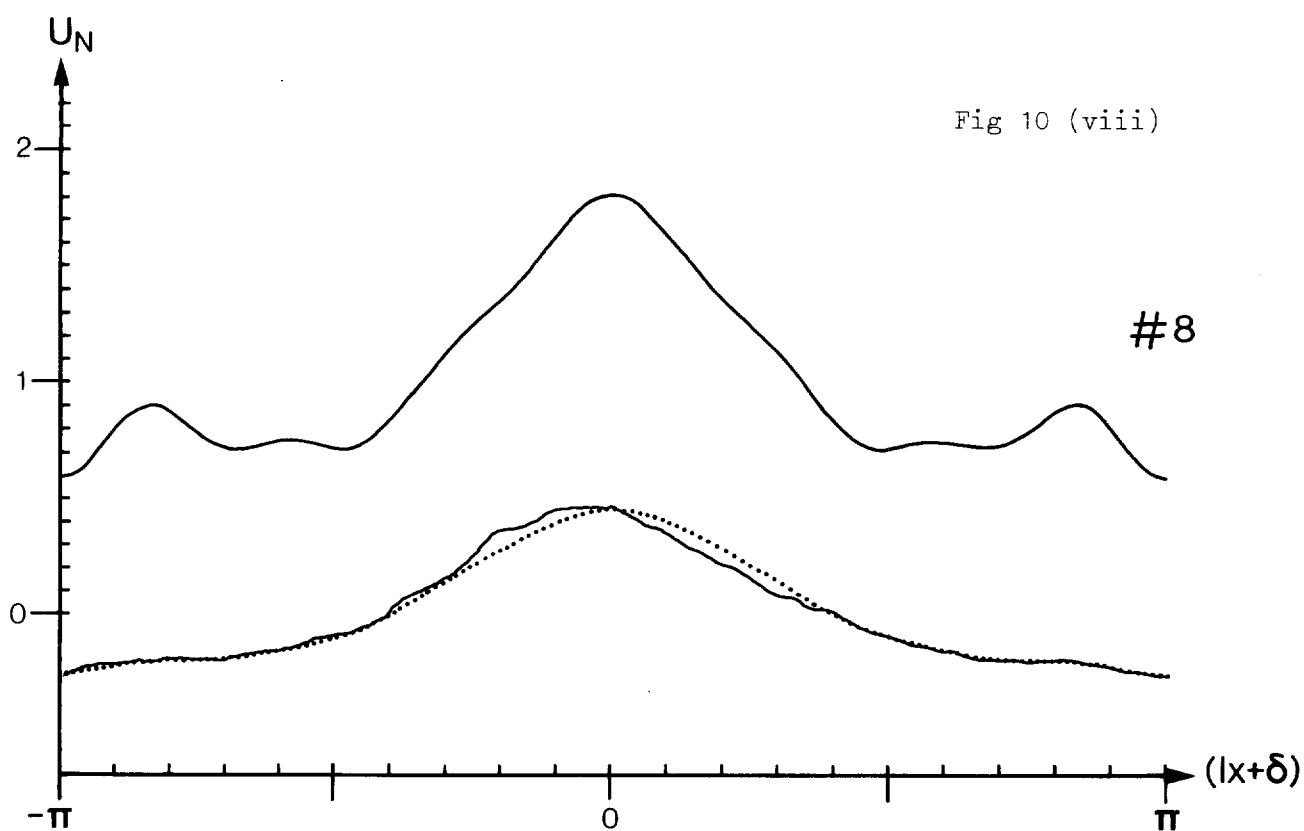
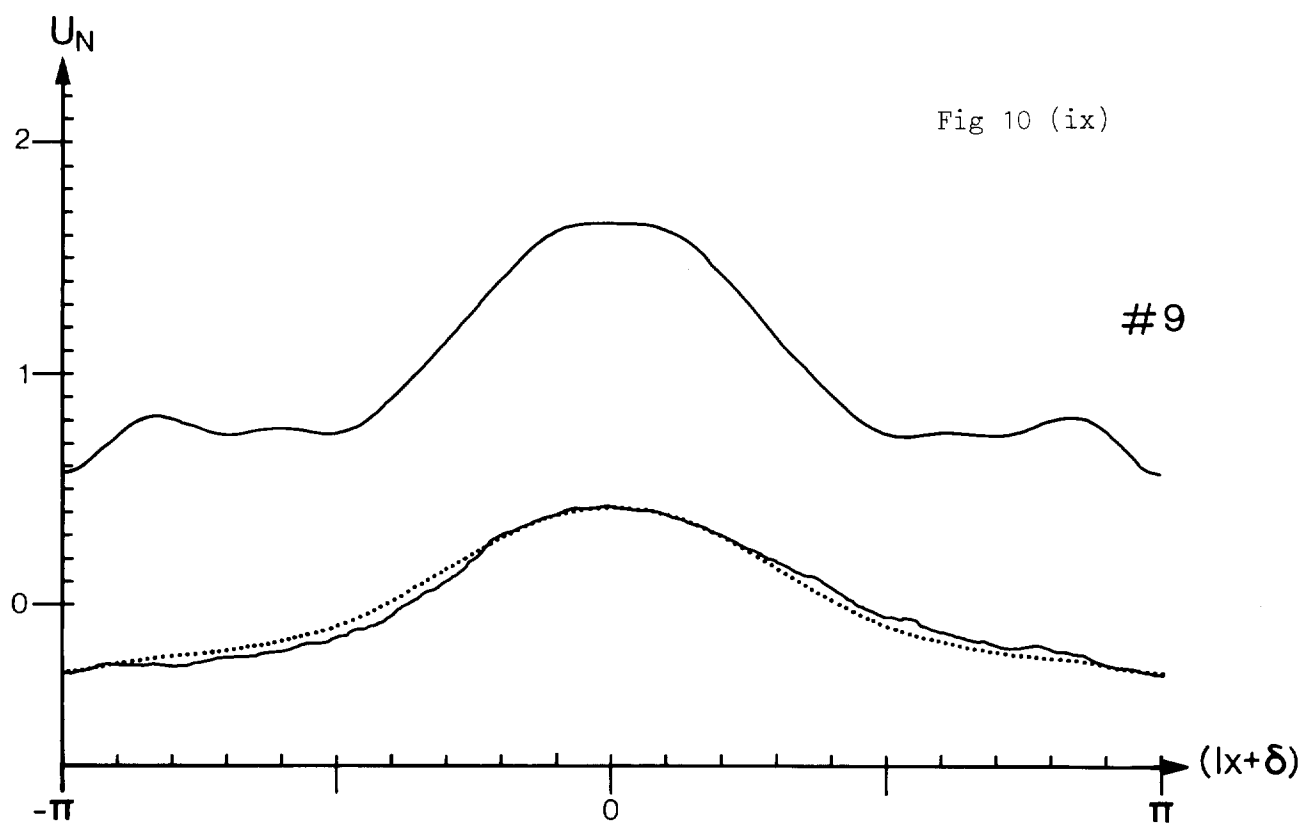


Fig 10 (viii)





maximum value quoted in Table 2 at the crest, and fall quite rapidly, and generally quite regularly, with distance from the crest positions. This is important in the context of sediment movement by waves since it helps to explain why, in certain circumstances, sediment may be observed moving as bedload in the region of the ripple crests, but not in the ripple troughs (see Davies and Wilkinson (1979)). Contributions to  $U_n$  from the higher harmonics are superimposed on the overall trends. However, these have little or no general significance, and, following the earlier discussion, it may be noted that corresponding variations are barely perceptible in the simulated ripple profiles in Fig 10. The minimum value of  $U_n$  occurs in the trough, except in cases in which a 'secondary crest' is present. For example, in the case of Ripple # 1,  $U_n$  achieves a value of 1.15 on the secondary crest, indicating a velocity which is greater locally than the unperturbed (flat bed) value.

In Fig 11, two typical examples of results for asymmetrical ripples are shown. The particular cases are for Ripples # 1 and 8, with  $N = 16$  in Eq (52), and the same smoothing procedure carried out as above. The simulated profiles exhibit small variations which were not present in the equivalent smoothed (symmetrical) curves in Fig 10 and, as a consequence, the velocity amplitude results contain quite marked local variations. Once again, however, these have no general significance and, in fact, the overall trends in the results are much the same as for the equivalent smoothed profiles in Fig 10. For Ripple # 1, a comparison of the peak normalized velocity amplitudes at the crest position gives values for  $U_n$  of 1.62 for both the asymmetrical and symmetrical cases. For Ripple # 8 the equivalent respective values are 1.86 and 1.81. Evidently, the fine detail of the ripple profile does not influence the peak velocity results too greatly, and this supports the earlier suggestion that, in modelling the deep flow over nearly symmetrical (wave-generated) sand ripples, it is adequate to work with smoothed symmetrical profiles, defined by about eight Fourier harmonics. For strongly asymmetrical cases, it is clearly necessary to retain the full details of the profiles, as discussed in the next section for the case of sandwaves in shallow water.

In the earlier section on the influence of the free surface on the results, the height  $\hat{y}$  above the bed to which the effects of ripples are important was discussed. For a deep flow above a sinusoidal bed of wavelength  $\bar{L}$ , this height was quoted as  $\hat{y} = 0.733\bar{L}$  and, in the present examples, the same result must hold with  $\bar{L} = 2\pi/\ell$  taken as the wavelength of the fundamental constituent ( $m = 1$ ). The heights of influence of the higher harmonic constituents,  $\hat{y}_m$ ,  $m = 2, N$ , are all smaller than this (viz.  $\hat{y}_m = 0.733\bar{L}/m$ ) and, in general,



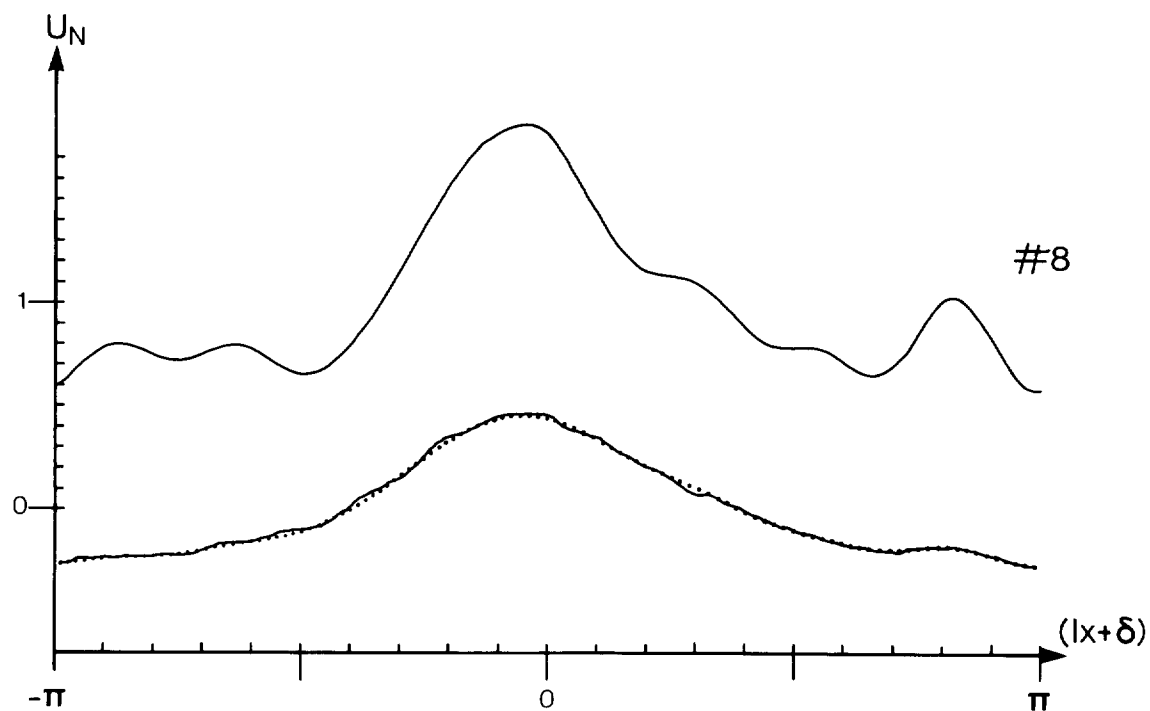
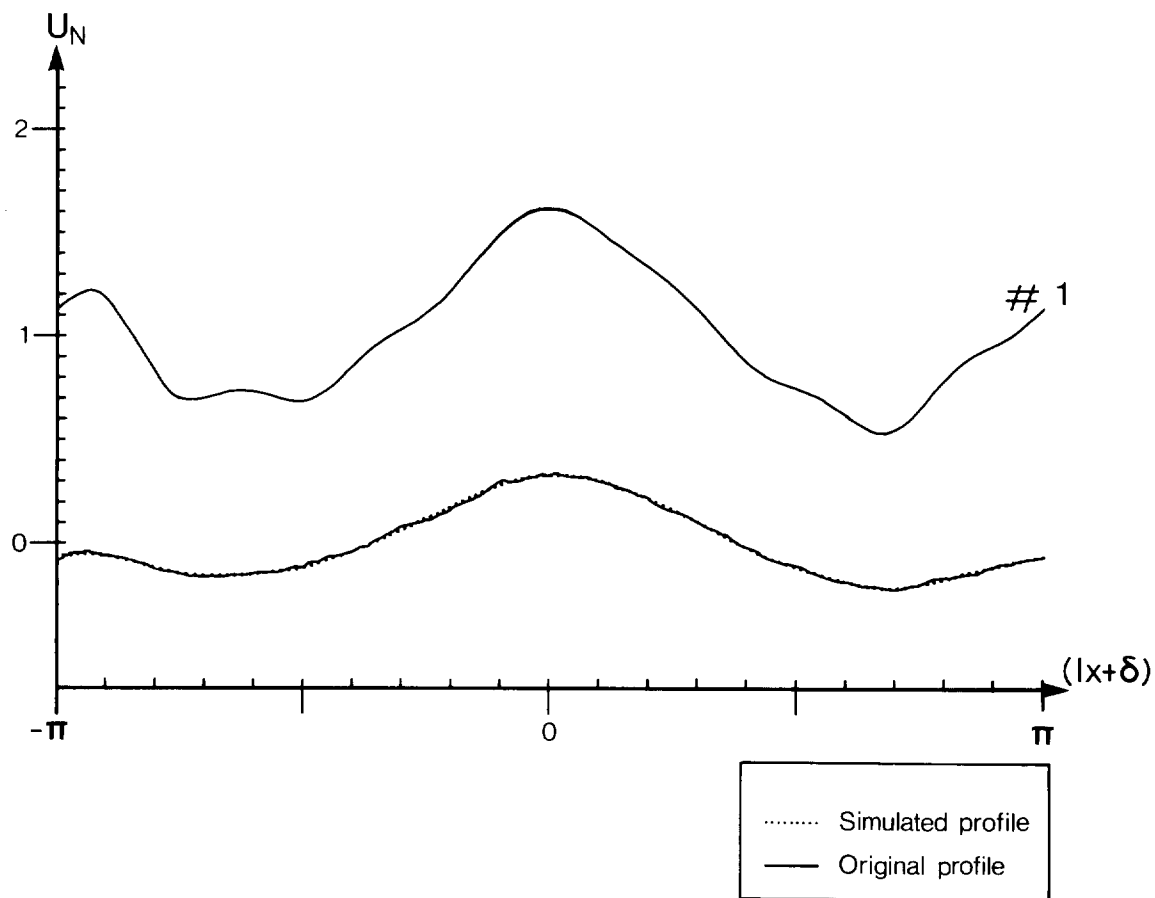


Fig 11 Normalized values of peak velocity at the bed surface over a complete wavelength of the bed for Ripples #1 and #8. The graphs are of the type shown in Fig 10, except that here unsmoothed asymmetrical bed profiles are considered.

need not be considered.

Finally, it should be noted that in Eq (53) conditions of resonance occur for each harmonic. These resonances arise where  $m\ell = \pm 2k$  ( $m = 1, N$ ). The condition  $\ell = 2k$  was examined earlier and is further commented on in the Discussion section. Clearly, for ripples in deep water, it is generally expected that  $\ell \gg k$ , so that no conditions of resonance are satisfied on the above rule. Bearing in mind also that the predicted resonances are given by an analysis which assumes the rippled bed to be of infinite horizontal extent, it is unlikely that the full effects of resonance described earlier would occur in real cases in which the rippled bed is of limited horizontal extent.

## 6.2 Results for sandwaves in shallow water

In contrast to the above examples relating to sand ripples, for which comparisons with deep flow results are appropriate, the flow velocities above two natural sandwaves in relatively shallow water are now discussed. In particular, the orbital velocity amplitudes at the bed surface are considered for waves progressing over a sandwave field assumed to be of indefinite extent in the positive and negative directions of  $x$ . Variations in orbital velocity over the surface of a sandwave have quite important implications since, although the basic sandwave forms may be tidally generated, there is evidence that surface waves can cause modifications to these basic profiles.

Sandwaves in shallow water have been discussed by Langhorne (1978) and, in the present exercise, sandwave profiles observed by Langhorne in Start Bay, South Devon, have been used to provide the necessary input to the present model. In addition, the examples have been based upon recorded water depths, and typical wave periods for Start Bay. Although the velocity amplitude results presented in this section are in a normalized form which is independent of surface wave amplitude 'a', it can be shown that the present theory is valid in respect of criteria (27) and (28) in all cases presented. (The criteria involving 'a' can be satisfied by restricting the wave amplitude to a small value.)

In Fig 12 the selected sandwave profiles are shown, together with their principal dimensions. Each profile has been digitized in a way which preserves its overall shape, bed surface undulations of very short wavelength having been smoothed out. These small undulations could be accounted for by the inclusion of many more digitized points in each sandwave length but, alternatively, can be handled by an independent subsequent analysis of the type given above for natural ripples in deep flow. The sandwave profiles are clearly asymmetrical and so, in

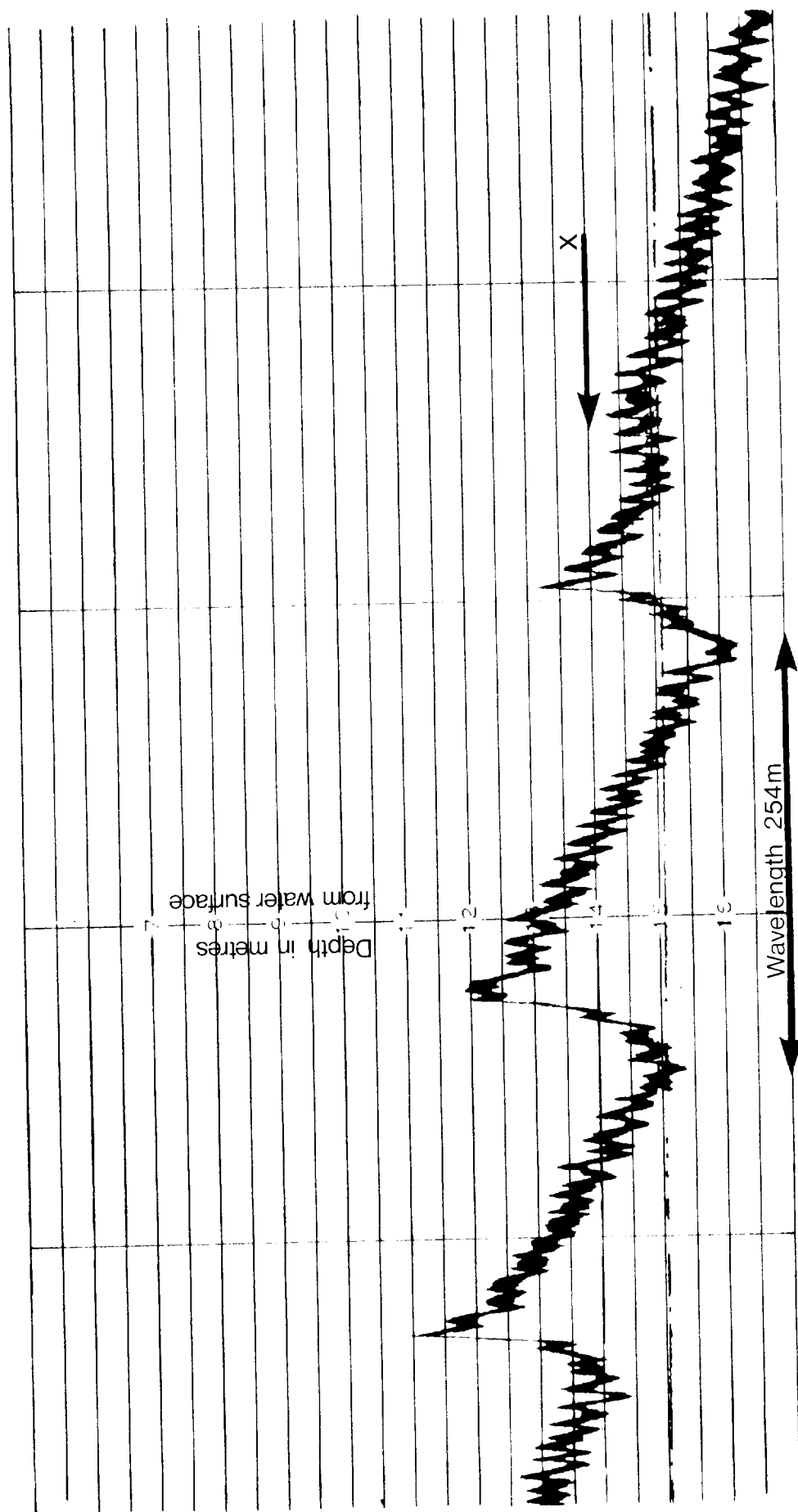


Fig 12 (i) SANDWAVE #1 : Sandwave height = 3.1m Overall steepness = 0.0121  
Mean water depth = 14.0m

Fig 12 In Fig 12 (i) and 12 (ii) echo-sounder runs show the two sandwave profiles. Their principal dimensions are as indicated. In 12 (iii) the digitized points taken to represent the sandwaves are shown together with the simulated profiles. Note the different vertical exaggerations in this diagram, and also that the sandwave length has been scaled to equal 1.0.

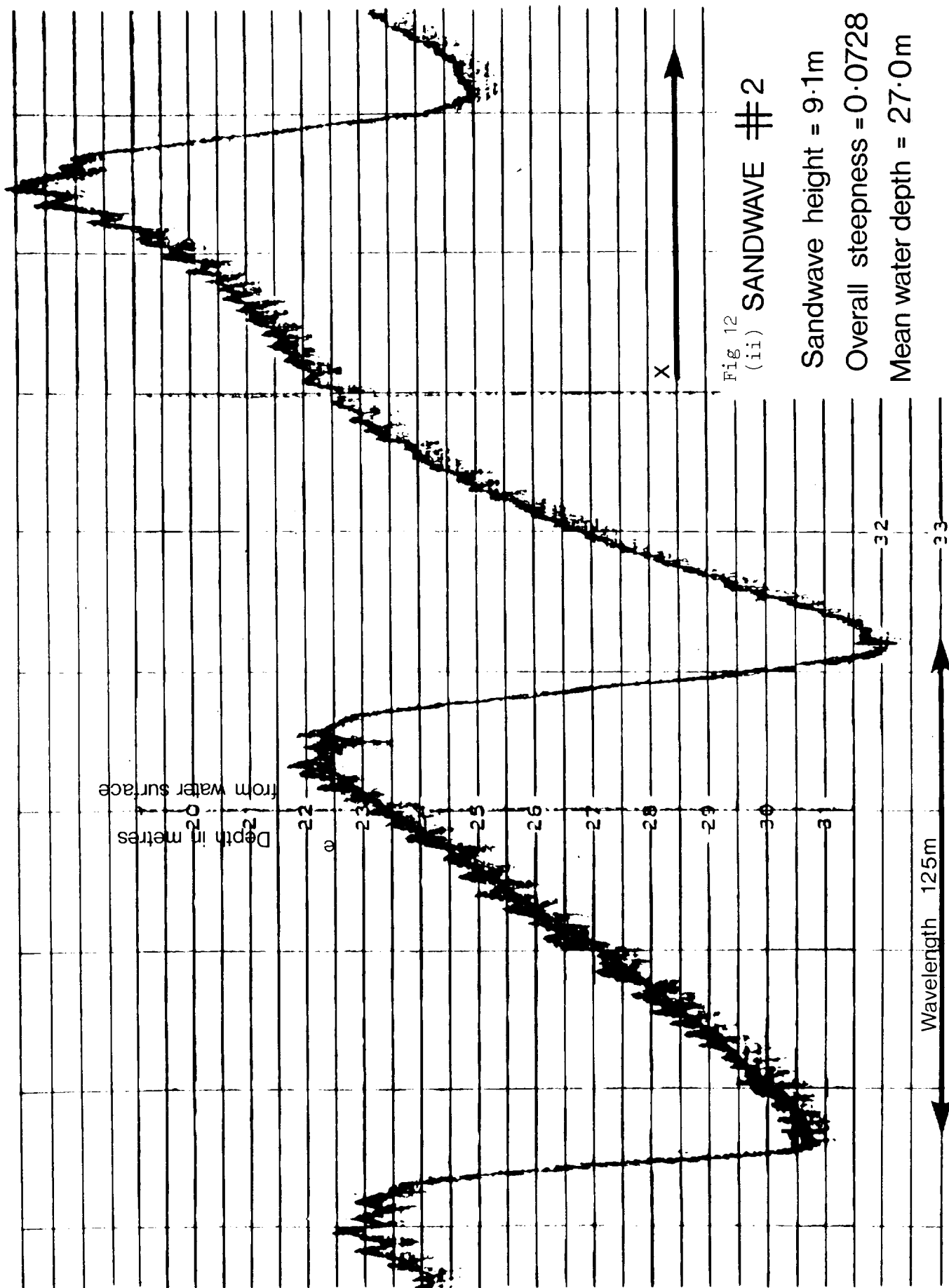


Fig 12

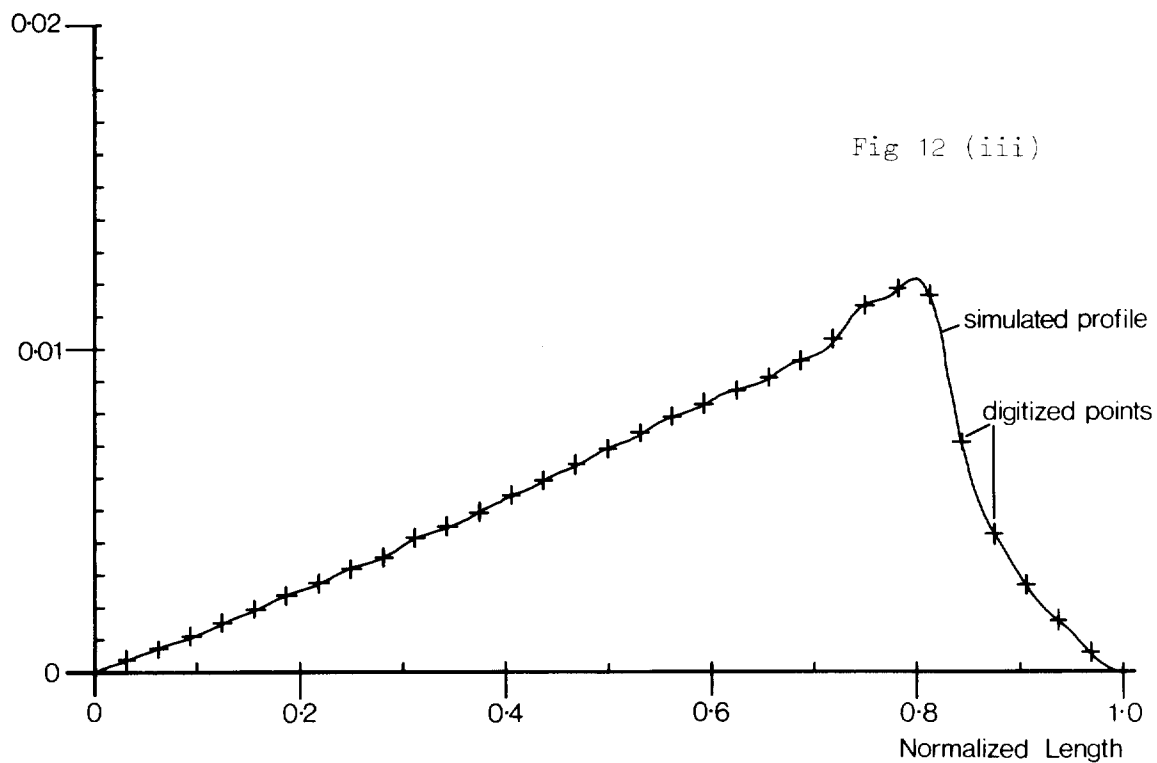
# (ii) SANDWAVE #2

Sandwave height = 9.1m

Overall steepness = 0.0728

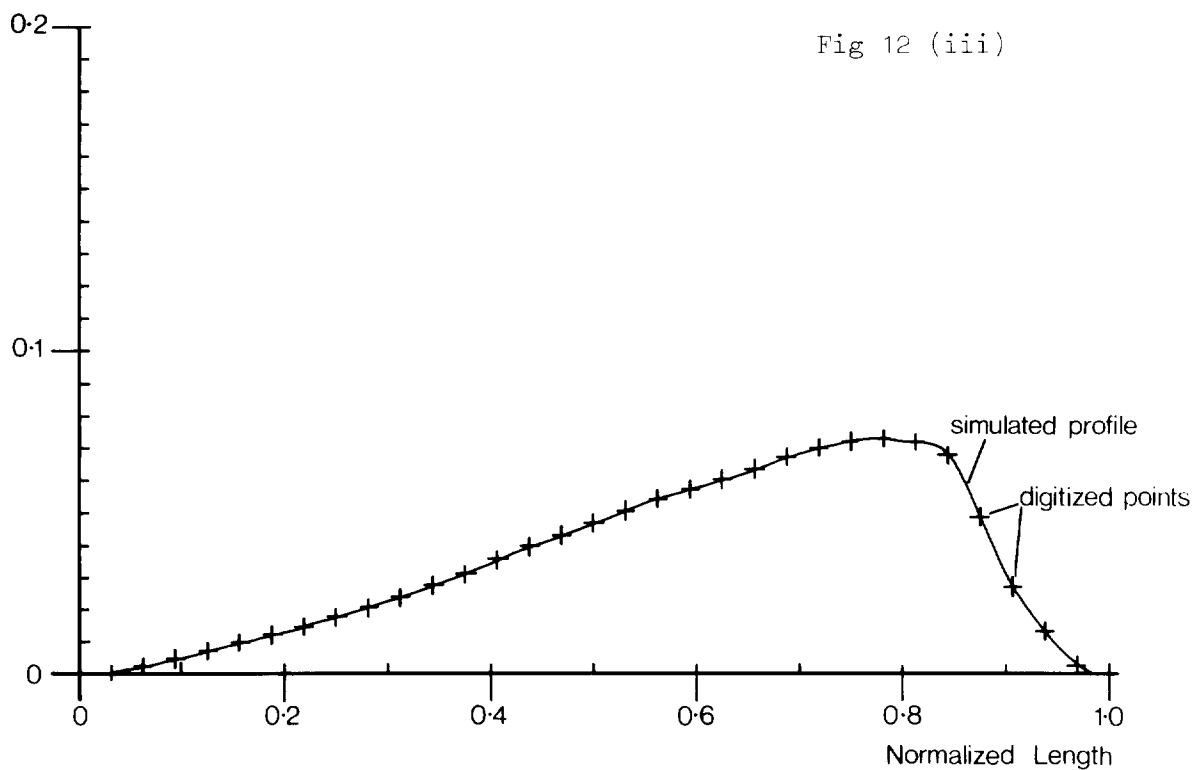
Mean water depth = 27.0m

Normalized Height



SANDWAVE N01

Normalized Height



SANDWAVE N02

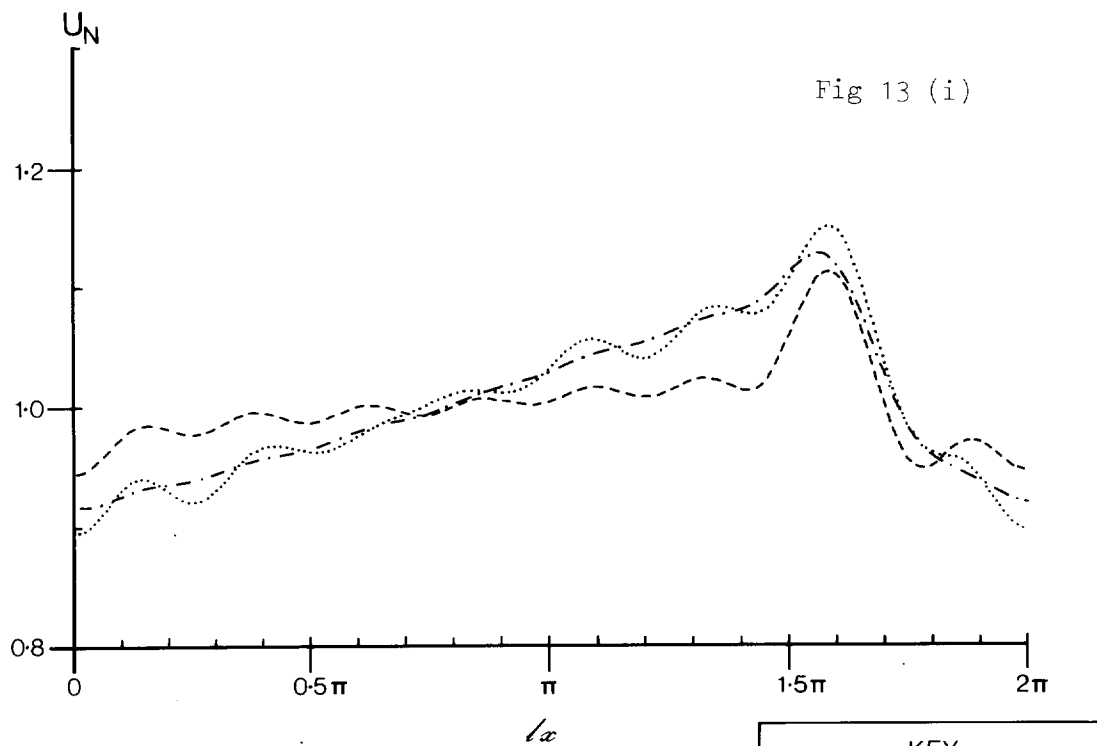
writing down the Fourier series for each profile, it is necessary to quote values for both  $b_m$  and  $\delta_m$  ( $m = 1, N$ ) in Eq (52). Each profile is represented by 32 digitized points ( $N = 16$ ) per wavelength (see Table 3). The first harmonic ( $m = 1$ ) is dominant, as expected, and contributions are present elsewhere to represent the overall asymmetry of the sandwaves.

Normalized peak horizontal velocity amplitudes at the surface of each sandwave are shown in Figs 13 and 14. These results are of the same type as those presented for the ripples in Figs 10 and 11, the Fourier series representing the sandwave profiles having been truncated at the eighth harmonic. For a given sandwave profile and a given mean water depth, the results can be seen to vary with the wave period. The extreme values of velocity amplitude on the bed surface are always found at the crest and trough positions, while elsewhere on the profiles the velocities are strongly influenced by both the overall asymmetry and local undulations of the bed. It is interesting to note that the peak values plotted do not necessarily occur when the surface wave crest is directly overhead ( $kx - \omega t = \pi/2$ ). However, the phase differences involved here have not been found to exceed a few degrees.

In Figs 13 and 14, typical results obtained using the present method are compared both with deep flow results for the same sandwaves, and with 'quasi-uniform' results in which the normalized velocity is assumed to depend only upon the local water depth and the wave period. Comparisons of both these types were made earlier for purely sinusoidal profiles. Since  $\bar{h}/h = 18.6$  for Sandwave #1, it is not surprising that variations exist between the predictions of the present method and the deep flow results which, as expected, tend to minimize departures from the unperturbed (flat bed) value. These variations, which are most noticeable for short wave periods ( $T \approx 6$  sec), are progressively reduced as wave period increases. In general, the deep flow results provide easily calculated, but conservative, bounds for the overall perturbation in velocity amplitude. For Sandwave #2, for which  $\bar{h}/h = 4.6$ , the deep flow results are in quite good agreement with the predictions of the present method over the entire profile due to the relatively larger water depth. A comparison of the general trend in the present results, with results based on the quasi-uniform assumption, indicates reasonable overall agreement for both sandwaves, at least away from the region of the crests where depth variations occur rapidly with horizontal distance, and where the effects of higher harmonics in the profiles complement one another. Here results based on the quasi-uniform assumption should be treated with caution, since, in general, they greatly underestimate the perturbations predicted by the present method.

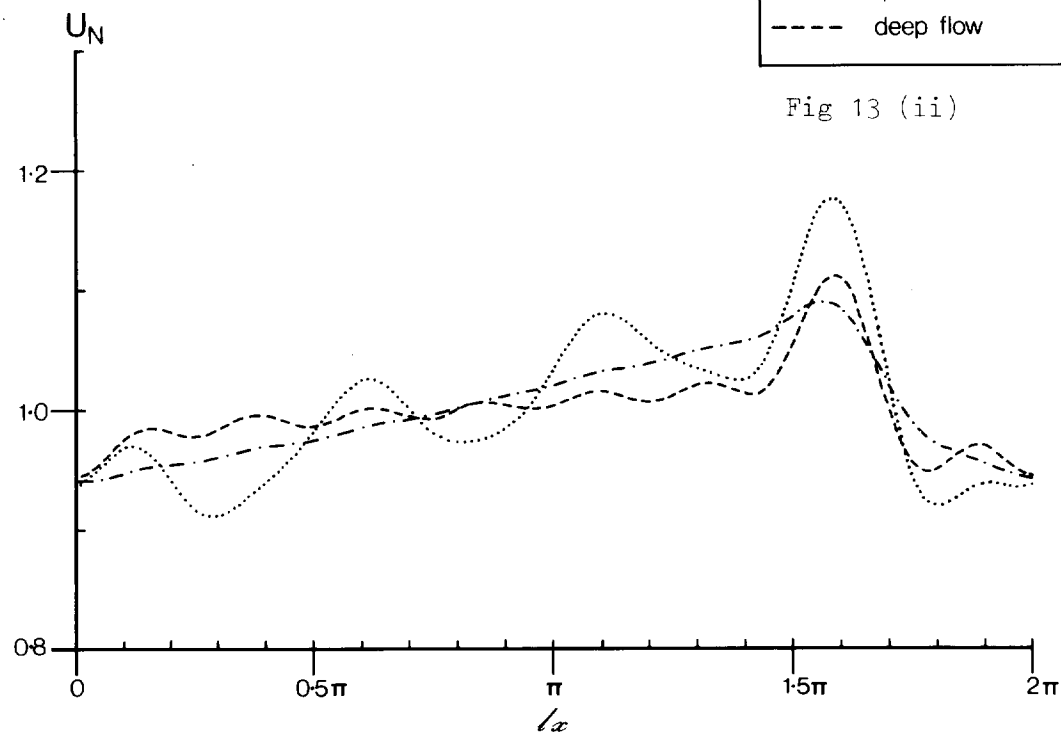
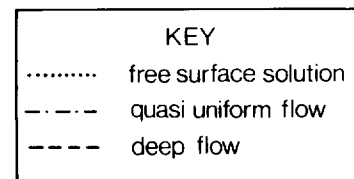
TABLE 3

[illegible]



SANDWAVE N<sup>o</sup> 1

$T = 8 \text{ sec}$

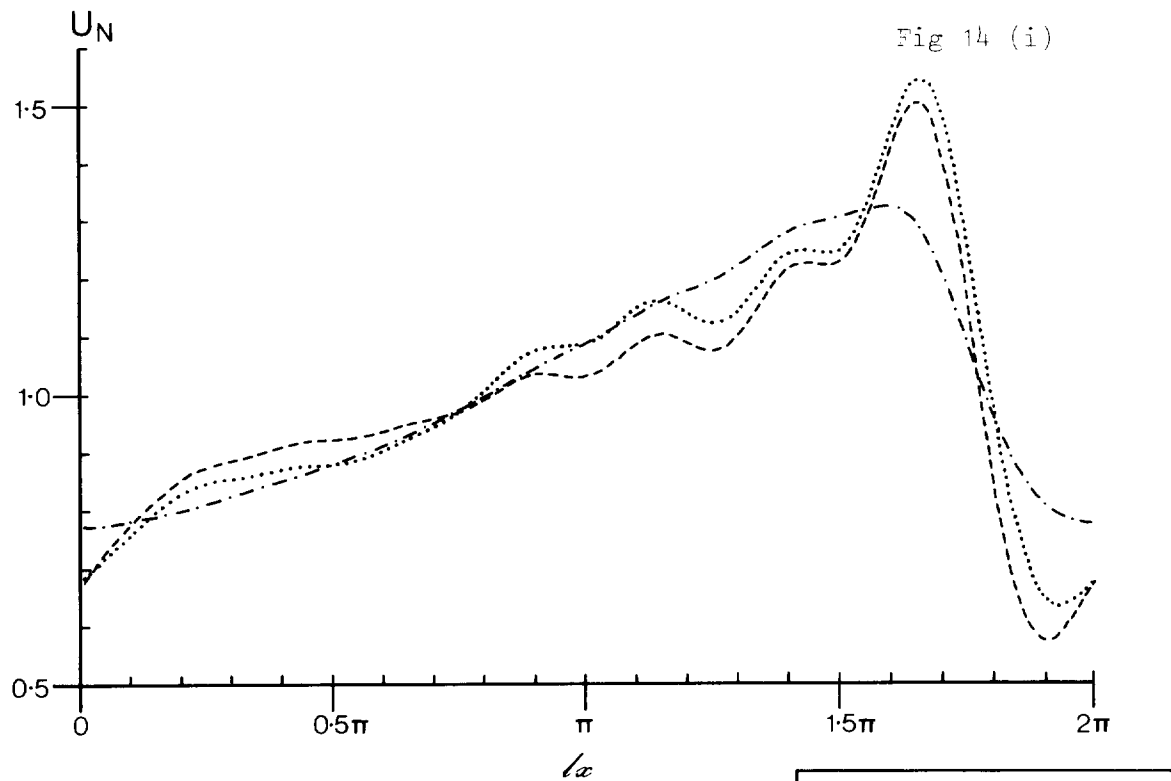


SANDWAVE N<sup>o</sup> 1

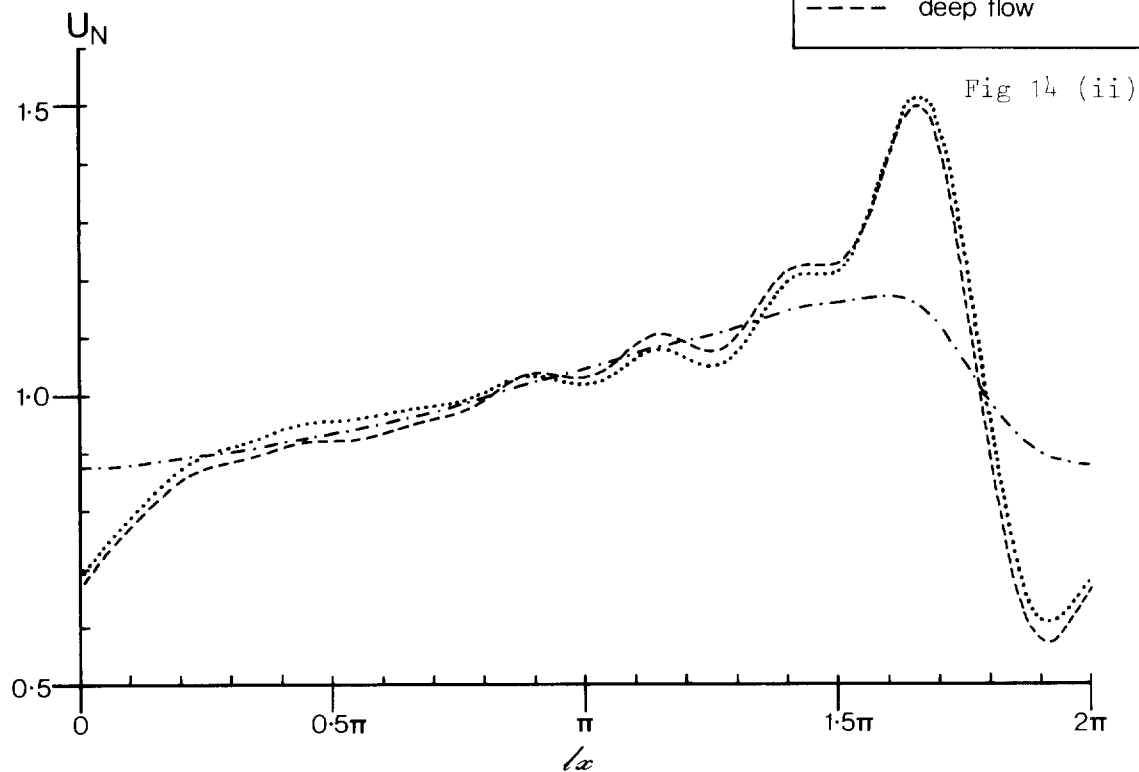
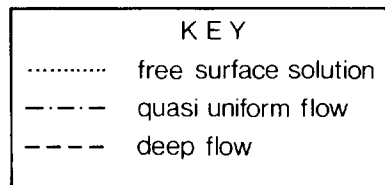
$T = 12 \text{ sec}$

Fig 13 A comparison of peak normalized horizontal velocities at the bed surface for Sandwave # 1. Normalization is with respect to the velocity amplitude on an equivalent flat bed. Results from the present method (Eq (53)) are labelled 'free surface solution', results for an assumed deep flow are labelled 'deep flow', and results based upon the local water depth are labelled 'quasi uniform flow'. Fig 13 (i) is for wave period  $T = 8 \text{ sec}$ , and 13 (ii) for  $T = 12 \text{ sec}$ .





SANDWAVE N<sup>o</sup> 2       $T=8\text{sec}$



SANDWAVE N<sup>o</sup> 2       $T=12\text{sec}$

Fig 14 Results equivalent to those in Fig 13 for Sandwave#2.  
 Fig 14 (i) is for wave period  $T = 8$  sec and Fig 14 (ii)  
 for  $T = 12$  sec.

Although sandwaves are 'non-equilibrium' profiles, in the sense of not being wave formed, possibilities of resonant interactions between the water surface and the bed arise if  $m\ell = \pm 2k$ , for any integral value of  $m \leq N$ . We noted earlier that the solution is not uniformly valid in the ratio of  $\ell$  to  $k$  at least for large bed wavelengths, and as a consequence any important harmonic constituent of the overall sandwave shape may interact with the surface waves to reflect incident wave energy. In making predictions of the amount of wave reflection, some doubt may arise in practice as to the reliability of the Fourier representation of the sandwave profile, particularly if an insufficient number of points has been adopted to define the location of the bed. Also, the qualifications made in the previous section concerning the assumed infinite horizontal extent of the bedforms apply here. However, if a matching of the surface wavelength and any constituent of the sandwave length occurs according to the above rule, it might be expected that a significant proportion of the incident wave energy in a narrow frequency band corresponding to the resonant surface wavenumber would be reflected. For Sandwave #1, the resonances in the range of wave period (6,15) seconds occur at 11.7, 9.7, 8.4, 7.5, 6.8 and 6.3 sec corresponding to  $m = 4$  to 9 respectively ( $k\ell \leq 1.6$  in all cases). For Sandwave #2, they occur at 9.6, 7.4 and 6.4 sec, corresponding to  $m = 2$  to 4 respectively ( $k\ell \leq 2.7$ ). In Fig 13 (ii) the effect of the nearby resonance with the fourth harmonic of the bed profile is clearly apparent. Evidently, therefore, the results in any particular run need to be interpreted carefully, since they may be unrealistic on account of the assumption of an infinite number of bottom undulations. Furthermore, in shallow water, the possibility of the surface waves breaking above the sandwave crests should not be ignored nor, in a real situation in which the bedforms are actually three dimensional, should the effects of refraction be discounted. In short, the mechanism of selective wave reflection described above may be just one of several mechanisms leading to a reduction in the amount of wave energy transmitted across a region of seabed topography.

## §7. DISCUSSION

The most striking features of the solutions presented earlier are the conditions of resonance between the rippled bed and the surface waves. The strongest of the resonances occurs when  $\ell = 2k$ , and some comments have been made about the behaviour of the solution close to such points. That discussion is now extended to cases in which the bed is erodible. In particular, the question

posed is whether an initially small periodic disturbance of the bed is likely to grow or be destroyed as a result of resonant interaction.

Close to the resonance point  $\ell = 2k$ , it was shown earlier that the solution  $\phi_2^{(1)}$  corresponds to waves progressing in the negative  $x$ -direction and, therefore, the superimposition of  $\phi_1$  and  $\phi_2^{(1)}$  produces a partially progressing and partially standing wave structure. If the combined wave pattern is sufficient to move sediment at the bed surface, there are two possible reasons why the standing wave component might be associated with the formation of bed features.

Firstly, on general intuitive grounds, it can be argued that beneath the antinodes of a standing wave, where the lowest velocities are found close to the bed surface, sedimentation rather than erosion might be expected. Conversely, beneath the nodes, where there is greatest horizontal activity near the bed, erosion rather than sedimentation might be expected. These statements hang entirely on the general tendency for accumulation of material to occur in relatively undisturbed parts of the bed, and for erosion to occur in relatively disturbed parts, where sediment threshold velocities will, if anywhere, be exceeded. In the context of the earlier analysis, a difficulty arises in applying this common sense argument since, if  $\ell \approx 2k$ , the weakest horizontal velocities occur above the ripple crests, suggesting the likely growth of existing bed features, but if  $\ell \approx 2k$  the strongest bed velocities occur at the crests, suggesting their possible erosion. Evidently, the conditions for growth and destruction of initially small bed features are rather finely balanced near the resonance point and it follows that a small change in surface wave length, in relation to the rather less readily changed bed wavelength, might have dramatic consequences in terms of the bed features if that change involves a jump across the singularity ( $\ell < 2k$  to  $\ell > 2k$ , or vice versa).

Secondly, it can be argued that the effect of bottom friction under a standing wave is to produce a pattern of residual velocities which, when superimposed on the first order motion, might tend overall to drag sand grains towards preferred points on the bed surface, and away from other points. For both laminar and turbulent boundary layers, this residual motion occurs in cells of length  $(\pi/2k)$ , the positioning of which is tied to the nodes and antinodes of the standing wave. The residual flow varies in magnitude depending upon position within each cell and, furthermore, for both laminar and turbulent cases and assuming a smooth flat bed, the direction of the residual velocity changes at a certain height above the bed. This height is the upper bound of an 'inner layer' adjacent to the bed, and

for a laminar boundary layer has the value  $0.93 \delta_*$  (Longuet-Higgins (1953)), where  $\delta_*$  is the Stokes layer thickness ( $= \sqrt{2\nu/\omega}$  and  $\nu$  is the kinematic viscosity). In the turbulent case, the inner layer thickness is considerably larger than this (Johns (1970)). The water particle residual motion in the inner layer is towards the positions of greatest horizontal first order motion, and away from the positions of where the motion is purely vertical. In the 'outer layer' above this, the residual motion is in the opposite direction. For the laminar case, Johns has suggested that any material in motion near the bed will probably be present in the outer layer (by virtue of the very small inner layer thickness) and that the drift velocity in this layer will probably give an indication of the direction and magnitude of sediment transport. This direction is towards the positions of lowest first order motion and, in the present analysis, this implies movement of material towards the crests, and therefore bedform growth, for  $\ell \approx 2k$ . However, in the physically more interesting case of a turbulent boundary layer, the greater thickness of the inner layer suggests that sediment motion may be confined to this layer within which the residual motion of water particles, and hence sediment, is towards the positions of greatest horizontal first-order activity. In the present analysis, this is towards the ripple crests, implying bedform growth, for  $\ell \approx 2k$ .

The laboratory experiments of Nielsen (1979, § 6) provide a convincing picture of dune growth beneath standing waves. Sediment accumulation is shown to occur at antinodes of surface elevation, and Nielsen's interpretation of his observations rests on the residual transport pattern described above for a laminar boundary layer. In the context of the present analysis, Nielsen's observations tie in with bedform growth of the type characterized above by  $\ell \approx 2k$ , both on the basis of the earlier intuitive argument and on the basis of the mass transport argument. For the very fine sand used by Nielsen (grain diameter 0.08 mm) an upwardly convected cloud of grains was observed above the evolving dune crests. This is consistent with the residual convection cell which is expected to occupy the entire flow depth above the 'outer' boundary layer. Dune formation in a turbulent boundary layer is less readily explained than in a laminar boundary layer, since the intuitive and mass-transport mechanisms are now in opposition. It is possible, therefore, that dunes having  $\ell \approx 2k$  are less inclined to form than those having  $\ell \approx 2k$ .

In conclusion, the overall picture presented by the two lines of argument above contains contradictions which may not be fully resolved without carefully controlled laboratory experiments to test the general ideas presented here for

discussion. The possibility of finding dunes having  $\ell \approx 2k$  on the seabed is a little remote, at least in locations with a fairly high tidal range, since wavenumber  $k$  changes considerably during a tidal cycle for waves of fixed frequency, and the bedforms would have insufficient time to adjust their wavelength accordingly. In this connection, it should be realized also that resonances of the type  $\ell = 2k$  are a consequence of the bed features being assumed of indefinite horizontal extent. Although conditions of the type  $\ell = 2k$  still take on a physical importance if the ripples occupy only a finite region of the bed, the singularities found in the present solution  $\phi_2^{(2)}$  do not arise. Consequently, while the various resonances mentioned earlier might look somewhat damaging to the usefulness of the solution, this is probably not too worrying in practice.

No attempt has been made in the present report to give an explanation for the possible development of any bed features other than dunes formed by the resonant interaction mechanism. Sand ripples are commonly formed in deep flow by a process of scour and deposition, associated with vortex formation above the lee slopes of ripples in each wave half cycle. The present theory, which does not account for flow separation, unfortunately provides little information about this case of obvious practical importance. Flow separation appears to occur in cases in which the near bed orbital diameter exceeds the equilibrium ripple wavelength (Sleath (1975)). (No cases in which flow separation is likely to have occurred on this criterion have been presented as examples earlier.) So the results given in this report should be viewed as being applicable only to rigid wavy beds, to relict (or fossil) rippled beds of sand or to equilibrium 'rolling grain' rippled beds (Sleath (1976)), above which the flow is nonseparating.

## § 8. CONCLUSIONS

The theory presented enables the velocity field to be calculated beneath surface waves progressing over a rippled bed structure. The flow has been assumed nonseparating at the seabed, and a variety of other limitations on the application of the small amplitude theory have been stated. These limitations do not prevent use of the theory over wide and practically important ranges of both surface wave and seabed parameters however.

The theory predicts a substantial enhancement of the orbital velocity amplitude above each crest on the bed surface, and a consequent reduction above each trough, compared with the velocity amplitude on an equivalent flat bed. To the order of approximation adopted, the theory also predicts a steepening of the

surface wave crests, and a lengthening and flattening of the troughs.

If  $\bar{\lambda}/h \approx 2$ , where  $\bar{\lambda}$  is the ripple wavelength and  $h$  is the mean water depth, the influence of the free surface is negligible and 'deep flow' results can be used to assess variations in orbital velocity due to the topography. Equation (3) can be used to calculate the surface velocity at the ripple crest for a purely sinusoidal bed, and Eq (54) can be used for a rather more general ripple profile. These equations indicate how the steepnesses of the various harmonic constituents present in a given ripple profile strongly influence the final result. If  $\bar{\lambda}/h \approx 2$  the free water surface introduces variations from the 'deep flow' velocity at the bed, which may be substantial if  $\bar{\lambda}/h \approx 7$ . It follows that the use of deep flow results in this regime will generally lead to underestimates of velocity amplitude above the dune crests, and the full theory presented in this report should be used in such cases. Contrasting practical examples of results for deep and shallow flows, in particular results for the flows above natural ripple shapes and above natural sandwaves on the seabed, have been presented. The variations in the surface velocities from crest to trough in both cases have important implications for sediment transport. Since they deal with two rather extreme situations, these examples serve as a convincing illustration of the usefulness of the theory.

In general terms, it is found that the interaction of progressing incident surface waves and sinusoidal undulations on the bed, gives rise to two new waves whose wavenumbers are the sum and difference of those of the incident wave ( $k$ ) and the bed ( $\ell$ ). If the incident wavenumber is the smaller of the two ( $k < \ell$ ) the difference wave is back reflected. Furthermore, if the bed wavenumber is twice the incident wavenumber ( $\ell = 2k$ ) the theory predicts an infinite, resonant interaction between the bed and the free surface. In principle, such an interaction may occur between surface waves and any harmonic constituent of a given ripple profile, but the dominant interaction is likely to be with the fundamental constituent. Although the theory breaks down where the solution is singular (at  $\ell = 2k$ ), a strong reflection of incident wave energy by the bedforms is predicted in the neighbourhood of this singularity. The amount of reflected wave energy is negligible for all other ratios  $\ell:k$ . The general physical significance of this result is that reflection of incident wave energy may tend to gradually reduce the wave height of an incoming swell wave, and thereby reduce its potential for erosion at the seabed. Although the present theory is unsuitable for comparing incident and transmitted wave energies, since the bedforms are assumed to be of infinite horizontal extent, it does cast some light on the way

in which wave reflection occurs. The theory is of interest and possible importance also in suggesting mechanisms for the formation of bar structures on an erodible seabed. The positioning of such bars is likely to be linked to the positions of the antinodes in surface elevation of the standing wave component arising from the wave reflection mechanism.

## § 1. INTRODUCTION

If surface water waves travel into a region of undulating seabed topography, it is of considerable interest to know how much of the incident wave energy is reflected by the topography and how much is transmitted across it. This scattering of wave energy is a matter of practical importance both in respect of coastal protection and also of possible dune growth if the bed is erodible. The problem tackled here is depicted in Fig 1. The bed surface is prescribed about its mean level  $Y = -h$  as

$$Y(x) = \begin{cases} 0 \\ Y_b(x) \\ 0 \end{cases} \quad \text{in} \quad \begin{array}{l} -\infty < x < L_1 \\ L_1 < x < L_2 \\ L_2 < x < \infty \end{array} \quad (1)$$

and the departure of the free water surface from its mean level is given by

$\eta(x,t)$ . The theoretical basis is that which was developed in Part I; in particular, the interaction of a prescribed first order velocity potential with the bedforms is given by Eqs (18b)-(21b) of Part I. In the examples considered later, we shall be concerned particularly with wave reflection by a patch of ripples and by an isolated bar on the seabed. However, the theory is presented in § 2. and 3. in a general way, such that the basic results can be used with any prescribed bottom topography.

The general aim of Part II is to develop a method to calculate the size of the reflected wave in cases in which the fluid domain is rather complicated, as in Fig 1. Such methods already exist for cases in which it is known how to map the fluid domain into some simpler domain - for example, if the fluid domain can be mapped into a strip, the method of Kreisel (1949) may be used to place bounds on the size of the reflected wave. In practice, however, the mapping is generally not known (even though it almost certainly exists according to the Riemann mapping theorem). This is so in the cases of interest here involving seabed topography and it is useful, therefore, to have available an alternative method, albeit an approximate one, to calculate the sizes of the reflected and transmitted waves.

We assumed in Part I that the bedforms were of infinite horizontal extent and we did not pay attention to any conditions to be imposed at infinity to ensure the uniqueness of the steady state perturbation solution obtained. We merely satisfied boundedness conditions at infinity which ensured that the solution had realistic physical characteristics. Since in Part II we consider a region of topography



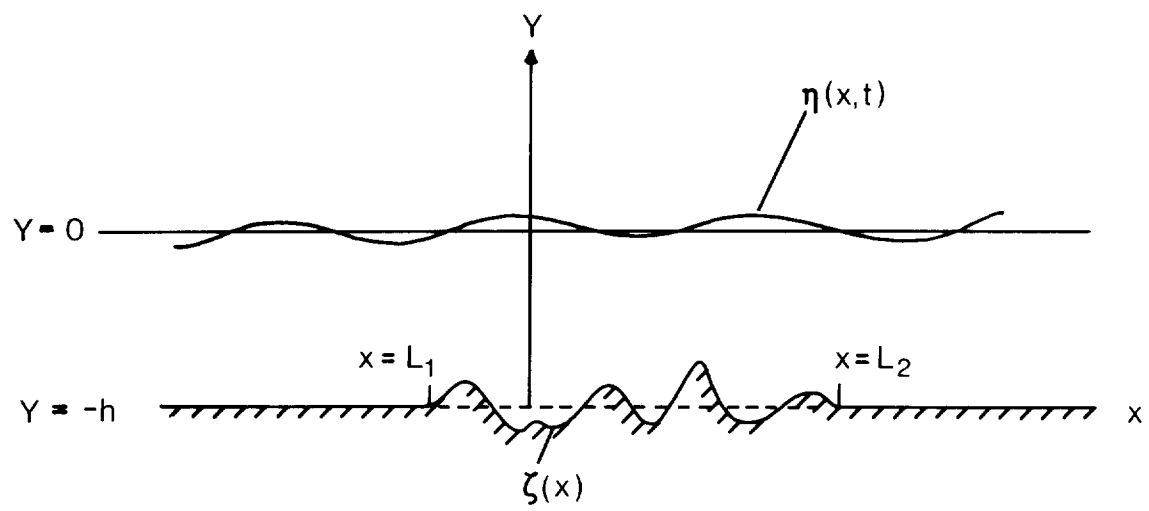


Fig 1 Definition sketch

which is of finite extent, we must now satisfy the radiation, or Sommerfeld, condition; in other words, we must ensure that the wave at infinity in the perturbation solution behaves like an outgoing wave. Stoker (1953) has argued that, if one adopts an initial value formulation in problems of this type, it should be sufficient to impose only boundedness conditions at infinity to ensure uniqueness of solution. If, on the other hand, one tackles the steady state problem directly, it may be unclear what conditions should be imposed at infinity - in fact, in § 2. we use the artifice of linear friction both to make the solution of the steady state problem determinate and to ensure that the radiation condition is satisfied.

In § 2. we discuss the steady state approach and adopt a modified form of Eq (20b) including linear friction to ensure that the solution obtained is determinate. In § 3. we describe the initial value formulation in which we follow closely the procedure of Stoker (1953). Both approaches involve a Fourier transformation of the governing equation and boundary conditions in respect of the horizontal space variable, enabling solutions to be obtained for the transform of the perturbation potential. The integrals resulting from the inversion of the respective solutions are handled by contour integration procedures. Although the two approaches yield the same final result, they in no way overlap one another, and both are included here since one is no more easy than the other. In § 4. first estimates for the amplitude of the reflected and transmitted waves are obtained in the special cases of progressive waves incident upon a patch of dunes and upon an isolated hump, and in § 5. these estimates are improved upon by an approximate iterative method. As in Part I, we are concerned only with two dimensional irrotational free-surface flow above an impermeable bed, and thus we take no account in this study of the effects of wave refraction, bottom friction or percolation.

## §2. THE STEADY STATE FORMULATION AND SOLUTION

The governing equation and boundary conditions, correct to second order, are given by Eqs (18b)-(21b) of Part I which, with slight changes of notation, we write here as follows:<sup>1</sup>

$$\nabla^2 \phi = 0 \quad \text{in} \quad -L < Y < 0 \quad (2)$$

$$\zeta_t + \phi_Y = 0 \quad \text{on} \quad Y = 0 \quad (\text{kinematic condition}) \quad (3)$$

$$\eta \zeta - \phi_t = 0 \quad \text{on} \quad Y = 0 \quad (\text{pressure condition}) \quad (4)$$

$$-\phi_x \zeta_x + \phi_Y + \zeta \phi_{YY} = 0 \quad \text{on} \quad Y = -L \quad (\text{kinematic condition}) \quad (5)$$

in which the subscripts indicate differentiation and the origin of the vertical axis has been taken in the free water surface. The prescribed first order velocity potential is denoted by  $\phi(x, Y, t)$ , the perturbation potential by  $\phi(x, Y, t)$ , the bed surface by  $\zeta(x)$  and the perturbed surface elevation by  $\eta(x, t)$ .

From Eqs (1) and (5), the interaction of the first order motion  $\phi$  with the bed  $\zeta$  can be seen to involve a velocity perturbation at  $Y = -L$  only in  $L_1 < x < L_2$ .

The effects of this disturbance on the fluid as a whole are described by Eqs (2)-(4). We shall be concerned here with the asymptotic behaviour of  $\phi$  as  $|x| \rightarrow \infty$ ; by virtue of the radiation condition, we require a solution which corresponds to an outgoing wave in this limit.

If we prescribe  $\phi$  as a periodic function of time and seek a steady state solution of Eqs (2)-(5), we find, for reasons which will become apparent later, that the solution is indeterminate. We therefore employ the familiar device, described by Lamb (1932, Art 242) and attributed to Lord Rayleigh, of introducing into the problem a small amount of friction proportional to the relative velocity. Although the coefficient of friction is set ultimately to zero, the device ensures the convergence of the integrals arising in the analysis and the uniqueness of the solution of the problem. Friction is introduced in Eq (4) in such a way that it does not interfere with the irrotational nature of the motion, but it should be noted

---

<sup>1</sup> The equation numbers, and figure numbers, in Part II both start at one. This should cause no confusion however, since no further cross-referencing is made between Parts I and II. Note also that, for convenience, the origin on the vertical axis in Part II has been redefined ( $Y = y - L$ ), and that the second order perturbation potential is written  $\phi$  in order to distinguish it from  $\phi_2^{(u)}$  in Part I.

that the "law of friction" is essentially a mathematical device which does not accurately represent the way in which dissipation occurs in the flow in reality. Lamb has used the approach in the problem of a surface disturbance to a steady stream, and an early application in wave theory is Havelock's (1917) study of surface waves caused by a submerged obstacle.

A slightly different approach to the steady state problem, but one which has the same mathematical consequences, is described by Lighthill (1978, Section 3.9) and Whitham (1974, Section 13.9), with particular reference to disturbances on the surface of a steady stream. If used in the present context, this alternative approach would involve the bed features "growing up slowly" to their present height from an initially flat surface; no attenuation of wave energy occurs in the approach by the introduction of dissipation into the system. We note, finally, that Adams and Buchwald (1969) have solved a steady state problem for continental shelf waves on essentially the same basis, though they merely add a small imaginary part to the real wave frequency, and show that this has the desired mathematical effect.

If we combine (3) and (4) and then introduce the linear friction term, the surface boundary condition becomes

$$\eta \varphi_r + \varphi_{tt} + \mu \varphi_t = 0 \quad \text{on} \quad \gamma = 0 \quad (6)$$

in which  $\mu (> 0)$  is the coefficient of friction. For convenience, we shall rewrite Eq (5) in a form compatible with Eq (1), so that the bottom boundary condition becomes

$$\varphi_r = \begin{cases} 0 & -\infty < x < L_1 \\ -V(x,t) & L_1 < x < L_2 \\ 0 & L_2 < x < \infty \end{cases} \quad \text{on} \quad \gamma = -h \quad (7)$$

in which  $V(x,t)$  is the vertical velocity at the bed surface given by

$$V(x,t) = -\Phi_x(x, -h, t) \cdot \zeta_x + \Phi_{rr}(x, -h, t) \cdot \zeta$$

We now Fourier transform the governing equation (1) and the boundary conditions (6) and (7) in respect of the horizontal space variable  $x$ , according to the definition

$$\hat{\varphi}(\xi, \gamma, t) = \frac{1}{\sqrt{2\pi}} \int_{-\infty}^{\infty} \varphi(x, \gamma, t) e^{i\xi x} dx$$

which has the inverse

$$\varphi(x, y, t) = \frac{1}{\sqrt{2\pi}} \int_{-\infty}^{\infty} \hat{\varphi}(\xi, y, t) e^{-i\xi x} d\xi$$

Thus Eq (2) becomes

$$\hat{\varphi}_{yy} - \xi^2 \hat{\varphi} = 0 \quad \text{in} \quad -L < y < 0 \quad (8)$$

Eq (6) becomes

$$g \hat{\varphi}_y + \hat{\varphi}_{tt} + \mu \hat{\varphi}_t = 0 \quad \text{on} \quad y = 0 \quad (9)$$

and Eq (7) becomes

$$\begin{aligned} \hat{\varphi}_y &= \frac{1}{\sqrt{2\pi}} \int_{-\infty}^{\infty} \varphi_y(x, -L, t) e^{i\xi x} dx \\ &= \frac{-1}{\sqrt{2\pi}} \int_{L_1}^{L_2} V(x, t) e^{i\xi x} dx \\ &= \frac{1}{\sqrt{2\pi}} \Lambda(\xi, t) \end{aligned} \quad , \text{ say.} \quad (10)$$

The solution of Eq (8) is

$$\hat{\varphi}(\xi, y, t) = \tilde{A}(\xi, t) \cosh(\xi y) + \tilde{B}(\xi, t) \sinh(\xi y) \quad (11)$$

and this satisfies the boundary conditions if

$$g \xi \tilde{B}(\xi, t) + \tilde{A}_{tt}(\xi, t) + \mu \tilde{A}_t(\xi, t) = 0 \quad (12)$$

and

$$-\xi \tilde{A}(\xi, t) \sinh(\xi L) + \xi \tilde{B}(\xi, t) \cosh(\xi L) = \frac{1}{\sqrt{2\pi}} \Lambda(\xi, t) \quad (13)$$

We now make the solution specific to the case of waves having frequency  $\sigma$  by taking <sup>1</sup>

$$\tilde{A}(\xi, t) = A_1(\xi) \cos(\sigma t) + A_2(\xi) \sin(\sigma t)$$

<sup>1</sup> These forms are consistent with the specification of  $V(x, t)$  as a real function of space and time, with the potential  $\varphi$  real also. The same final result for the steady state problem is achieved, however, if the complex forms  $\tilde{A}(\xi, t) = A(\xi) e^{i\sigma t}$  etc, are adopted, though the details of the procedure are different in this case.

$$\tilde{B}(\xi, t) = B_1(\xi) \cos(\sigma t) + B_2(\xi) \sin(\sigma t) \quad (14)$$

and

$$\mathcal{L}(\xi, t) = \mathcal{L}_1(\xi) \cos(\sigma t) + \mathcal{L}_2(\xi) \sin(\sigma t)$$

Substituting the expressions for  $\tilde{A}(\xi, t)$  and  $\tilde{B}(\xi, t)$  into Eq (11), and taking the inverse Fourier transform, the final solution for the velocity potential can be written in the form

$$\varphi(x, y, t) = \int_{-\infty}^{\infty} \frac{1}{\sqrt{2\pi}} \left[ \{A_1 \cosh(\xi y) + B_1 \sinh(\xi y)\} \cos(\sigma t) + \{A_2 \cosh(\xi y) + B_2 \sinh(\xi y)\} \sin(\sigma t) \right] e^{-i\xi x} d\xi \quad (15)$$

$$= \int_{-\infty}^{\infty} \mathcal{F}(\xi) d\xi \quad , \text{ say } ,$$

in which, from (12) and (13),

$$A_1 = \frac{\tilde{a} \mathcal{L}_1 + \tilde{b} \mathcal{L}_2}{\sqrt{2\pi} (\tilde{a}^2 + \tilde{b}^2)}$$

$$A_2 = \frac{\tilde{a} \mathcal{L}_2 - \tilde{b} \mathcal{L}_1}{\sqrt{2\pi} (\tilde{a}^2 + \tilde{b}^2)}$$

$$B_1 = \frac{\sigma^2 A_1 - \mu \sigma A_2}{g \xi}$$

$$B_2 = \frac{\sigma^2 A_2 + \mu \sigma A_1}{g \xi}$$

where  $\tilde{a}(\xi) = \frac{\sigma^2}{g} \cosh(\xi h) - \xi \sinh(\xi h)$

and  $\tilde{b}(\xi) = \frac{\mu \sigma}{g} \cosh(\xi h)$

2.1 The evaluation of  $\varphi(x, y, t)$  by contour integration

We obtain our final result from (15) by contour integration using the residue theorem. Firstly, we replace the range of integration  $-\infty < \xi < \infty$  in (15) by integration around a closed contour consisting of the portion  $(-r_0, r_0)$  of the  $\xi$ -axis and a semi-circle centred at the origin and having radius  $r_0$ .

In the limit  $\tau_0 \rightarrow \infty$ , the required range of integration is recovered, since the semi-circle makes a zero contribution. The semi-circle is chosen in the upper half plane or lower half plane such that the radiation condition is satisfied. In particular, we find that the linear friction term has the effect of placing the singularities of the integrand of (15) in the upper or lower half plane, and the correct choice of contour ensures outgoing waves from the undulating part of the bed. For  $\mu > 0$  the waves are damped as  $|x|$  increases, but as  $\mu \rightarrow 0$  an oscillatory solution is obtained as  $|x| \rightarrow \infty$ . In fact, we shall be concerned here only with the solutions in the two asymptotic limits  $x \rightarrow \pm \infty$ .

It is necessary initially to identify the positions of the singularities in (15) which arise as a result of the term  $(\tilde{a}^2 + \tilde{b}^2)$  in the denominators of  $A_1, A_2, B_1$  and  $B_2$ . These positions must be established in terms of a complex dummy variable of integration, and so we take  $\xi$  to be the real part of a new variable  $\lambda = \xi + i\chi$ .

The singularities ( $\lambda = \lambda_p$ ) corresponding to  $(\tilde{a}^2 + \tilde{b}^2) = 0$  must lie near the positions ( $\lambda = \lambda_0$ ) which satisfy  $\tilde{a}^2 = 0$ , since  $\tilde{b} \sim \mu$  and  $\mu$  is small. These positions are given by

$$\lambda_0 \tanh(\lambda_0 l) = \frac{\sigma^2}{g} \quad (16)$$

and, if we introduce at this stage the dispersion relation for the surface waves prescribed in the first order solution  $\Phi$ , namely

$$k \tanh(kh) = \frac{\sigma^2}{g} \quad (17)$$

where  $k$  is the wavenumber, we note that (16) is satisfied by  $\lambda_0 = \xi_0 = \pm k$  on the real axis of  $\lambda$ . In addition, we note an infinite number of poles on the imaginary axis of  $\lambda$  which are given by  $\lambda_0 = i\chi_0$ , where  $\chi_0$  satisfies

$$-\chi_0 \tanh(\chi_0 l) = \frac{\sigma^2}{g} \quad (18)$$

If we now relate  $\lambda_p$  to  $\lambda_0$  by

$$\lambda_p = \lambda_0 + \tilde{a}\mu$$

we can determine  $\tilde{a}$  by equating terms  $O(\mu)$  in the equation  $\tilde{a} = \pm i\tilde{b}$ , or

$$(\sigma^2 \pm i\mu\sigma) \cosh(\lambda_p h) - g\lambda_p \sinh(\lambda_p h) = 0$$

It follows that

$$\tilde{a} = \pm \frac{ig\lambda_0}{\sigma(\sigma^2 h - g - g^2 \lambda_0^2 h / \sigma^2)}$$

and so the positions of the poles of the integrand in (15) are

$$\lambda_p = \lambda_0 \left\{ 1 \pm i g \mu / \sigma (\sigma^2 k - g - g^2 \lambda_0^2 k / \sigma^2) \right\}$$

This implies that each of the original poles  $\lambda_0$  is replaced by two poles upon the introduction of the linear friction term. In particular, each of the poles on the real axis of  $\lambda$  is replaced by two poles, one of which is displaced slightly into the upper half plane, the other into the lower half plane. So the new poles do not lie on the path of integration  $(-\infty, \infty)$ , which is the desired effect on the friction term. Similarly, each of the poles  $\lambda_0$  on the imaginary axis is replaced by two poles associated with small positive and negative real displacements.

To evaluate (15) by contour integration, we must choose a contour in the  $\lambda$ -plane such that the solution has the correct physical behaviour in the asymptotic limits  $x \rightarrow \pm\infty$ . In the first place, we require that any transients in  $x$  decay in these limits and our choice of contour is therefore governed by the term  $e^{-i\xi x}$  in (15). In the complex  $\lambda$ -plane this term becomes  $e^{-i\lambda x}$  and so, if  $\lambda_p = \xi_p + i\chi_p$ , the transient behaviour is given by  $e^{\chi_p x}$ . For a pole in the upper half plane ( $\chi_p > 0$ ), this implies an increasing behaviour as  $x \rightarrow +\infty$  and a decaying behaviour as  $x \rightarrow -\infty$ . Conversely, for a pole in the lower half plane ( $\chi_p < 0$ ),  $e^{\chi_p x}$  implies a decaying behaviour as  $x \rightarrow +\infty$  and an increasing behaviour as  $x \rightarrow -\infty$ . It follows that, for the calculation of the asymptotic value of the integral as  $x \rightarrow +\infty$ , the selected contour must contain only those poles which lie in the lower half plane if the solution is to converge; and, for  $x \rightarrow -\infty$ , the contour must contain only those poles in the upper half plane. Although initially all the poles in the problem give rise to transients in the solution on account of the linear friction in the system, the two poles close to  $\xi_0 = \pm k$  are the only ones to make non-zero oscillatory contributions in the limits  $x \rightarrow \pm\infty$  as  $\mu \rightarrow 0$ , and it will be shown that these contributions correspond to outgoing waves as required.

We shall consider the contours  $C_1$  and  $C_2$  shown in Fig 2. The asymptotic limit  $x \rightarrow -\infty$  is handled by taking  $C_1$ , and the limit  $x \rightarrow +\infty$  by  $C_2$ . Ultimately, the radius of the semi-circular portion of each contour is assumed to tend to infinity, so that the range of integration in (15), consisting of the real axis, forms a part of each contour. The residue theorem states that

$$\oint_C f(\lambda) d\lambda = 2\pi i \times \left\{ \text{sum of the residues of } f(\lambda) \text{ in } C \right\}$$



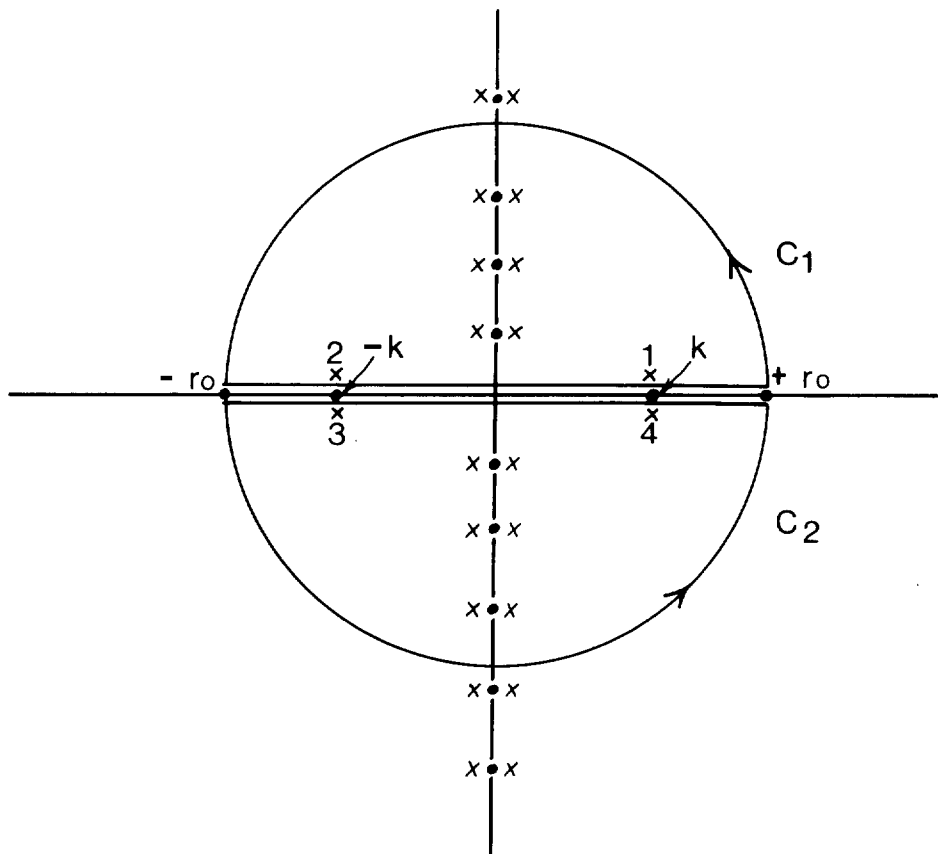


Fig 2 Sketch of contours  $C_1$  and  $C_2$  in the  $\lambda$ -plane

and in order to calculate the residues at the simple poles in the present problem we note first that

$$\lim_{\lambda \rightarrow \lambda_p} \frac{\tilde{a}(\lambda)(\lambda - \lambda_p)}{\tilde{a}^2(\lambda) + \tilde{b}^2(\lambda)} = - \frac{\cosh(\lambda_p h)}{2\lambda_p h + \sinh(2\lambda_p h)} \\ = - R_* \Big|_{\lambda_p}, \text{ say.}$$

If we write

$$A_1 = \frac{\tilde{a} A_{1*}}{\sqrt{2\pi}(\tilde{a}^2 + \tilde{b}^2)}, \quad B_1 = \frac{\tilde{a} B_{1*}}{\sqrt{2\pi}(\tilde{a}^2 + \tilde{b}^2)}, \quad A_2 = \frac{\tilde{a} A_{2*}}{\sqrt{2\pi}(\tilde{a}^2 + \tilde{b}^2)} \text{ and } B_2 = \frac{\tilde{a} B_{2*}}{\sqrt{2\pi}(\tilde{a}^2 + \tilde{b}^2)}$$

then the residue of the integrand of (15) at  $\lambda_p$  may be expressed

$$R_p = -\frac{1}{2\pi} R_* \Big|_{\lambda_p} \left[ \{A_{1*} \cosh(\lambda\gamma) + B_{1*} \sinh(\lambda\gamma)\} \Big|_{\lambda_p} \cos(\sigma t) + \{A_{2*} \cosh(\lambda\gamma) + B_{2*} \sinh(\lambda\gamma)\} \Big|_{\lambda_p} \sin(\sigma t) \right] e^{-i\lambda_p x} \quad (19)$$

### 2.1.1 Solution in the asymptotic limit $x \rightarrow -\infty$

We are concerned here with contour  $C_1$  in Fig 2 including poles 1 and 2 and also, as  $\mu \rightarrow \infty$ , all the poles closely adjacent to the positive imaginary axis of  $\lambda$ . If we consider pole 1 at  $\lambda_{p1} = k + i\mu k_0$  ( $k_0 > 0$ ), say, the residue is given by Eq (19) with  $\lambda_p = \lambda_{p1}$ . It may be noted that since  $e^{-i\lambda_p x} = e^{-ikx} e^{\mu k_0 x}$ , this contribution to the final result contains a decaying transient for  $x < 0$  since  $\mu > 0$ . The same is true of pole 2 at  $\lambda_{p2} = -k + i\mu k_0$ . Clearly, in the limit  $\mu \rightarrow 0$ ,  $e^{-i\lambda_p x} \sim e^{-ikx}$  in both cases, giving a purely oscillatory behaviour as required.

For pole 1, the residue is given by

$$R_1 = \frac{1}{2\pi} \left\{ \frac{-\cosh(\lambda_{p1} h)}{2\lambda_{p1} h + \sinh(2\lambda_{p1} h)} \right\} \left[ \left\{ \left( L_1 + \frac{\tilde{b}}{\tilde{a}} L_2 \right) \cosh(\lambda_{p1} \gamma) + \frac{1}{g\lambda_{p1}} \left( (\sigma^2 + \mu\sigma \frac{\tilde{b}}{\tilde{a}}) L_1 + (\sigma^2 \frac{\tilde{b}}{\tilde{a}} - \mu\sigma) L_2 \right) \sinh(\lambda_{p1} \gamma) \right\} \cos(\sigma t) \right. \\ \left. + \left\{ \left( L_2 - \frac{\tilde{b}}{\tilde{a}} L_1 \right) \cosh(\lambda_{p1} \gamma) + \frac{1}{g\lambda_{p1}} \left( (\mu\sigma - \sigma^2 \frac{\tilde{b}}{\tilde{a}}) L_1 + (\sigma^2 + \mu\sigma \frac{\tilde{b}}{\tilde{a}}) L_2 \right) \sinh(\lambda_{p1} \gamma) \right\} \sin(\sigma t) \right] e^{-i\lambda_{p1} x}$$

and since  $\lim_{\mu \rightarrow 0} (\tilde{b}/\tilde{a})_{\lambda_{p1}} = i$ , this reduces in the limit  $\mu \rightarrow 0$  to

$$R_1 \Big|_{\mu=0} = -\frac{1}{2\pi} \left\{ \frac{\cosh(kh)}{2kh + \sinh(2kh)} \right\} e^{-ikx} \left[ \left\{ (\mathcal{L}_1 + i\mathcal{L}_2) \Big|_k \cosh(kY) + \tanh(kh) (\mathcal{L}_1 + i\mathcal{L}_2) \Big|_k \sinh(kY) \right\} \cos(\omega t) \right. \\ \left. + \left\{ (\mathcal{L}_2 - i\mathcal{L}_1) \Big|_k \cosh(kY) + \tanh(kh) (\mathcal{L}_2 - i\mathcal{L}_1) \Big|_k \sinh(kY) \right\} \sin(\omega t) \right] \\ = -\frac{1}{2\pi} \left\{ \frac{\cosh k(Y+h)}{2kh + \sinh(2kh)} \right\} e^{-i(kx+\omega t)} \left[ \mathcal{L}_1 + i\mathcal{L}_2 \right]_k \quad (20)$$

For pole 2,  $\lim_{\mu \rightarrow 0} (\tilde{b}/\tilde{a})_{\lambda_{p2}} = -i$  and the residue reduces in the limit  $\mu \rightarrow 0$  to

$$R_2 \Big|_{\mu=0} = \frac{1}{2\pi} \left\{ \frac{\cosh k(Y+h)}{2kh + \sinh(2kh)} \right\} e^{i(kx+\omega t)} \left[ \mathcal{L}_1 - i\mathcal{L}_2 \right]_{-k} \quad (21)$$

As far as the poles closely adjacent to the imaginary axis are concerned, typically at  $\lambda_p = \mu\chi_1 + i\chi_0$  where  $\chi_0$  is given by (18) and  $\chi_1$  is small and real, the behaviour of the residues is again governed by  $e^{-i\lambda_p x} = e^{-i\mu\chi_1 x} e^{-\chi_0 x}$ . As  $\mu \rightarrow 0$ ,  $e^{-i\lambda_p x} \sim e^{\chi_0 x}$ . For finite values of  $x$ , all such terms will make contributions to the final result. However, in the asymptotic limit  $x \rightarrow -\infty$ , these poles make a zero contribution, and for this reason we shall not consider them further. It follows that

$$\oint_{C_1} f(\lambda) d\lambda = 2\pi i (R_1 + R_2) \Big|_{\mu=0} \quad (x \rightarrow -\infty)$$

We need to establish finally that the integral around the semi-circular portion of  $C_1$  is zero as  $t_0 \rightarrow \infty$ . If we write  $\lambda = t_0 e^{i\theta}$  in (15), this part of the integral becomes

$$\int_0^\pi \frac{1}{\sqrt{2\pi}} \left[ \{A_1 \cosh(t_0 e^{i\theta} Y) + B_1 \sinh(t_0 e^{i\theta} Y)\} \cos(\omega t) + \{A_2 \cosh(t_0 e^{i\theta} Y) + B_2 \sinh(t_0 e^{i\theta} Y)\} \sin(\omega t) \right] e^{-it_0 e^{i\theta} x} \cdot it_0 e^{i\theta} d\theta \quad (22)$$

For simplicity, consider a typical term in the brace in the above integrand, viz.

$$A_1 \cosh(t_0 e^{i\theta} Y) = \frac{\tilde{a}\mathcal{L}_1 + \tilde{b}\mathcal{L}_2}{\tilde{a}^2 + \tilde{b}^2} \cosh(t_0 e^{i\theta} Y)$$

Setting  $Y = -\mathcal{L}$  to maximize the magnitude of this term in respect of  $Y$  and dividing throughout by  $\cosh^2(t_0 e^{i\theta} \mathcal{L})$ , this becomes

$$A_1 \cosh(t_0 e^{i\theta} \mathcal{L}) = \frac{\{-t_0 e^{i\theta} \tanh(t_0 e^{i\theta} \mathcal{L}) + \sigma^2/g\} \mathcal{L}_1 + \{\mu\sigma/g\} \mathcal{L}_2}{(t_0 e^{i\theta})^2 \tanh^2(t_0 e^{i\theta} \mathcal{L}) - 2t_0 e^{i\theta} \frac{\sigma^2}{g} \tanh(t_0 e^{i\theta} \mathcal{L}) + \{(\sigma^2/g)^2 + (\mu\sigma/g)^2\}} \\ \sim \mathcal{L}_{1,2} / t_0 \quad \text{as} \quad t_0 \rightarrow \infty$$

Each of the remaining terms in the brace in (22) has a similar behaviour, which means that the integrand as a whole behaves as

$$\sim \frac{\Lambda_{1,2}}{r_0} \exp\{-i r_0 e^{i\theta} x\} \cdot i r_0 e^{i\theta} \sim \Lambda_{1,2} \exp\{-i r_0 e^{i\theta} x\}$$

The transient contribution in the integrand is then  $\exp\{+x \sin\theta\}$ . For  $0 < \theta < \pi$ ,  $\sin\theta > 0$  and so, for  $x < 0$ ,  $r_0 x \sin\theta < 0$ . In other words, in the limit  $r_0 \rightarrow \infty$ ,  $\exp\{+x \sin\theta\} \rightarrow 0$  and so, assuming that the terms  $\Lambda_{1,2}$  do not display an exponentially increasing dependence on  $r_0$  (as is the case in the later examples), we arrive at the final result, as  $x \rightarrow -\infty$ ,

$$\begin{aligned} \Phi(x, y, t) &= \int_{-\infty}^{\infty} f(\xi) d\xi = 2\pi i (R_1 + R_2) \Big|_{\mu=0} \\ &= i \frac{\cosh k(y+l)}{2kh + \sinh(2kh)} \left[ e^{i(kx+ct)} \{ \Lambda_1 - i \Lambda_2 \}_{-k} - e^{-i(kx+ct)} \{ \Lambda_1 + i \Lambda_2 \}_k \right] \end{aligned} \quad (23)$$

This solution corresponds to an outgoing wave in water of finite depth, as required.

### 2.1.2 Solution in the asymptotic limit $x \rightarrow +\infty$

We are concerned here with contour  $C_2$  in the lower half plane in Fig 2. This contains poles 3 and 4 and also, as  $r_0 \rightarrow \infty$ , all the poles closely adjacent to the negative imaginary axis of  $\lambda$ . By the same argument as used in § 2.1.1 we find that in the limit  $\mu \rightarrow 0$  the residue at pole 3 is

$$R_3 \Big|_{\mu=0} = \frac{1}{2\pi} \cdot \frac{\cosh k(y+l)}{2kh + \sinh(2kh)} e^{i(kx-ct)} \left[ \Lambda_1 + i \Lambda_2 \right]_{-k} \quad (24)$$

and the residue at pole 4 is

$$R_4 \Big|_{\mu=0} = -\frac{1}{2\pi} \cdot \frac{\cosh k(y+l)}{2kh + \sinh(2kh)} e^{-i(kx-ct)} \left[ \Lambda_1 - i \Lambda_2 \right]_k \quad (25)$$

where we have used the results

$$\lim_{\mu \rightarrow 0} \left( \tilde{b} / \tilde{a} \right)_{\lambda_{p3}} = i \quad \text{and} \quad \lim_{\mu \rightarrow 0} \left( \tilde{b} / \tilde{a} \right)_{\lambda_{p4}} = -i$$

As far as the poles closely adjacent to the imaginary axis are concerned, these now make a zero contribution to the final result in the asymptotic limit  $x \rightarrow +\infty$  and we are left with

$$\oint_{C_2} f(\lambda) d\lambda = 2\pi i (R_3 + R_4) \Big|_{\mu=0} \quad (x \rightarrow +\infty)$$

Since, by an argument closely similar to that given in § 2.1.1, the contribution to the integral on the semi-circular part of  $C_2$  can be shown to be zero as  $r_0 \rightarrow \infty$ , we have in this case, as  $x \rightarrow +\infty$ ,

$$\begin{aligned} \varphi(x, y, t) &= \int_{-\infty}^{\infty} f(\xi) d\xi = -2\pi i (R_3 + R_4) \Big|_{\mu=0} \\ &= -i \frac{\cosh k(y+h)}{2kh + \sinh(2kh)} \left[ e^{i(kx - \omega t)} \{ \mathcal{L}_1 + i \mathcal{L}_2 \}_k - e^{-i(kx - \omega t)} \{ \mathcal{L}_1 - i \mathcal{L}_2 \}_k \right] \end{aligned} \quad (26)$$

Again this solution corresponds to an outgoing wave as required. To proceed any further it is necessary to prescribe  $V(x, t)$  in Eq (7) and hence determine  $\mathcal{L}_1$  and  $\mathcal{L}_2$ . Some examples of the use of Eqs (23) and (26) are discussed in § 4.

We have been concerned here only with the properties of the solution (15) in the asymptotic limits  $x \rightarrow \pm\infty$ . It is, of course, possible to evaluate the solution in the immediate vicinity of the region of bed disturbance. The solution then involves not only the propagating modes associated with the poles at  $\lambda_0 = \pm k$ , but also the infinite number of non-propagating modes associated with the poles on the imaginary axis, given by Eq (18). These non-propagating modes satisfy the free surface and bottom conditions, and each decays exponentially in  $x$  away from the region of topography. In practice, at a distance of a few depths from this region, the non-propagating modes are negligibly small, and the solution effectively comprises only the outgoing propagating modes.

## 2.2 Limitations on the solution for $\varphi(x, y, t)$

In Part I of this report (§ 3.5) we discussed in some detail the physical limitations on the solutions of the linearized equations (2)-(5) (Eqs (17b)-(21b) in Part I). It was shown that these limitations arise on account of terms dropped in the process of linearizing the boundary conditions, and also on account of general requirements of the type  $|\varphi| \ll |\Phi|$ . For the solution in Part I, it was possible to state the limitations as a series of simple conditions between the various length scales in the problem. For the rather more complicated solution (Eq (15)) arrived at in Part II, the limitations are less readily obtained and, in fact, we defer the discussion of this matter to § 4. However, since the principal example to be taken concerns a bed of the type considered in Part I (except that the undulations on the bed surface are of finite horizontal extent), we expect the conditions of Part I to carry over in almost unchanged form to

Part II. In addition, in § 5, we shall require the solution to satisfy a certain condition in relation to wave energy flux, using the general results (23) and (26) for the limits  $x \rightarrow \pm \infty$ . Essentially, we shall ensure that the incident component of wave energy flux on the undulating part of the bed is balanced approximately by the sum of the reflected and transmitted components.

### 2.3 Discussion of the steady state problem

The central difficulty in the steady state formulation is the requirement that the velocity potential be Fourier transformable. If the problem is set up without the linear friction term (or some equivalent device), the solution is found to be given by the inverse Fourier transform of a function which is singular on the path of integration; in other words, the velocity potential in the problem posed does not possess a Fourier transform. The introduction of linear friction is a device which produces transient time variations in the problem, having the mathematical effect of moving the poles of the integrand off the contour of integration and thus ensuring that the modified velocity potential is Fourier transformable. Ultimately the steady state solution is obtained by setting the friction coefficient to zero.

The difficulty just described does not arise if a time dependent solution is considered, and in particular it does not arise if an equivalent initial value problem is solved. We illustrate this in § 3. where we follow quite closely the procedure of Stoker (1953). Essentially Stoker argues that, if a full time dependent problem is considered, the cause of the singular behaviour of the function for which the inverse Fourier transform is required is readily apparent, and it is clear how the difficulty which it presents can be overcome. Thus the introduction of time dependence in the problem leads to the consideration of a function which does have a proper Fourier transform, and in the limit of large time the solution is found to be the same as that obtained from the above steady state formulation. As far as the boundary conditions at infinity are concerned, the physical requirements in the steady state problem are met if the velocity potential is bounded at infinity, and also if the radiation condition is satisfied. However, in the initial value problem, it is sufficient to impose boundedness conditions at infinity only.

## § 3. THE INITIAL VALUE PROBLEM AND ITS SOLUTION

The procedure of Stoker (1953) for the solution of the steady state problem in the asymptotic limits  $|x| \rightarrow \infty$  is as follows: firstly, an initial value

problem is posed and solved; secondly, a passage of the solution to the limit time approaching infinity is made; and thirdly, the space variable  $x$  is allowed to approach infinity. The order in which the second and third steps are carried out is not reversible due to the finite propagation speed of water waves. Clearly, if the order was reversed, no wave would be found in the perturbation solution at infinity. This general approach has been adopted also by Harband (1977) in a study of the propagation of long waves over slowly varying topography.

We start with Eqs (2)-(5), but now assume the perturbation  $\varphi(x, y, t)$  to the velocity potential  $\Phi(x, y, t)$  to be zero for  $t \leq 0$ . So the governing equation is

$$\nabla^2 \varphi = 0 \quad -L < y < 0, \quad t > 0 \quad (2a)$$

the boundary condition at the free surface is

$$g \varphi_y + \varphi_{tt} = 0 \quad \text{on} \quad y = 0, \quad t > 0 \quad (6a)$$

and at the bed is

$$\varphi_y = \begin{cases} 0 & -\infty < x < L_1 \\ -V(x, t) & L_1 < x < L_2 \\ 0 & L_2 < x < \infty \end{cases} \quad \text{on} \quad y = -L, \quad t > 0 \quad (7a)$$

where  $V(x, t)$ , the vertical velocity at the bed surface, is given again by

$$V(x, t) = -\Phi_x(x, -L, t) \cdot \zeta_x + \Phi_{yy}(x, -L, t) \cdot \zeta$$

Following Stoker, we require only boundedness of the solution at infinity, and in particular that  $\varphi$  and its first and second derivatives tend to zero as  $|x| \rightarrow \infty$  at time  $t$  in such a way that Fourier transforms exist in  $x$ . We make no formal statement about the behaviour of  $\varphi$  as  $t \rightarrow \infty$ , but impose the initial conditions

$$\left. \begin{aligned} \varphi(x, 0, 0) &= 0 \\ \varphi_t(x, 0, 0) &= 0 \end{aligned} \right\} \quad (t = 0) \quad (27)$$

which imply that the free surface is initially at rest in its horizontal equilibrium position.

Upon taking the Fourier transforms of (2a), (6a) and (7a), we have

$$\hat{\Phi}_{\gamma\gamma} - \xi^2 \hat{\Phi} = 0 \quad -L < \gamma < 0, \quad t > 0 \quad (8a)$$

$$g \hat{\Phi}_\gamma + \hat{\Phi}_{tt} = 0 \quad \gamma = 0, \quad t > 0 \quad (9a)$$

$$\begin{aligned} \hat{\Phi}_\gamma &= -\frac{1}{\sqrt{2\pi}} \int_{L_1}^{L_2} V(x, t) e^{i\xi x} dx \\ &= \frac{1}{\sqrt{2\pi}} \mathcal{L}(\xi, t) \quad t > 0 \end{aligned} \quad (10a)$$

The solution of (8a) is

$$\hat{\Phi}(\xi, \gamma, t) = \tilde{A}(\xi, t) \cosh(\xi \gamma) + \tilde{B}(\xi, t) \sinh(\xi \gamma) \quad (11a)$$

and (9a) and (10a) lead as before to equations for  $\tilde{A}$  and  $\tilde{B}$  as follows:

$$g \xi \tilde{B}(\xi, t) + \tilde{A}_{tt}(\xi, t) = 0 \quad (12a)$$

$$-\tilde{A}(\xi, t) \cdot \xi \sinh(\xi L) + \tilde{B}(\xi, t) \xi \cosh(\xi L) = \frac{1}{\sqrt{2\pi}} \mathcal{L}(\xi, t) \quad (13a)$$

Now however, rather than making the solution specific to the case of waves of frequency  $\sigma$  as in (14), we solve (12a) and (13a), firstly by eliminating  $\tilde{B}(\xi, t)$  and secondly by using the method of variation of parameters to solve for  $\tilde{A}(\xi, t)$ . The differential equation for  $\tilde{A}(\xi, t)$  is

$$\begin{aligned} \tilde{A}_{tt} + (g \xi \tanh(\xi L)) \tilde{A} &= -\frac{g}{\sqrt{2\pi} \cosh(\xi L)} \mathcal{L}(\xi, t) \\ &= \nu(\xi, t) \quad , \text{ say } , \end{aligned} \quad (28)$$

and the general solution of (28) is

$$\tilde{A}(\xi, t) = \left\{ \tilde{A}_1 + \int_0^t \frac{\cos(e\tau) \nu(\xi, \tau)}{e} d\tau \right\} \sin(et) + \left\{ \tilde{A}_2 - \int_0^t \frac{\sin(e\tau) \nu(\xi, \tau)}{e} d\tau \right\} \cos(et) \quad (29)$$

where  $\tilde{A}_1$  and  $\tilde{A}_2$  are constants and

$$e^2 = g \xi \tanh(\xi L)$$



From the initial conditions,

$$\tilde{A}(\xi, 0) = 0$$

$$\tilde{A}_t(\xi, 0) = 0$$

which imply that  $\tilde{A}_1 = \tilde{A}_2 = 0$  and so (29) becomes

$$\begin{aligned}\tilde{A}(\xi, t) &= \int_0^t \frac{\{\cos(e\tau) \sin(et) - \sin(e\tau) \cos(et)\}}{e} \varpi(\xi, \tau) d\tau \\ &= \int_0^t \frac{\sin e(t-\tau) \varpi(\xi, \tau)}{e} d\tau \\ &= \int_0^t \frac{\sin(e\tau) \varpi(\xi, t-\tau)}{e} d\tau\end{aligned}$$

It follows from (12a) or (13a) that

$$\tilde{B}(\xi, t) = \frac{1}{g\xi} \left\{ -\varpi(\xi, t) + e^2 \int_0^t \frac{\sin(e\tau) \varpi(\xi, t-\tau)}{e} d\tau \right\}$$

and so  $\hat{\phi}(\xi, \gamma, t)$  is given from (11a) by

$$\begin{aligned}\hat{\phi}(\xi, \gamma, t) &= \left\{ \cosh(\xi\gamma) + \frac{e^2 \sinh(\xi\gamma)}{g\xi} \right\} \int_0^t \frac{\sin(e\tau) \varpi(\xi, t-\tau)}{e} d\tau - \frac{\varpi(\xi, t) \sinh(\xi\gamma)}{g\xi} \\ &= \frac{\cosh \xi(\gamma+k)}{\cosh(\xi k)} \int_0^t \frac{\sin(e\tau) \varpi(\xi, t-\tau)}{e} d\tau - \frac{\varpi(\xi, t) \sinh(\xi\gamma)}{g\xi}\end{aligned}$$

Upon taking the inverse transform we arrive at the solution

$$\phi(x, \gamma, t) = \int_{-\infty}^{\infty} \frac{1}{\sqrt{2\pi}} \left\{ \frac{\cosh \xi(\gamma+k)}{\cosh(\xi k)} \int_0^t \frac{\sin(e\tau) \varpi(\xi, t-\tau)}{e} d\tau - \frac{\varpi(\xi, t) \sinh(\xi\gamma)}{g\xi} \right\} e^{-i\xi x} d\xi \quad (30)$$

Equation (30) can be viewed as being at one stage removed from the time-dependent solution discussed in § 2. and, clearly, we expect to recover this latter solution in the limit  $t \rightarrow \infty$ . The important point to note at this stage is that, for non-singular choices of  $\varpi(\xi, t)$ , the integrand in (30) has no singularities on the path of integration. This is central to the argument which follows in which we declare  $\xi$  to be the real part of a complex variable, and then deform the path of integration in the complex plane. This operation is legitimate by Cauchy's theorem since, in the process of deformation from the old to the new paths, no singularities of the integrand which lie off the real axis in the complex plane are crossed.

To proceed further it is necessary to specify  $\varpi(\xi, t)$ , and in (30) we shall assume that

$$\left. \begin{aligned}
 V(x,t) &= V_1(x) \cos(\sigma t) + V_2(x) \sin(\sigma t) && \text{in (7a)} \\
 \therefore \mathcal{L}(\xi,t) &= \mathcal{L}_1(\xi) \cos(\sigma t) + \mathcal{L}_2(\xi) \sin(\sigma t) && \text{from (10a)} \\
 \therefore \omega(\xi,t) &= \omega_1(\xi) \cos(\sigma t) + \omega_2(\xi) \sin(\sigma t) && \text{from (28)}
 \end{aligned} \right\} \quad (31)$$

as a result of a prescribed first order motion of frequency  $\sigma$  satisfying (17). It follows that

$$\sin(e\tau)\omega(\xi,t-\tau) = \omega_1 \sin(e\tau) \cos \sigma(t-\tau) + \omega_2 \sin(e\tau) \sin \sigma(t-\tau)$$

which, when written in exponential form and integrated w.r.t.  $\tau$ , can be expressed as the sum of the following four terms

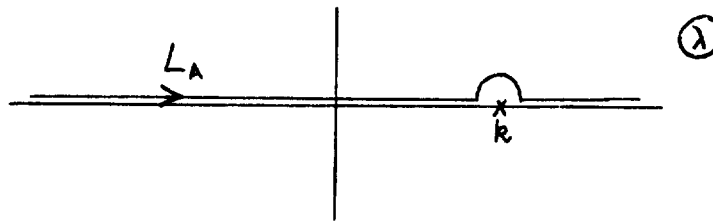
$$\begin{aligned}
 \int_0^t \sin(e\tau)\omega(\xi,t-\tau) d\tau &= \frac{1}{4} e^{i\sigma t} \left\{ \frac{e^{i(e-\sigma)t} - 1}{e - \sigma} \right\} \{-\omega_1 + i\omega_2\} && \text{Term A} \\
 &+ \frac{1}{4} e^{i\sigma t} \left\{ \frac{e^{-i(e+\sigma)t} - 1}{-(e+\sigma)} \right\} \{\omega_1 - i\omega_2\} && \text{Term B} \\
 &+ \frac{1}{4} e^{-i\sigma t} \left\{ \frac{e^{i(e+\sigma)t} - 1}{(e+\sigma)} \right\} \{-\omega_1 - i\omega_2\} && \text{Term C} \\
 &+ \frac{1}{4} e^{-i\sigma t} \left\{ \frac{e^{-i(e-\sigma)t} - 1}{-(e-\sigma)} \right\} \{\omega_1 + i\omega_2\} && \text{Term D}
 \end{aligned}$$

where it will be noted that each term is regular. In handling (30) we are at liberty to carry each of these terms separately through the limiting processes  $t \rightarrow \infty$ ,  $x \rightarrow \pm \infty$  in such a way that the solution has the desired physical behaviour. In particular, before we resubstitute Terms A to D in (30), we follow Stoker (1953) in anticipating certain singularities which are found to lie on the path of integration  $-\infty < \xi < \infty$  as  $t \rightarrow \infty$ . These singularities originate in the integration with respect to  $\tau$  in (30), and inspection of Terms A to D indicates their locations to be associated with  $(e-\sigma)^{-1}$ ,  $(e+\sigma)^{-1}$ ,  $(e+\sigma)^{-1}$  and  $(e-\sigma)^{-1}$  respectively. Adopting the convention that the positive root of  $\sqrt{g\xi \tanh(\xi h)} = c$  is taken on the positive axis of  $\xi$ , these singularities arise at  $\xi = +k$ ,  $-k$ ,  $-k$  and  $+k$  for Terms A to D respectively. As mentioned above, it is convenient to evaluate (30) by taking  $\xi$  to be the real part of a complex variable  $\lambda = \xi + i\chi$

and to by-pass the singularities by choosing a set of new paths of integration in the  $\lambda$ -plane, namely  $L_A$ ,  $L_B$ ,  $L_C$  and  $L_D$  for Terms A to D respectively. It will be noted that, since  $e = e(\lambda)$  in the complex plane, additional singularities of the integrand occur on the imaginary axis of  $\lambda$  as in section 2. However, in the arguments which follow, these singularities are not to be found within the areas bounded by the old and the new paths of integration and, therefore, need not be considered further. The particular choices for the new paths ( $L_A$ , etc) are made such that the solution corresponding to each of Terms A, B, C and D is bounded as  $t \rightarrow \infty$ . It then remains only to verify, term by term, that the radiation condition is satisfied in the asymptotic limits  $|x| \rightarrow \pm \infty$ .

#### Consider Term A

In anticipation of a singularity at  $\lambda = +k$ , we replace the path of integration  $-\infty < \xi < \infty$  in (30) by the contour  $L_A$  which is indented into the upper half plane at  $\lambda = +k$ . The choice of the upper half plane is governed by the need for a solution containing only decaying transients in time.



Following the change of contour we have

$$\mathcal{Q}_A(x, y, t) = \int_{L_A} \frac{1}{\sqrt{2\pi}} \cdot \frac{\cosh \lambda (y+k)}{\cosh (\lambda h)} \cdot \frac{e^{i\omega t}}{4\rho} \cdot \{-\omega_1 + i\omega_2\} \left[ \frac{e^{i(e-\sigma)t}}{e-\sigma} - \frac{1}{e-\sigma} \right] e^{-i\lambda x} d\lambda$$

It may be noted that, in the form written above, the terms in the square brackets are separately singular at  $\lambda = +k$  ( $e = +\sigma$ ). The first of these terms is the result of the initial conditions and is expected, therefore, to provide a decaying transient contribution as  $t \rightarrow \infty$ . This we can see as follows:- On the semi-circle in the upper half plane the imaginary part of  $\lambda$  is positive, so the imaginary part of  $e$  is positive. It follows that the real part of  $i(e-\sigma)$  is negative,  $\sigma$  being real, and so the exponential in the square bracket has a negative real part. Therefore, as  $t \rightarrow \infty$ , this part of the path makes a contribution that tends to zero. As in Stoker's example, we argue that the remaining portions of  $L_A$ , which lie on the real axis, make

contributions which die out like  $1/t$ . This is discussed by Harband (1977), and can be shown by integration by parts. For large  $t$ , we are left with the following asymptotic representation for  $\mathcal{G}_A$ :

$$\mathcal{G}_A(x, y, t) = \int_{\mathcal{L}_A} \frac{1}{\sqrt{2\pi}} \cdot \frac{\cosh \lambda(k+h)}{\cosh(\lambda h)} \cdot \frac{e^{i\omega t}}{4e} \{-\nu_1 + i\nu_2\} \left[ \frac{-1}{e^{-\sigma}} \right] e^{-i\lambda x} d\lambda, \quad (t \rightarrow \infty) \quad (32)$$

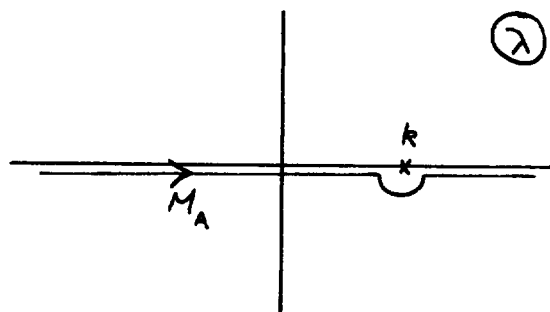
In the integrand of (32), we note the anticipated singularity at  $\lambda = +k$  ( $\rho = \sigma$ ). There is also a pole at  $\lambda = 0$  ( $\rho = 0$ ). However, it can be shown that this latter pole does not make a significant contribution to the final answer since, when its effect is added to the equivalent effects of the poles at  $\lambda = 0$  from Terms  $B$ ,  $C$  and  $D$ , the combined result is zero. (The poles at  $\lambda = 0$  from Terms  $B$ ,  $C$  and  $D$  are also left on the respective paths of integration as seen later.) We shall not discuss the poles at  $\lambda = 0$  further, therefore, but merely note that their appearance in (32) and the companion equations for Terms  $B$ ,  $C$  and  $D$ , is an artefact of the approach adopted here.

We now examine the behaviour of (32) in the asymptotic limits  $x \rightarrow \pm\infty$ , and we consider initially the limit  $x \rightarrow -\infty$ . On the semi-circular portion of  $\mathcal{L}_A$ , the imaginary part of  $\lambda$  is positive, so the real part of  $(-i\lambda)$  is positive. Clearly, therefore, by virtue of the exponential term  $e^{-i\lambda x}$ , the contribution to  $\mathcal{G}_A$  from the semi-circle must tend to zero in the limit  $x \rightarrow -\infty$ . On the remaining portions of  $\mathcal{L}_A$  lying on the real axis, a behaviour  $\sim 1/x$  can be seen to be exhibited by  $\mathcal{G}_A$  (by, for instance, integrating by parts). So the total contribution arising from Term  $A$  is zero in the limit  $x \rightarrow -\infty$ :

$$\mathcal{G}_A(x, y, t) = 0 \quad (x \rightarrow -\infty) \quad (33)$$

To evaluate (32) in the limit  $x \rightarrow +\infty$ , it is convenient to consider a new contour  $M_A$  which is indented into the lower half plane at  $\lambda = +k$ . We note initially that

$$\int_{M_A} [\ ] d\lambda - \int_{\mathcal{L}_A} [\ ] d\lambda = 2\pi i \left\{ \begin{array}{l} \text{Residue} \\ \text{at} \\ \lambda = +k \end{array} \right\} \quad \text{Term A}$$



where the square brackets imply the integrand of (32). On the semi-circular part of  $M_A$  the exponential term is such as to produce a zero contribution to the integral in the limit  $x \rightarrow +\infty$ . (This is not so on the semi-circular part of  $L_A$  in this limit.) Elsewhere on  $M_A$ , the contributions to the integral are also zero for the reasons given above. It follows that

$$\begin{aligned}\varphi_A(x, y, t) &= \int_{L_A} [\ ] d\lambda \\ &= -2\pi i \left\{ \begin{array}{c} \text{Residue} \\ \text{at} \\ \lambda = k \end{array} \right\}_{\text{Term A}} \quad (x \rightarrow +\infty)\end{aligned}$$

Since

$$\lim_{\lambda \rightarrow k} \frac{\lambda - k}{e^{-\sigma}} = \frac{2\sigma \cosh^2(kh)}{y \{ kh + \sinh(kh) \cosh(kh) \}}$$

it follows that the residue at  $\lambda = k$  is given by

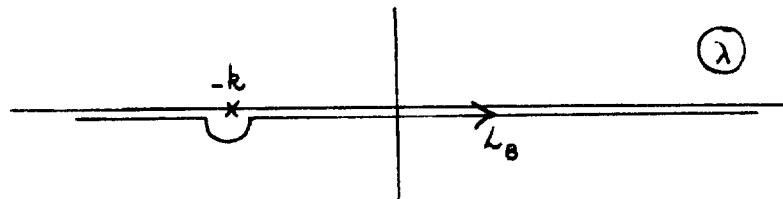
$$R_{+k,A} = -\frac{1}{\sqrt{2\pi}} e^{-i(kx-\sigma t)} \cdot \frac{\cosh k(Y+k)}{y \{ 2kh + \sinh(2kh) \}} \cdot \left\{ -\omega_1 \Big|_{+k} + i \omega_2 \Big|_{+k} \right\} \cosh(kh)$$

Upon using (28) this leads to the final result for Term A as  $x \rightarrow +\infty$ ,

$$\varphi_A(x, y, t) = i e^{-i(kx-\sigma t)} \cdot \frac{\cosh k(Y+k)}{\{ 2kh + \sinh(2kh) \}} \cdot \left\{ \omega_1 \Big|_{+k} - i \omega_2 \Big|_{+k} \right\}, \quad (x \rightarrow +\infty) \quad (34)$$

Consider Term B:

The argument adopted here differs from that for Term A only in its minor details. In anticipation of a singularity at  $\lambda = -k$  in the limit  $t \rightarrow \infty$  we start by replacing the path of integration in (30) by the path  $L_B$ . Thus we arrive at the asymptotic representation for  $\varphi_B$  (cf (32))

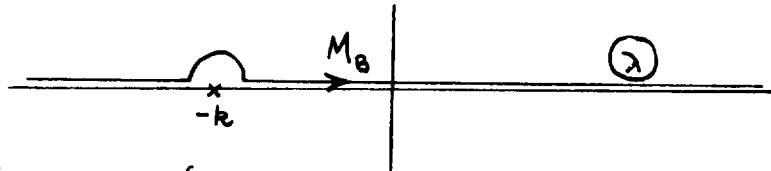


$$\varphi_B(x, y, t) = \int_{L_B} \frac{1}{\sqrt{2\pi}} \cdot \frac{\cosh \lambda(Y+k)}{\cosh(\lambda k)} \cdot \frac{e^{i\sigma t}}{4e} \cdot \left\{ \omega_1 - i \omega_2 \right\} \left[ \frac{1}{e+\sigma} \right] e^{-i\lambda x} d\lambda \quad (t \rightarrow \infty) \quad (35)$$

In the limit  $x \rightarrow +\infty$  this gives

$$\varphi_B(x, y, t) = 0 \quad (x \rightarrow +\infty) \quad (36)$$

To evaluate (35) in the limit  $x \rightarrow -\infty$ , we consider a new path  $M_B$  which is indented into the upper half plane at  $\lambda = -k$ . We see that



$$\int_{M_B} [\ ] d\lambda - \int_{L_B} [\ ] d\lambda = -2\pi i \cdot R_{-k,B}$$

where the square brackets now indicate the integrand of (35) and where  $R_{-k,B}$  is the residue at  $\lambda = -k$ . Since

$$\lim_{\lambda \rightarrow -k} \frac{\lambda + k}{e^{\lambda + \sigma}} = \frac{2\sigma \cosh^2(kh)}{g\{k\ell + \sinh(kh)\cosh(kh)\}}$$

we find that

$$R_{-k,B} = -\frac{1}{\sqrt{2\pi}} e^{i(kx + \sigma t)} \cdot \frac{\cosh k(\gamma + \ell)}{g\{2kh + \sinh(2kh)\}} \cdot \left\{ \mathcal{V}_1 \Big|_{-k} - i \mathcal{V}_2 \Big|_{-k} \right\} \cosh(kh)$$

and so, the contribution of the integral on  $M_B$  being zero as  $x \rightarrow -\infty$ , we arrive at the result for Term B that

$$\begin{aligned} \varphi_B(x, \gamma, t) &= \int_{L_B} [\ ] d\lambda \\ &= 2\pi i R_{-k,B} \quad (x \rightarrow -\infty) \\ &= i e^{i(kx + \sigma t)} \cdot \frac{\cosh k(\gamma + \ell)}{\{2kh + \sinh(2kh)\}} \cdot \left\{ \mathcal{L}_1 \Big|_{-k} - i \mathcal{L}_2 \Big|_{-k} \right\} \quad (x \rightarrow -\infty) \end{aligned} \quad (37)$$

Consider Term C:

We again anticipate a singularity at  $\lambda = -k$ , but now indent our initial contour,  $L_C$ , into the upper half plane at this point. Thus, as  $t \rightarrow \infty$ , we have

$$\varphi_C(x, \gamma, t) = \int_{L_C} \frac{1}{\sqrt{2\pi}} \cdot \frac{\cosh \lambda(\gamma + \ell)}{\cosh(\lambda \ell)} \cdot \frac{e^{-i\sigma t}}{4e} \cdot \{\mathcal{V}_1 + i\mathcal{V}_2\} \left[ \frac{1}{e^{\lambda + \sigma}} \right] e^{-i\lambda x} d\lambda \quad (t \rightarrow \infty) \quad (38)$$

In the limit  $x \rightarrow -\infty$

$$\varphi_C(x, \gamma, t) = 0 \quad (x \rightarrow -\infty) \quad (39)$$

and, in the limit  $x \rightarrow +\infty$ , we work with a new contour  $M_C$ , indented into the lower half plane at  $\lambda = -k$ , to arrive at the final result

$$\varphi_c(x, y, t) = -i e^{i(kx - \sigma t)} \cdot \frac{\cosh k(y + \ell)}{\{2kh + \sinh(2kh)\}} \cdot \left\{ L_1 \Big|_{-k} + i L_2 \Big|_{-k} \right\} \quad (x \rightarrow +\infty) \quad (40)$$

Consider Term  $\mathcal{D}$ :

We now anticipate a singularity at  $\lambda = +k$  and, accordingly, indent our initial contour  $\mathcal{L}_D$  into the lower half plane at this point. As  $t \rightarrow \infty$  we have

$$\varphi_D(x, y, t) = \int_{\mathcal{L}_D} \frac{1}{\sqrt{2\pi}} \cdot \frac{\cosh \lambda(y + \ell)}{\cosh(\lambda \ell)} \cdot \frac{e^{-i\sigma t}}{4\rho} \cdot \{z_1 + i z_2\} \left[ \frac{1}{e - \sigma} \right] e^{-i\lambda x} d\lambda \quad (t \rightarrow \infty) \quad (41)$$

In the limit  $x \rightarrow +\infty$

$$\varphi_D(x, y, t) = 0 \quad (x \rightarrow +\infty) \quad (42)$$

and, in the limit  $x \rightarrow -\infty$ , we work with a contour  $\mathcal{M}_D$ , indented into the upper half plane at  $\lambda = +k$ , to arrive at

$$\varphi_D(x, y, t) = -i e^{-i(kx + \sigma t)} \cdot \frac{\cosh k(y + \ell)}{\{2kh + \sinh(2kh)\}} \cdot \left\{ L_1 \Big|_k + i L_2 \Big|_k \right\} \quad (x \rightarrow -\infty) \quad (43)$$

The remaining part of (30) is the integral expression

$$- \frac{1}{\sqrt{2\pi}} \int_{-\infty}^{\infty} e^{-i\xi x} \cdot \frac{\psi(\xi, t) \sinh(\xi \ell)}{g \xi} d\xi$$

This has no singularities on the path of integration for non-singular choices of  $\psi(\xi, t)$  and so, in the asymptotic limits  $x \rightarrow \pm \infty$ , it makes no contribution to the final result. This can be demonstrated, for instance, by integrating by parts.

We obtain our final result in the limit  $x \rightarrow -\infty$ , by superimposing (33), (37), (39) and (43):

$$\varphi(x, y, t) = i \frac{\cosh k(y + \ell)}{\{2kh + \sinh(2kh)\}} \cdot \left[ e^{i(kx + \sigma t)} \left\{ L_1 - i L_2 \right\}_{-k} - e^{-i(kx + \sigma t)} \left\{ L_1 + i L_2 \right\}_k \right] \quad (44)$$

$(t \rightarrow \infty, x \rightarrow -\infty)$

This solution corresponds to an outgoing wave in water of finite depth and it confirms the earlier result (23) obtained by the linear friction method. In the limit  $x \rightarrow +\infty$ , we superimpose (34), (36), (40) and (42) to obtain

$$\varphi(x, y, t) = i \frac{\cosh k(y+l)}{\{2kh + \sinh(2kh)\}} \left[ e^{-i(kx-\sigma t)} \{ \mathcal{L}_1 - i \mathcal{L}_2 \}_k - e^{i(kx-\sigma t)} \{ \mathcal{L}_1 + i \mathcal{L}_2 \}_{-k} \right] \quad (45)$$

( $t \rightarrow \infty, x \rightarrow +\infty$ )

Again this solution corresponds to an outgoing wave and it confirms the earlier result (26). We have shown, therefore, that by imposing boundedness conditions on the solution (30) of the initial value problem (through our choice of the paths  $\mathcal{L}_A$ , etc) the radiation condition is satisfied in the limits  $|x| \rightarrow \infty$ . In § 4. we apply results (44) and (45) to certain special cases.

## § 4. APPLICATIONS OF THE THEORY

### 4.1 A simple piston action at the bottom boundary

By way of simple illustration of the use of Eqs (44) and (45), we consider first a vertical piston action at the bottom boundary. The piston is of length  $2L$  with its centre displaced a distance  $L_0$  from  $x = 0$ , and it makes a vertical oscillation about its mean height  $y = -L$  with velocity amplitude  $V_0(x)$ , such that <sup>1</sup>

$$V(x, t) = V_0 \cos(\sigma t) \quad \text{in} \quad -L + L_0 < x < L + L_0 \quad (46)$$

From (10)

$$\mathcal{A}(\xi, t) = - \int_{-L+L_0}^{L+L_0} V_0 \cos(\sigma t) e^{i\xi x} dx = -V_0 e^{i\xi L_0} \cdot \frac{2 \sin(\xi L)}{\xi} \cdot \cos(\sigma t)$$

and so from (14)

$$\mathcal{L}_1 = -2V_0 e^{i\xi L_0} \frac{\sin(\xi L)}{\xi}, \quad \mathcal{L}_2 = 0$$

---

<sup>1</sup> Here we do not deduce  $V(x, t)$  from the expression given in (7), but we simply prescribe it. If there is no first order motion ( $\Phi = \text{constant}$ ), and if the bottom is oscillating such that  $\zeta = \zeta(t) \sim \sin(\sigma t)$ , then strictly we require the addition of the term  $\zeta_\epsilon$  to the left hand side of the bottom boundary condition (5) in order to permit (46).



Substituting these expressions in (44) and (45) gives the final results

$$\varphi(x, y, t) = 4V_0 \frac{\cosh k(y+h)}{\{2kh + \sinh(2kh)\}} \cdot \frac{\sin(kh)}{k} \sin(kx + \sigma t - kh_0) \quad (x \rightarrow -\infty)$$

and

$$\varphi(x, y, t) = -4V_0 \frac{\cosh k(y+h)}{\{2kh + \sinh(2kh)\}} \cdot \frac{\sin(kh)}{k} \sin(kx - \sigma t - kh_0) \quad (x \rightarrow \infty)$$

We see here, firstly, that the velocity potential is real, as required; secondly, that the waves are outgoing and are slightly displaced in phase to account for the offset  $h_0$  specified in (46); thirdly, that the waves are properly attenuated with depth; and, finally, that the amplitude of the waves is proportional to  $\sin(kh)$ . This latter point has the effect that for integral values of the ratio  $2h/(\text{surface wavelength})$  the outgoing wave height becomes zero. On the other hand, if the ratio takes the values  $\frac{1}{2}, \frac{3}{2}, \dots$ , the outgoing wave height is maximised. This property is found also in the next application discussed. In general, however, the piston action at the bed in  $(-h+h_0, h+h_0)$  produces outgoing waves at the water surface as  $x \rightarrow \pm \infty$ .

The piston problem is quite similar in some respects to that discussed by Carrier (1966) in a study of the generation of tsunamis. Carrier's approach was to give the seabed in  $x < 0$  a displacement proportional to  $e^{a_1 x} t e^{-a_2 t}$  in  $t > 0$ , where  $a_1$  and  $a_2$  are positive constants, and to study the resulting transient motion in  $x > 0$  using linear theory. Further comments about his study are given in the earlier literature survey.

#### 4.2 A patch of ripples on an otherwise flat bed

We consider now a case of particular interest, namely the interaction of progressing surface waves with a patch of ripples on the bed<sup>1</sup>. In the assumed absence of any undulations on the bed, we prescribe a first-order motion

$\Phi(x, y, t)$  and then deduce the perturbation  $\varphi(x, y, t)$  to this motion resulting from the presence of the ripples. In following this procedure we use Eq (5) to determine  $V(x, t)$  in Eq (7).

For the first order motion we prescribe the velocity potential for waves of amplitude  $a$  and period  $\frac{2\pi}{\sigma}$ , progressing in the  $+x$  direction in water of depth  $h$ , namely

---

<sup>1</sup> The term 'ripple' is used here in a very general way, and does not imply any restrictions on the bed wavelength.

$$\bar{\Phi}_p = \frac{ga}{\sigma} \cdot \frac{\cosh k(Y+L)}{\cosh(kh)} \cos(kx - \sigma t) \quad (47)$$

which for illustration, and in order to build up a complete understanding of the solution, we shall treat as the sum of two standing waves

$$\begin{aligned} \bar{\Phi}_p &= \bar{\Phi}_{s1} + \bar{\Phi}_{s2} \quad \text{where} \\ \bar{\Phi}_{s1} &\sim \cos(kx) \cos(\sigma t) \quad (\text{Wave 1}) \\ \bar{\Phi}_{s2} &\sim \sin(kx) \sin(\sigma t) \quad (\text{Wave 2}) \end{aligned} \quad (48)$$

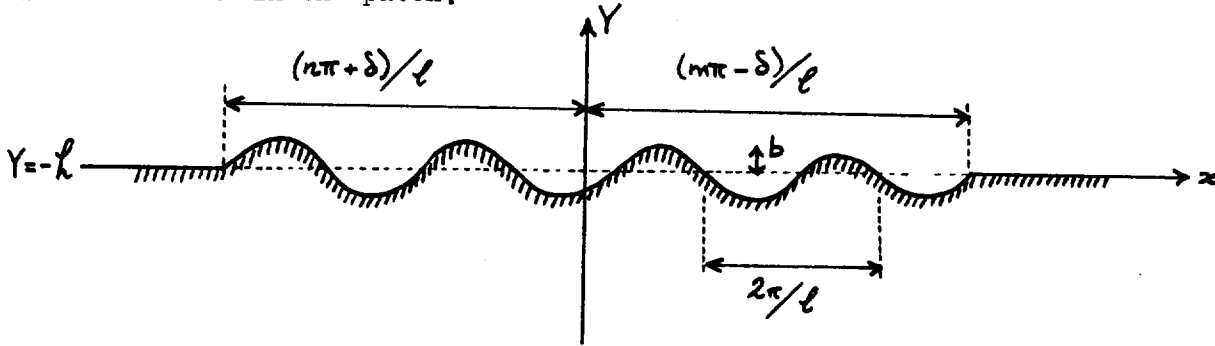
We prescribe the bed surface in Eq (1) as

$$Y_b(x) = b \sin(\ell x + \delta) \quad , \quad L_1 < x < L_2 \quad (49)$$

where  $\delta$  is a constant phase angle. For continuity of bed elevation we take

$$L_1 = (-n\pi - \delta)/\ell \quad \text{and} \quad L_2 = (m\pi - \delta)/\ell$$

where  $n$  and  $m$  are integers, so that there are  $(n+m)/2$  ripples of wavenumber  $\ell$  in the patch.



From (7), (10), (48) and (49), we have for Wave 1

$$V(x,t) = -g\eta \Big|_{-h} = C_* \{ \ell \sin(kx) \cos(\ell x + \delta) + k \cos(kx) \sin(\ell x + \delta) \} \cos(\sigma t)$$

where

$$C_* = \frac{gabk}{\sigma \cosh(kh)}$$

It follows that

$$\mathcal{L}_1 = C_* \int_{L_1}^{L_2} \{ -\ell \sin(kx) \cos(\ell x + \delta) - k \cos(kx) \sin(\ell x + \delta) \} e^{i\ell x} dx$$

and

$$\mathcal{L}_2 = 0$$

Hence, from (44) and (45), as  $\underline{x \rightarrow -\infty}$

$$\varphi(x, y, t) = \frac{-C_* \cosh k(y+x)}{2\{2kh + \sinh(2kh)\}} \cdot \left[ \frac{2k/\ell}{(2k/\ell)^2 - 1} \cdot \left\{ (-1)^m \sin(kx + \sigma t - 2kL_2) - (-1)^{\tilde{m}} \sin(kx + \sigma t - 2kL_1) \right\} \right. \\ \left. + (2k/\ell) \left( (-1)^m - (-1)^{\tilde{m}} \right) \sin(kx + \sigma t) \right] \quad (50)$$

and as  $\underline{x \rightarrow +\infty}$

$$\varphi(x, y, t) = \frac{C_* \cosh k(y+x)}{2\{2kh + \sinh(2kh)\}} \cdot \left[ \frac{2k/\ell}{(2k/\ell)^2 - 1} \cdot \left\{ (-1)^m \sin(kx - \sigma t - 2kL_2) - (-1)^{\tilde{m}} \sin(kx - \sigma t - 2kL_1) \right\} \right. \\ \left. + (2k/\ell) \left( (-1)^m - (-1)^{\tilde{m}} \right) \sin(kx - \sigma t) \right] \quad (51)$$

Similarly for Wave 2

$$V(x, t) = -\varphi_y \Big|_{-x} = C_* \left\{ -\ell \cos(kx) \cos(yx + \delta) + k \sin(kx) \sin(yx + \delta) \right\} \sin(\sigma t)$$

Hence

$$A_1 = 0$$

$$A_2 = C_* \int_{x_1}^{x_2} \left\{ \ell \cos(kx) \cos(yx + \delta) - k \sin(kx) \sin(yx + \delta) \right\} e^{i\frac{1}{2}x} dx$$

and, from (44) and (45), as  $\underline{x \rightarrow -\infty}$

$$\varphi(x, y, t) = \frac{C_* \cosh k(y+x)}{2\{2kh + \sinh(2kh)\}} \cdot \left[ -\frac{2k/\ell}{(2k/\ell)^2 - 1} \cdot \left\{ (-1)^m \sin(kx + \sigma t - 2kL_2) - (-1)^{\tilde{m}} \sin(kx + \sigma t - 2kL_1) \right\} \right. \\ \left. + (2k/\ell) \left( (-1)^m - (-1)^{\tilde{m}} \right) \sin(kx + \sigma t) \right] \quad (52)$$

and as  $\underline{x \rightarrow +\infty}$

$$\varphi(x, y, t) = \frac{C_* \cosh k(y+x)}{2\{2kh + \sinh(2kh)\}} \cdot \left[ -\frac{2k/\ell}{(2k/\ell)^2 - 1} \cdot \left\{ (-1)^m \sin(kx - \sigma t - 2kL_2) - (-1)^{\tilde{m}} \sin(kx - \sigma t - 2kL_1) \right\} \right. \\ \left. + (2k/\ell) \left( (-1)^m - (-1)^{\tilde{m}} \right) \sin(kx - \sigma t) \right] \quad (53)$$

It will be noted that each of the results (50)-(53) represents an outgoing wave. In other words, the interaction of each of the standing waves of (48) with the rippled bed gives rise to progressive waves travelling away from the

region of disturbance ( $L_1 < x < L_2$ ). If we now superimpose the above results, we obtain the solutions appropriate to the case of a progressive wave train incident on the patch of ripples. In particular, the interaction of the velocity potential (47) with the bed surface (49) gives, as  $x \rightarrow -\infty$

$$\varphi(x, y, t) = \frac{-C_* \cosh k(y+L)}{\{2kh + \sinh(2kh)\}} \cdot \frac{2k/\ell}{(2k/\ell)^2 - 1} \left[ (-1)^m \sin(kx + \sigma t - 2kL_2) - (-1)^n \sin(kx + \sigma t - 2kL_1) \right] \quad (54)$$

and as  $x \rightarrow +\infty$

$$\varphi(x, y, t) = \frac{C_* \cosh k(y+L)}{\{2kh + \sinh(2kh)\}} \cdot \left( \frac{2k/\ell}{(2k/\ell)^2 - 1} \right) \cdot \left( (-1)^m - (-1)^n \right) \sin(kx - \sigma t) \quad (55)$$

It can be seen that these results have a rather different character. For convenience, however, we shall discuss the solutions in two simpler special cases.

#### Special Case 1

Firstly, consider the case in which there is an integral number of ripple wavelengths in the patch  $L_1 < x < L_2$ , such that  $m = n$  and  $\delta = 0$  in (49). If we write  $m\pi/\ell = L$ , we find from (54) and (55) that, as  $x \rightarrow -\infty$

$$\varphi(x, y, t) = 2C_* \frac{\cosh k(y+L)}{\{2kh + \sinh(2kh)\}} \cdot \frac{2k/\ell}{(2k/\ell)^2 - 1} \cdot (-1)^m \sin(2kL) \cos(kx + \sigma t) \quad (56)$$

and as  $x \rightarrow +\infty$

$$\varphi(x, y, t) = 0 \quad (57)$$

Here, therefore, there is no disturbance in the perturbation solution on the down-wave side of the ripple patch, but there is a (reflected) disturbance on the up-wave side. The size of the reflected wave in relation to the incident wave can be assessed from the ratio of the amplitudes of the velocity potentials

$$\frac{\text{Amplitude } \{ \varphi(x, y, t) \}_{x \rightarrow -\infty}}{\text{Amplitude } \{ \Phi \}} = \frac{2bk}{\{2kh + \sinh(2kh)\}} \cdot \left[ (-1)^m \left( \frac{2k/\ell}{(2k/\ell)^2 - 1} \right) \cdot \frac{\sin(2k/\ell \cdot m\pi)}{(2k/\ell)^2 - 1} \right] \quad (58)$$

We can view this ratio as being composed of two parts. Consider firstly the part in the square brackets which we shall denote  $H_1(2k/\ell)$ , viz.

$$H_1(2k/\ell) = (-1)^m (2k/\ell) \cdot \frac{\sin(2k/\ell \cdot m\pi)}{(2k/\ell)^2 - 1}$$

We note initially that the amplitude of the reflected wave is highly oscillatory in the ratio of the overall length of the ripple patch  $(2m\pi/\ell)$  to the surface wavelength (see § 4.1). This result has been obtained for submerged rectangular parallelepipeds by, for example, Jeffreys (1944), Kreisel (1949), Newman (1965b) and Mei and Black (1969). We note next that  $H_1(2k/\ell)$  is not singular at  $2k/\ell = 1$  since

$$\lim_{2k/\ell \rightarrow 1} H_1(2k/\ell) = m\pi/2$$

In fact, what the limit shows is that  $H_1(1)$  increases linearly with the number of ripples ( $m$ ) in the patch. This can be seen in Fig 3 where  $H_1$  is plotted as a function of  $(2k/\ell)$  for  $m = 1, 2, 3$  and 4. The implication of the result is that as  $m$  increases, the amplitude of  $\phi(-\infty, y, t)$  at  $2k/\ell = 1$  increases, and this leads ultimately, as  $m \rightarrow \infty$ , to the condition of resonant interaction described in Part I (§ 4.1) of this report. It should be noted that  $H_1(2k/\ell)$  does not achieve its peak value at  $2k/\ell = 1$  but at a value  $2k/\ell > 1$ , since the slope of  $H_1$  at  $2k/\ell = 1$  is  $m\pi/4$ . This is most evident in the curve for  $m=1$  which has its maximum value at  $2k/\ell = 1.126$ ; the corresponding values for  $m = 2, 3$  and 4 are  $2k/\ell = 1.036, 1.0165$  and 1.009 respectively. This may have some significance in connection with § 7. of Part I, where it was suggested that ripple growth on an erodible bed of infinite horizontal extent is more likely for  $\ell \lesssim 2k$  than for  $\ell \gtrsim 2k$ . The present result suggests that in practical cases, where the number of ripples ( $m$ ) is finite, the strongest reflection of wave energy occurs for  $\ell \lesssim 2k$ , implying conditions which favour ripple growth rather than destruction. It was suggested in Part I that this growth is associated with the partially standing wave structure resulting from the superimposition of the incident  $(\phi)$  and reflected  $(\phi(-\infty, y, t))$  waves. Clearly, in the present case, standing waves will occur only on the up-wave side of the ripple patch, and so ripple growth is expected in  $-\infty < x < L$ , but not in  $L_2 < x < \infty$ .

More generally, given a constant ripple wavenumber  $\ell$ , the response curves in Fig 3 can be viewed as having the nature of wave attenuation functions of the surface wavenumber  $k$ . In particular, where  $H_1(2k/\ell) = 0$ , the amplitude of

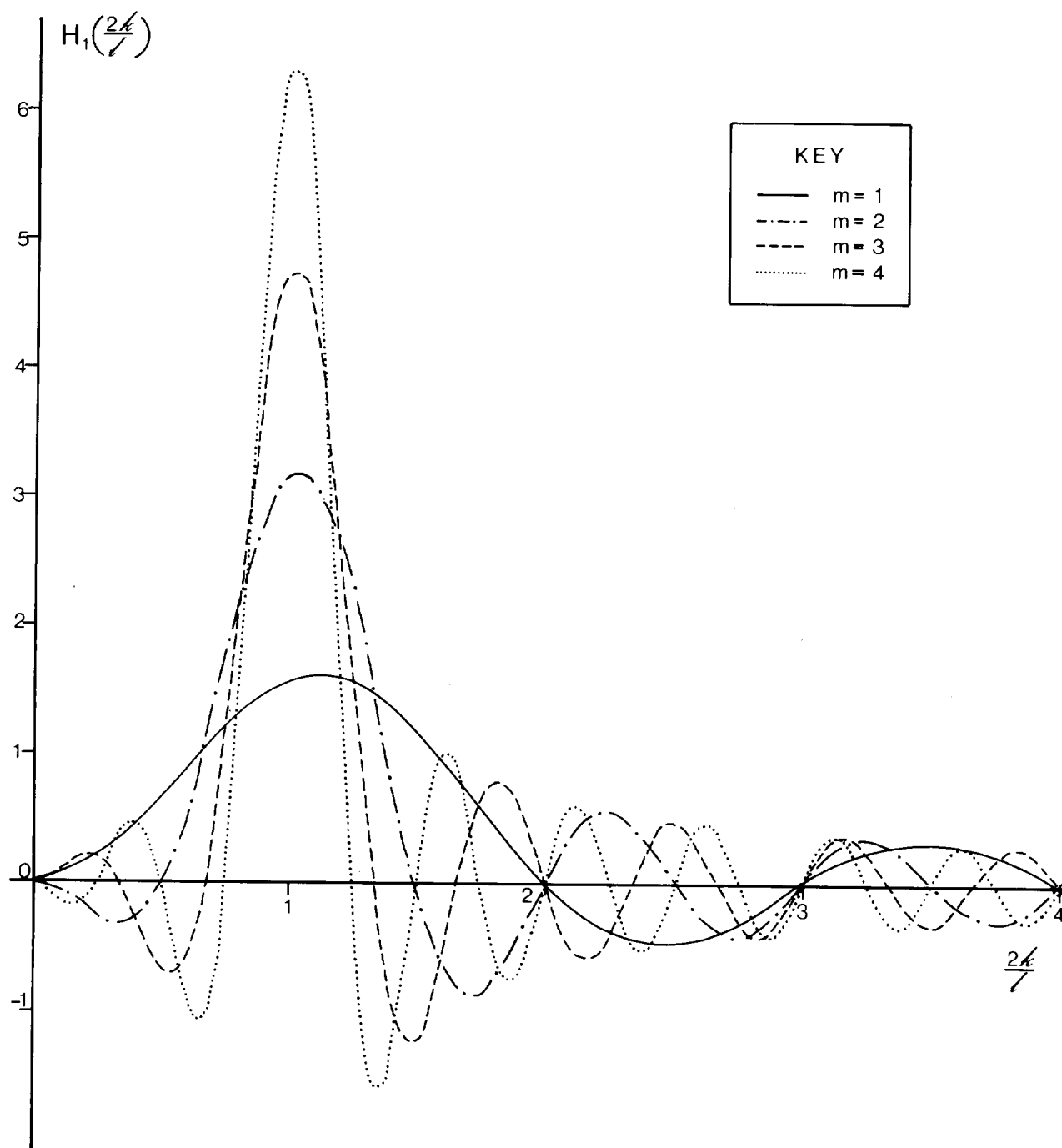


Fig 3 The response curve  $H_1\left(\frac{2k}{l}\right)$

the reflected wave  $\varphi(-\infty, y, t)$  is zero, implying that the incident waves are unaffected by the ripples on the bed. On the other hand, where  $H_1(2k/\ell)$  has its turning values, local maxima occur in the amount of wave energy reflected. It follows that, if a spectrum of surface waves is incident on a patch of ripples, significant reflections of wave energy may be expected to occur, but mainly in the neighbourhood of preferred values of  $k$ . In practice, this may cause a selective attenuation of the spectrum on the down-wave side of the ripples, compared with the incident wave spectrum. Conversely, any type of bed surface in  $L_1 < x < L_2$  may be described as a sum of Fourier harmonics and, since the theory is linear, it is possible to construct a general response curve for the predicted amplitude of the reflected wave as a function of  $k$  (see § 4.4).

The remaining part of the ratio in (58), namely  $2bk/\{2kh + \sinh(2kh)\}$ , indicates that the size of the reflected wave is dependent upon the ripple amplitude and the water depth. For long waves ( $kh \ll 1$ ) the term reduces to  $(b/2h)$ , and hence for long waves of wavenumber such that  $2k/\ell = 1$ ,

$$\frac{\text{Amplitude } \{\varphi(x, y, t)\}_{x \rightarrow -\infty}}{\text{Amplitude } \{\Phi\}} = \frac{b}{2h} \cdot \frac{\pi\pi}{2} \left( \frac{2k}{\ell} - 1, kh \ll 1 \right)$$

So in the typical physically interesting case of long wavelength dunes with, say,  $b/2h \approx 1/15$  the theory predicts that total reflection of wave energy will occur for  $m \geq 10$ . Although the theory is not expected to yield accurate results if  $|\varphi| \approx |\Phi|$  the general implication of this example is that it may take only a relatively small number of ripples to give rise in practice to total wave reflection, if the surface and ripple wavenumbers are such that  $2k/\ell = 1$ .

Results for the peak reflected wave amplitude  $a_r$  in the general case of intermediate water depth are shown in Fig 4, in which  $a_r/a$  is plotted against  $b/\ell$  for the range  $m = 1, 10$ , and for ripple steepness  $b\ell = \pi/20$  (Fig 4(i)) and  $b\ell = \pi/10$  (Fig 4(ii)). (Allen (1968) quotes the range of steepness of natural "large-scale ripples", having wavelength greater than 60 cm, as  $\pi/100 < b\ell < \pi/10$ .) The range of  $b/\ell$  has been taken as (0, 0.4) which is likely to encompass any naturally occurring features; strictly,  $b/\ell$  must be small for the theory to be valid (see § 3.5, Part I). The results plotted are the peak values of reflected wave amplitude which can arise as  $k$  varies. As suggested by Fig 3, this peak value is found where  $2k/\ell$  is close to unity and, in fact, it never exceeds the value at  $2k/\ell = 1$  itself by more than 0.01 for the curves plotted. Each curve has zero slope at the origin, an increasing slope for small  $b/\ell$  and, thereafter, a point of inflection and the tendency towards a linear behaviour in

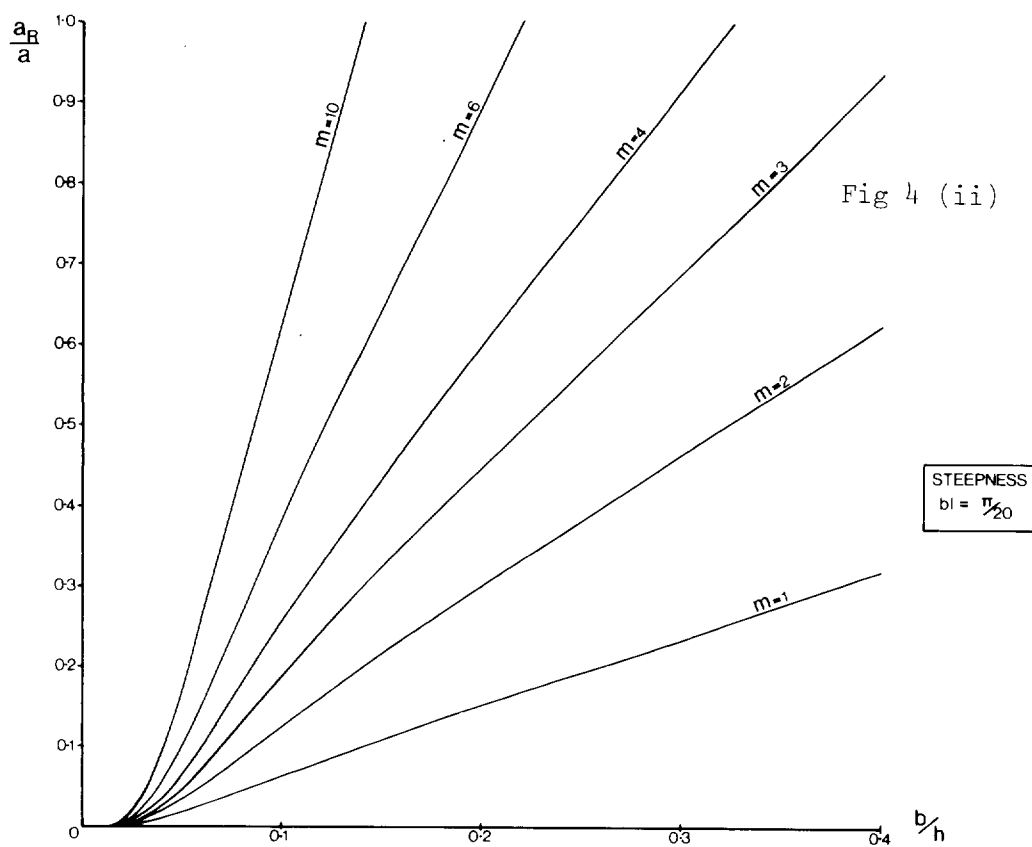
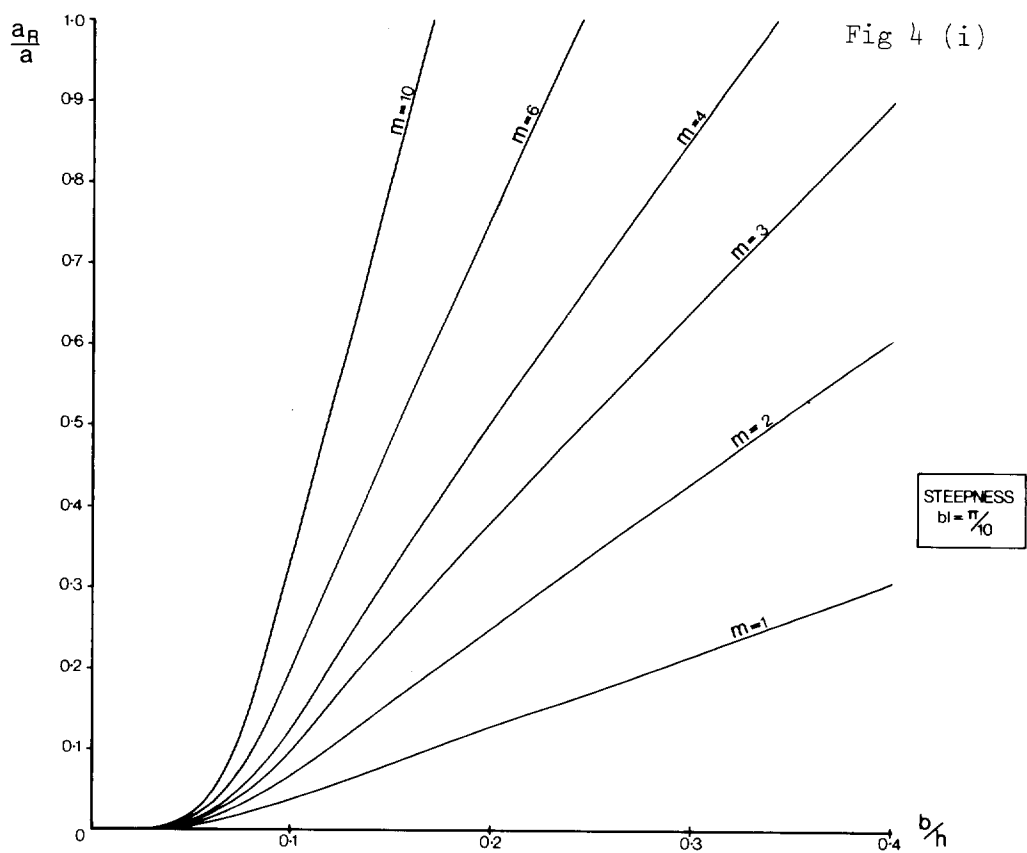


Fig 4 The reflected wave amplitude as a function of  $m$  and  $\frac{b}{h}$  for  $bl = \frac{\pi}{20}$  (Fig 4 (i)) and  $bl = \frac{\pi}{10}$  (Fig 4 (ii))



$(b/\ell)$  for large values of this quotient (in particular, for values such that  $b/\ell \gg 2b\ell$ ). It might be noted that, for  $2k/\ell = 1$ , the slopes of the linear portions of the curves are given by  $(m\pi/4)$ , regardless of steepness  $(b\ell)$ , but that the points of inflection occur at larger values of  $(b/\ell)$  as  $(b\ell)$  increases at a given value of  $m$ . The curves show that relatively few ripples having  $2k/\ell \approx 1$  are needed to produce a large reflected wave amplitude and that, for given  $(b/\ell)$  and  $m$ , the smaller the ripple steepness the greater is the size of the reflected wave.

Following the remaining examples in this section, we extend the results for this special case of the patch of ripples, in order to overcome certain deficiencies in (54) and (58). In particular, we attempt to produce a proper energy balance in the solution such that the transmitted wave energy flux (as  $x \rightarrow +\infty$ ) is equal to the difference between the incident and reflected fluxes. In (47), (56) and (57) this balance is not established and, in fact, Eq (56) should be viewed as providing an upper bound on the size of the reflected wave. This is true also of the example which follows, and of the examples in § 4.3 and 4.4.

### Special Case 2

Now consider the case in which there is a non-integral number of ripple wavelengths in the patch. In particular, consider the case in which  $m = n+1$  and  $\delta = 0$  in (49). From (54) and (55), as  $x \rightarrow -\infty$

$$\phi(x, y, t) = 2C_* \frac{\cosh k(y+\ell)}{\{2kh + \sinh(2kh)\}} \cdot \frac{2k/\ell}{(2k/\ell)^2 - 1} \cdot (-1)^n \cos\{(2n+1)k\pi/\ell\} \sin(kx + \sigma t - k\pi/\ell) \quad (59)$$

and, as  $x \rightarrow +\infty$

$$\phi(x, y, t) = 2C_* \frac{\cosh k(y+\ell)}{\{2kh + \sinh(2kh)\}} \cdot \frac{2k}{\ell} \cdot (-1)^{n+1} \sin(kx - \sigma t) \quad (60)$$

So in this case the transmitted wave (60) is non-zero and, when combined with  $\bar{\Phi}$ , produces small changes in the amplitude and phase of the waves on the down-wave side of the ripple patch. This is so even in cases of zero reflection. While the size of the transmitted wave  $\phi(\infty, y, t)$  increases linearly in  $(k/\ell)$ , there is no suggestion of a resonance in (60) as  $n \rightarrow \infty$ . Such a resonance occurs only in the reflected wave (59) as  $n \rightarrow \infty$ . In Fig 5 the function

$$H_2(2k/\ell) = (-1)^{n+1} \cdot \frac{2k}{\ell} \cdot \frac{\cos((2n+1)k\pi/\ell)}{(2k/\ell)^2 - 1}$$

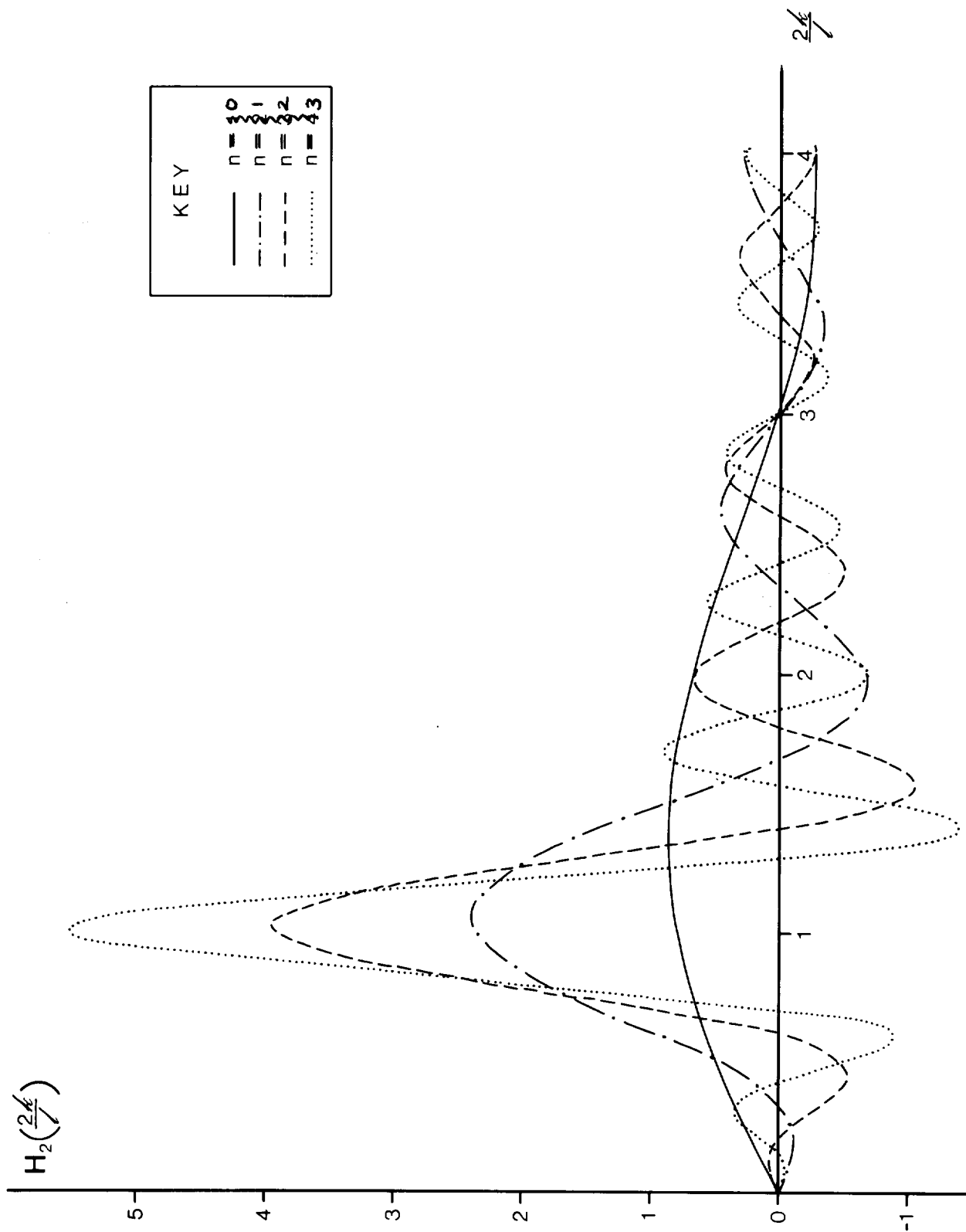


Fig 5 The response curve  $H_2(2k/l)$

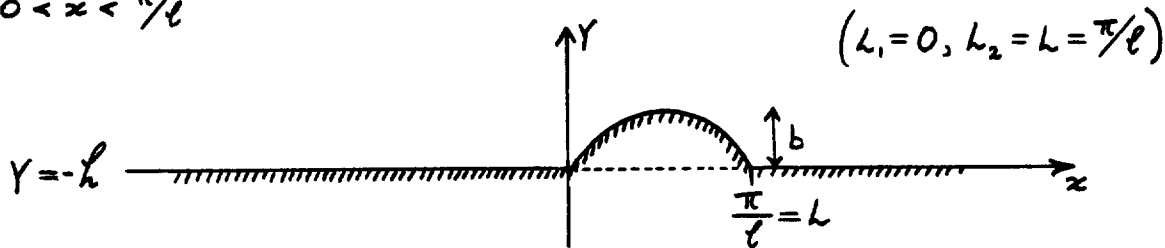
is plotted for  $0 \leq 2k/\ell \leq 4$  and for  $n = 0, 1, 2$  and  $3$ . As in the case of Eq (56), we note that Fig 5 implies that (59) is non-singular at  $2k/\ell = 1$  for finite  $n$ ; in fact,  $H_2(1) = \left(\frac{2n+1}{4}\right)\pi$ . Also, as was the case for  $H_1(2k/\ell)$  in Fig 3, the function  $H_2(2k/\ell)$  does not achieve its peak value at  $2k/\ell = 1$ , but at a value  $2k/\ell \gtrsim 1$ . This is most evident in the curve for  $n = 0$  ( $m = 1$ ) which has its maximum at  $2k/\ell = 1.367$ ; the corresponding values for  $n = 1, 2$  and  $3$ , ( $m = 2, 3$  and  $4$ ), are  $2k/\ell = 1.061, 1.023$  and  $1.012$  respectively.

In general, we see from the two special cases that the transmitted wave in the perturbation solution is either zero or non-zero depending upon whether there is an integral or non-integral number of wavelengths in the ripple patch. The magnitude of the transmitted wave is proportional to  $k/\ell$ . The reflected wave in the perturbation solution is rather more complicated in that its magnitude is periodic in the ratio  $k/\ell$ . The strongest reflection of incident wave energy occurs for  $2k/\ell \gtrsim 1$ , the amplitude of the reflected wave increasing with the number of ripples in the patch.

#### 4.3 A single sand bar or sandbank

Consider now another case having some relevance to coastal protection, namely the propagation of waves over a submerged sand bar or sandbank. Again we shall assume that the progressive waves in the first order solution have the velocity potential  $\Phi$  given by (47).

One approach is the extension of the results of § 4.2 for the special case in which  $\delta = 0$ ,  $m = 1$  and  $n = 0$ . This implies a single sinusoidal profile in  $0 < x < \pi/\ell$



and gives the results, as  $x \rightarrow -\infty$

$$\Phi(x, Y, t) = 2C_* \frac{\cosh k(Y+L)}{\{2kh + \sinh(2kh)\}} \cdot \frac{2k/\ell}{(2k/\ell)^2 - 1} \cdot \cos(kh) \sin(kx + \omega t - kL) \quad (61)$$

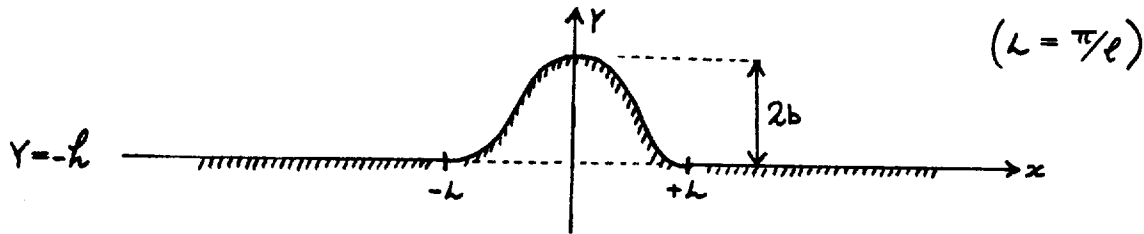
and, as  $x \rightarrow +\infty$

$$\varphi(x, y, t) = -2C_* \frac{\cosh k(y+L)}{\{2kh + \sinh(2kh)\}} \cdot \frac{2k}{\ell} \cdot \sin(kx - \sigma t) \quad (62)$$

The magnitude of the reflected wave in (61) is proportional to  $|H_2(2k/\ell)|$  with  $n = 0$  (see Fig 5), implying the strongest reflection of wave energy at wavenumber  $k$  such that  $2k/\ell = 1.367$ . The presence of a non-zero, but generally small, transmitted wave in (62) is the consequence of the bar comprising a non-integral number of wavelengths of the basic sinusoidal profile. It suggests a phase shift in the transmitted wave, even in cases of zero reflection.

An alternative way to proceed, and a way which ensures continuity of bed slope at the end points of the bar, is to define the bed by, say

$$Y_b(x) = b(1 + \cos(\ell x)) \quad \text{in} \quad -L < x < L \quad (63)$$



In contrast to the approach leading to (61) and (62), this introduces additional terms in the calculation of  $\mathcal{Q}_Y$  (from  $\mathcal{S}\Phi_{YY}$  in (5)); these terms arise as a result of the  $x$ -independent part of the right hand side of (63). The final results are, as  $x \rightarrow -\infty$

$$\varphi(x, y, t) = 2C_* \frac{\cosh k(y+L)}{\{2kh + \sinh(2kh)\}} \cdot \frac{\sin(2kL)}{(2k/\ell)^2 - 1} \cdot \sin(kx + \sigma t) \quad (64)$$

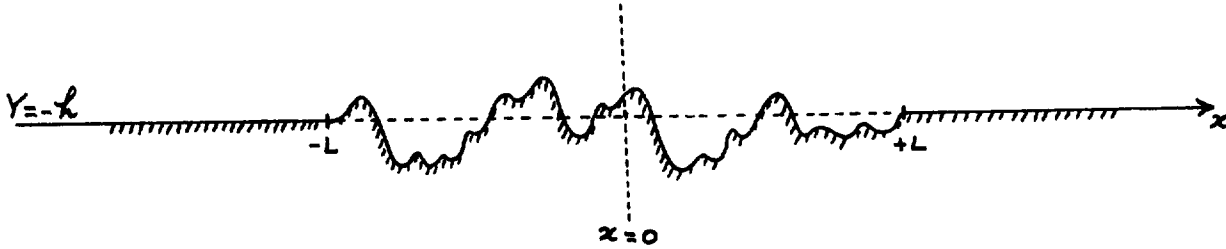
and, as  $x \rightarrow +\infty$

$$\varphi(x, y, t) = 0 \quad (65)$$

We see in this case that the magnitude of the reflected wave is proportional to  $\sin(2kL)/\{(2k/\ell)^2 - 1\}$  which has its most important turning value at  $2k/\ell = 0.837$ . The transmitted wave is zero as a result of there now being an integral number of wavelengths of the basic sinusoidal profile in  $-L < x < L$ .

#### 4.4 The general result

For completeness we take finally a case which is more general than those described above, involving Fourier series representations for both the bed features and the first-order surface waves. We suppose for simplicity that the region of topography is of extent  $2L$  in the  $x$ -direction with the origin of the  $x$ -axis at the midpoint of this range.



The bed is given by

$$Y_b(x) = \sum_{q=0}^{\infty} b_q \sin(qLx + \delta_q) \quad \text{in } -L < x < L \quad (65)$$

where  $L = \pi/l$  and in which  $b_0$  and  $\delta_0$  are chosen to ensure continuity of elevation at  $x = \pm L$ . The incident waves are given to first order by a series written in terms of surface wavenumber as follows:

$$\Phi(x, y, t) = \sum_{r=1}^{\infty} \Phi_r(x, y, t)$$

where

$$\Phi_r(x, y, t) = \frac{a_r g}{\sigma_r} \cdot \frac{\cosh k_r(y+h)}{\cosh(k_r h)} \cos(k_r x - \sigma_r t + \Delta_r) \quad (66)$$

and

$$k_r = +k \quad \text{with} \quad \sigma_r^2 = g k_r \tanh(k_r h)$$

The perturbing velocity at the bed is given as before by (7) in which  $\zeta$  and  $\bar{\phi}$  are now the infinite series given by (65) and (66) respectively and, as  $x \rightarrow \pm \infty$ , the general results may be built up by superimposing solutions of the type (44) and (45), viz.

$$\varphi(x, y, t) = \sum_r \sum_q \varphi_{qr}(x, y, t) \quad (67)$$

where  $\varphi_{qr}$  is the typical term arising from the  $q$ th term of (65) and the  $r$ th term of (66). (We assume in writing (67) that the orders of integration and summation may be reversed in calculating  $\mathcal{L}_1$  and  $\mathcal{L}_2$  in (44) and (45); in practice, truncated Fourier series will be taken for both  $\zeta$  and  $\bar{\phi}$  and so problems of convergence are not considered here.) Thus we arrive at the final results, as  $x \rightarrow -\infty$

$$\begin{aligned} \varphi_{qr}(x, y, t) = 2 C_{qr} \frac{\cosh k_r(y+l)}{\{2k_r l + \sinh(2k_r l)\}} \cdot (-1)^q \sin(2k_r L) \left[ \frac{k_r + l_q}{2k_r + l_q} \cos(k_r x + \sigma_r t - \Delta_r - \delta_q) \right. \\ \left. + \frac{l_q - k_r}{2k_r - l_q} \cos(k_r x + \sigma_r t - \Delta_r + \delta_q) \right] \quad (68) \end{aligned}$$

and, as  $x \rightarrow +\infty$ ,

$$\varphi_{qr}(x, y, t) = 0 \quad (69)$$

where

$$C_{qr} = \frac{a_r g b_q k_r}{\sigma_r \cosh(k_r l)} \quad \text{and} \quad l_q = q l$$

On substituting (68) into (67) we obtain a solution which, given the discrete spectral representations for the bed in (65) and the incident waves in (66), may be used to determine the spectrum of reflected waves. It is to be expected that this reflection will be selective in the manner shown in Figs 3 and 5; in effect, as each new harmonic constituent of either the bed or the incident waves is introduced, we build up the perturbation solution by establishing a set of response curves of the type shown in these figures and, ultimately, we superimpose the results obtained. In general, this will lead to the conclusion that energy reflection from the incident spectrum occurs at preferred wavenumbers or in preferred groups of wavenumbers. We note finally

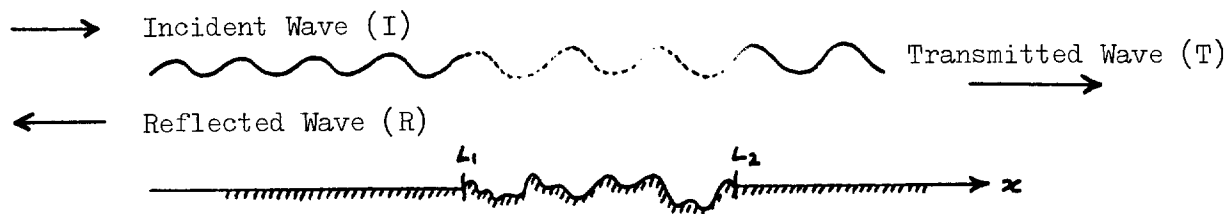
that the transmitted wave in the perturbation solution is zero. This is as a result of the fact that each constituent of the spectrum of bed features comprises an integral number of wavelengths in  $(-L, L)$ .

#### 4.5 Discussion

It was suggested earlier that results (56), (59), (61), (64) and (68) should be treated as providing upper bounds for the magnitudes of the reflected waves in the various applications discussed. The reason for this is that a proper energy balance is not established in the solution as a whole; in particular, there is an imbalance between the incident wave energy flux and the sum of the reflected and transmitted energy fluxes. This comes about on account of the fact that the linearized analysis does not permit any attenuation of the incident waves  $(\Phi)$  as they travel over the region of topography in  $(-L, L)$ , causing the predicted reflected wave in the perturbation solution to be overestimated and the transmitted wave to be generally zero. In practice, if the reflected wave is non-zero, there must be a progressive attenuation of the incident wave in  $(-L, L)$  and, in § 5. we discuss an ad hoc method of recovering an energy balance in the solution, and of thereby establishing more accurate predictions for the magnitudes of the reflected and transmitted waves. The true result may, in fact, hang on either a single reflection of the incident wave, or be a compounded effect of several reflections (see Newman (1965b)). Fortunately, the final result for the overall reflection coefficient appears to be rather insensitive to such details.

### § 5. CORRECTION PROCEDURE TO ESTABLISH A PROPER ENERGY BALANCE IN THE SOLUTION

We now seek to establish a balance of energy fluxes in the final results by an ad hoc iterative procedure. Suppose that waves (I) are incident on the bedforms from the left hand side



then, in general, we require for waves of given frequency that

$$\bar{E}_I = \bar{E}_R + \bar{E}_T \quad (70)$$

where  $\bar{E}$  stands for energy density and where the subscripts are defined in the figure. Eq (70) must be satisfied since the water is of the same constant mean depth at  $\pm \infty$  and, therefore, the group velocities of the three wave trains are the same. In terms of the amplitudes of the respective waves, it follows that

$$a^2 = a_I^2 = a_R^2 + a_T^2 \quad (71)$$

Suppose that, subject to (71), we identify the incident wave (I) and the transmitted wave (T) with the first order solution, and suppose further that wave reflection occurs uniformly<sup>1</sup> from  $x = L_1$  to  $L_2$ . There is some support for such an assumption in § 4.2 where we noted at  $2k/l = 1$ , that is near the condition for maximum wave reflection, that the amplitude of the reflected wave was proportional to the number ( $m$ ) of ripples in the patch. It may not be unreasonable, therefore, to assume a linear attenuation of incident wave amplitude from a prescribed starting value at  $x = L_1$  to some new lower value to be determined at  $x = L_2$ . On this basis, the general results (44) and (45) may be used in an iterative scheme to recalculate  $\varphi(x, y, t)$  as  $x \rightarrow \pm \infty$ , and to achieve a final result which satisfies (71) approximately.

For a modified incident wave amplitude which varies linearly from a value  $a_I = a$  at  $x = L_1$  to  $a_T$  at  $x = L_2$ , it is appropriate in calculating  $\Lambda(\xi, t)$  to replace  $V(x, t)$  given by (7), by  $\tilde{V}(x, t)$  where

$$\tilde{V}(x, t) = V(x, t) \left\{ \frac{L_2 - x}{L_2 - L_1} + \frac{a_T}{a} \cdot \frac{x - L_1}{L_2 - L_1} \right\} \quad \text{in } (L_1, L_2) \quad (72)$$

Here the term in the brace provides the assumed linear behaviour and, for  $a_T < a$ , it has the desired effect of producing a weaker interaction on the down-wave side of the region of bedforms than is obtained by taking  $V(x, t)$  itself (ie  $a_T = a$ ). If, for convenience, we write

$$F'_*(x, \xi, t) = F'_1(x, \xi) \cos(\sigma t) + F'_2(x, \xi) \sin(\sigma t) = \frac{1}{a} V(x, t) e^{i\xi x}$$

---

<sup>1</sup>Strictly we relax here the requirement that the redefined first order waves ( $I \rightarrow T$ ) satisfy the potential equation in  $(L_1, L_2)$ . Although this is not stated explicitly, it is the consequence of introducing a linear attenuation term into the perturbing velocity  $V(x, t)$  at the bed, Eq (72).



where a dash indicates differentiation with respect to  $x$ , it follows that the new expression for  $\mathcal{L}(\xi, t)$  may be written

$$\begin{aligned}\tilde{\mathcal{L}}(\xi, t) &= \tilde{\mathcal{L}}_1(\xi) \cos(\sigma t) + \tilde{\mathcal{L}}_2(\xi) \sin(\sigma t) \\ &= - \int_{L_1}^{L_2} \left\{ a \cdot \frac{L_2 - x}{L_2 - L_1} + a_\tau \cdot \frac{x - L_1}{L_2 - L_1} \right\} F'_*(x, \xi, t) dx\end{aligned}$$

and hence

$$\left. \begin{aligned}\tilde{\mathcal{L}}_1(\xi) &= a F_1(L_1, \xi) - a_\tau F_1(L_2, \xi) - \left\{ \frac{a - a_\tau}{L_2 - L_1} \right\} \int_{L_1}^{L_2} F_1(x, \xi) dx \\ \tilde{\mathcal{L}}_2(\xi) &= a F_2(L_1, \xi) - a_\tau F_2(L_2, \xi) - \left\{ \frac{a - a_\tau}{L_2 - L_1} \right\} \int_{L_1}^{L_2} F_2(x, \xi) dx\end{aligned} \right\} \quad (73)$$

These results may be used in (44) and (45) to give new perturbation solutions  $\tilde{\Phi}(x, y, t)$  in the limits  $x \rightarrow \pm\infty$ .

To satisfy (71) the following iterative scheme may be employed. Firstly, as in § 4, the reflected and transmitted waves may be calculated in the perturbation solution, assuming no attenuation of wave amplitude in the first order solution; in other words, if  $a_\tau^{(0)}$  is set equal to  $a$  (where the superscript denotes the stages in the calculation), then  $a_R^{(1)}$  and  $a_\tau^{(1)}$  may be calculated in the perturbation solution. Since, in general,  $a$ ,  $a_R^{(1)}$  and  $a_\tau^{(1)}$  will not satisfy (71), a new value  $\tilde{a}_\tau^{(1)} = \sqrt{a^2 - (a_R^{(1)})^2}$  may be calculated. If it is then found (as is most likely in the applications of interest here) that  $|\tilde{a}_\tau^{(1)}| \gg |a_\tau^{(1)}|$ , then  $\tilde{a}_\tau^{(1)}$  may be taken as the new wave amplitude at  $x = L_2$ . Thus new values of reflected and transmitted wave amplitudes,  $a_R^{(2)}$  and  $a_\tau^{(2)}$ , may be obtained from the linear attenuation argument above, and so the iterative scheme proceeds until  $a_R$  has converged to a value  $a_R^{(FINAL)}$ . This may be taken as a terminal and more accurate estimate of reflected wave amplitude provided the associated transmitted wave in the perturbation solution is negligibly small, that is provided  $|a_\tau^{(FINAL)}| \ll \sqrt{a^2 - (a_R^{(FINAL)})^2}$ . In the next section, this scheme is used in the case of the patch of ripples in  $(L_1, L_2)$ , that is in the case discussed in § 4.2. The iterative method is found to converge quite rapidly, and it suggests quite a substantial difference between  $a_R^{(1)}$  and  $a_R^{(FINAL)}$ .

### 5.1 Application in the case of a patch of ripples on an otherwise flat bed

The first order potential is given by (47) and the bed elevation in  $L_1 < x < L_2$  by (49). With  $V(x, t)$  calculated from (7) and modified to  $\tilde{V}(x, t)$  according to (72), the following results are obtained for  $\tilde{\Phi}$ , in the limits  $x \rightarrow -\infty$

$$\tilde{\varphi}(x, y, t) = \frac{C_* \cosh k(y+k)}{a \{2kh + \sinh(2kh)\}} \left[ \frac{2k/\ell}{(2k/\ell)^2 - 1} \cdot \left\{ a_r (-1)^m \sin(kx + \sigma t - 2kL_2) - a (-1)^n \sin(kx + \sigma t - 2kL_1) \right\} \right. \\ \left. + \left\{ \frac{a - a_r}{\ell(L_2 - L_1)} \right\} \cdot \frac{2}{(2k/\ell)^2 - 1} \cdot \left\{ (-1)^m \cos(kx + \sigma t - 2kL_2) - (-1)^n \cos(kx + \sigma t - 2kL_1) \right\} \right] \quad (74)$$

and  $x \rightarrow +\infty$

$$\tilde{\varphi}(x, y, t) = \frac{C_* \cosh k(y+k)}{a \{2kh + \sinh(2kh)\}} \left[ \left( \frac{2k}{\ell} \right) (a_r (-1)^m - a (-1)^n) \sin(kx - \sigma t) - \frac{2(a - a_r)}{\ell(L_2 - L_1)} \{ (-1)^m - (-1)^n \} \cos(kx - \sigma t) \right] \quad (75)$$

Upon setting  $a_r = a$ , Eqs (54) and (55) are recovered from (74) and (75) respectively. In the case of an integral number of bed wavelengths in the patch ( § 4.2, Special Case 1), such that  $m = n$  and  $\delta = 0$ , we have as  $x \rightarrow -\infty$

$$\tilde{\varphi}(x, y, t) = \frac{C_* \cosh k(y+k)}{a \{2kh + \sinh(2kh)\}} \left[ \frac{2k/\ell}{(2k/\ell)^2 - 1} \cdot (-1)^m \left\{ (a - a_r) \cos(2kL) \sin(kx + \sigma t) + (a + a_r) \cos(kx + \sigma t) \right. \right. \\ \left. \left. \cdot \sin(2kL) \right\} - 2 \left\{ \frac{(a - a_r) \cdot (-1)^m}{\pi \{ (2k/\ell)^2 - 1 \}^2} \cdot \sin(2kL) \sin(kx + \sigma t) \right\} \right] \quad (76)$$

and as  $x \rightarrow +\infty$

$$\tilde{\varphi}(x, y, t) = \frac{C_* \cosh k(y+k)}{\{2kh + \sinh(2kh)\}} \cdot \frac{2k}{\ell} \cdot \frac{a_r - a}{a} \cdot (-1)^m \sin(kx - \sigma t) \quad (77)$$

Now setting  $a_r = a$ , Eqs (56) and (57) are recovered respectively. It may be noted that the transmitted waves in the modified perturbation solutions (75) and (77) are no longer zero, the potentials taking values  $\sim (a - a_r)$ . This is due to the fact that the vertical motion  $\tilde{V}(x, t)$  at the bed is not now purely sinusoidal in time and space, and the result is a small phase shift in the transmitted wave.

Application of the iterative scheme described above enables a terminal value of reflected wave amplitude  $a_r^{(\text{FINAL})}$  to be obtained from the initial value  $a_r^{(i)}$ . The final value of  $a_r$  has been taken as the value  $a_r^{(i+1)}$  for which  $|(a_r^{(i+1)} - a_r^{(i)})/a_r^{(i+1)}| < 0.001$ ; in the present example, with Eqs (76) and (77), this has required about 5 steps for  $a_r^{(i)}/a \approx 0.5$  and about 18 steps for  $a_r^{(i)}/a \approx 1.0$ . It has been found that the ratio  $(a_r^{(i)} - a_r^{(\text{FINAL})})/a_r^{(i)}$  is a function of  $a_r^{(i)}/a$  only, as shown in Fig 6. In the case of zero reflection, the initial result ( $a_r^{(i)} = 0$ ) clearly requires no correction. If the first estimate is  $a_r^{(i)} = 0.5a$  the final result satisfying (71) is  $a_r^{(\text{FINAL})} \approx 0.47a$ . In the extreme case of total reflection in the first estimate ( $a_r^{(i)} = a$ ), the terminal value is

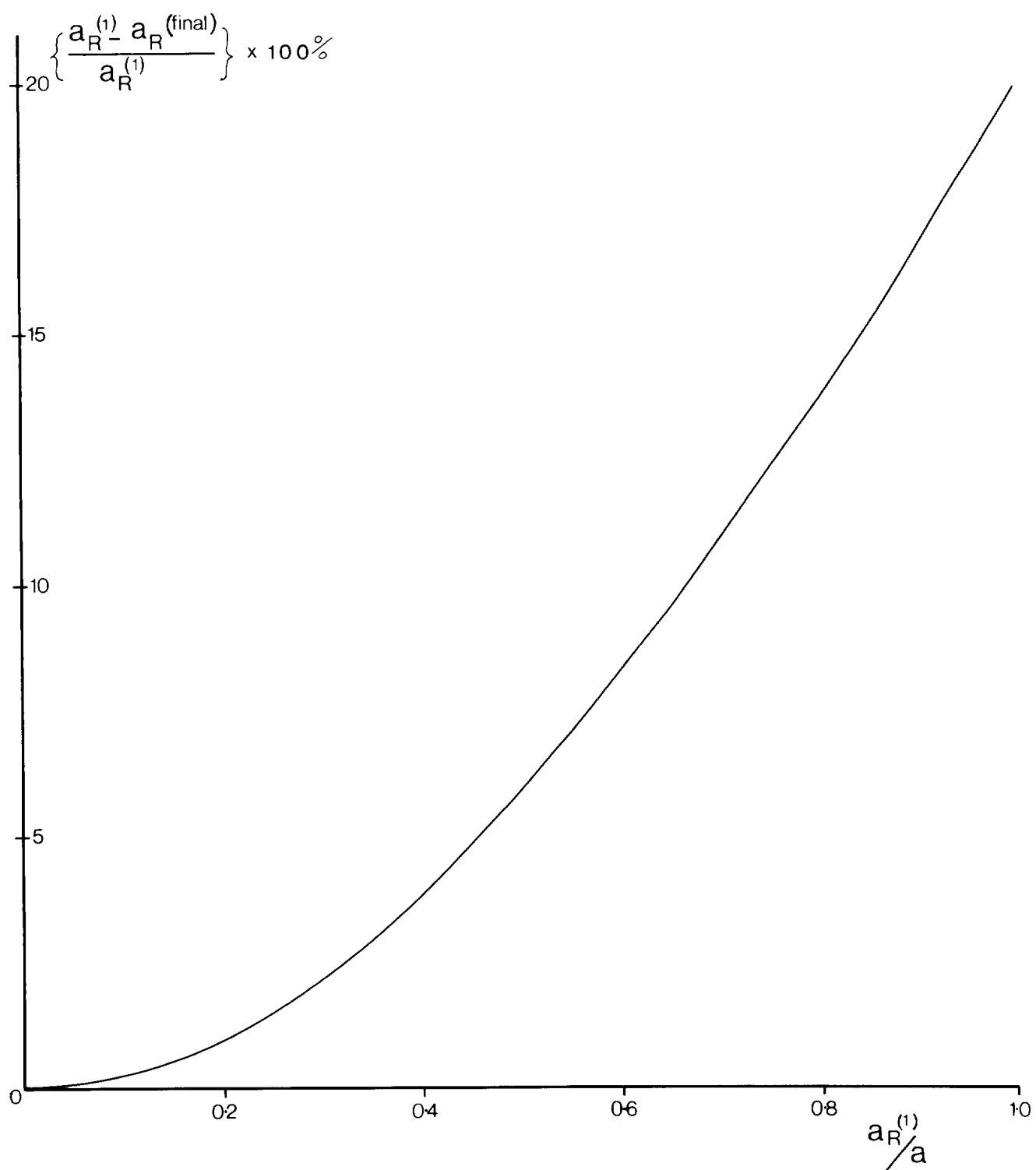


Fig 6 Correction curve for the reflected wave amplitude.

$a_r^{(\text{FINAL})} = 0.8 a$  . In terms of energy flux this indicates an overestimate of reflected energy flux of 36%. Despite the need for substantial corrections of this type for conditions of large wave reflection, the principal value of the present method is in providing the estimate  $a_r^{(1)}$  by way of (44) and (45) in the first place.

The final result is rather insensitive to the particular attenuation assumption which is made. In fact, the correction curve in Fig 6 may be obtained in this particular example by making a simpler modification to  $V(x,t)$  than (72), namely  $\tilde{V}(x,t) = \{(a+a_r)/2a\} V(x,t)$ . Equations (56) and (57) may then be re-used successively to iterate to the final result. The transmitted wave in the perturbation solution is zero on this assumption however, and it is preferable, in general, to adopt (72) or some similar, rather more realistic, attenuation rule.

In Part I of this report, for the case of a sinusoidal bed of infinite horizontal extent, limitations on the perturbation solution were stated as a set of restrictions on the sizes of various non-dimensionalized length scales in the problem, together with the further restriction that near  $2k/\ell = 1$  the solution is invalid due to the infinite resonance in the potential. In Part II the limitations are the same, except that now the perturbation solution is merely resonant, and not infinitely resonant, near  $2k/\ell = 1$ , and so the first estimate for the perturbation potential will be valid near  $2k/\ell = 1$  provided  $a_r^{(1)} \ll a$ . In fact, the correction procedure described in this section, despite its shortcomings, enables even this restriction to be relaxed, so that we do not formally require  $a_r^{(\text{FINAL})} \ll a$  in the final result. It follows that, having applied the correction procedure, we need only satisfy the restrictions on the various combinations of length scales in the problem. As argued earlier, these restrictions do not prevent the use of the solution in physically interesting cases.

## § 6. DISCUSSION

### 6.1 Consequences for sediment transport

It was shown in § 4.2 that for surface waves incident upon sinusoidal bedforms of finite horizontal extent, maximum reflection occurs at surface wavenumbers for which  $2k/\ell \approx 1$ . Since in Part I, for a bed of infinite extent it was suggested that there may be a coupling between wave reflection and dune growth if  $2k/\ell \approx 1$ , this result has certain consequences for sediment

transport, at least if the bed on the up-wave side of the ripple patch is erodible. The existence of a partially standing wave structure in  $-\infty < x < L_1$ , caused by wave reflection, may deform this part of the bed into dunes having the preferred bed wavenumber  $\ell \approx 2k$ . The general picture may then be as follows: if a spectrum of waves is incident on a region of bedforms of wavenumber  $\ell$ , only those waves having  $k \approx \ell/2$  will be strongly reflected by the topography. These reflected waves may cause the formation of new bed features in  $-\infty < x < L_1$ , and, as these grow, so the nature of the wave reflection will change and become concentrated near the point in the spectrum where  $2k/\ell = 1$ . Evidently, no mechanism exists for the formation of new bed features in the region  $L_2 < x < \infty$  by surface/seabed interaction.

It is worth contrasting this situation with that which would arise in steady flow over bedforms of initially finite horizontal extent. In this case, the equivalent perturbation solution leads to the prediction of a standing wave on the downstream side of the bedforms<sup>1</sup>. Therefore any new bedform growth is to be expected only on the downstream side ( $L_2 < x < \infty$ ) of the initial disturbance on the bed. In respect of implications for sediment transport, this is the fundamental difference between the cases involving waves and currents.

## 6.2 Momentum flux considerations

In § 5. we established an approximate balance between the incident, reflected and transmitted wave energy fluxes. Since, in general, the bedforms are found to reflect wave energy, they must also reflect horizontal momentum, and hence be subject to a mean horizontal force. This may be calculated if the incident, reflected and transmitted wave amplitudes are known. By the conservation of mean momentum, we expect the bedforms to be subject to a mean horizontal force in the direction of incident wave travel which, for non-breaking waves of small amplitude, is equal to

$$\frac{1}{4} \rho_w g (a^2 + a_r^2 - a_t^2) \left( 1 + \frac{2kh}{\sinh(2kh)} \right) \quad (78)$$

per unit width of wavefront, where  $\rho_w$  is the water density and  $g$  is gravity (Longuet-Higgins (1977)). For totally submerged bodies, it has been found experimentally that the mean force can be less than the expected value given by (78), due partly to the presence of a second harmonic in the transmitted

---

<sup>1</sup>This is by analogy with, for example, Lamb (1932, Art 243)

wave (see also Jolas (1960)). This arises under circumstances in which the wave amplitude above the submerged body becomes a significant fraction of the local depth, though the waves are not necessarily breaking. This situation is clearly not accounted for by the present theory but, in § 3.5 of Part I, it was argued that we require  $a/k, b/k \ll 1$  for the theory to be valid. Longuet-Higgins (1977) has studied the forces on a submerged model bar, mounted on wheels and free to move horizontally on a smooth flat bed in either direction. The observed direction of motion of this bar was governed by forces due to wave set-up and set-down; in particular, long low incident waves tended to move the bar in the direction of wave propagation, but short steep breaking waves tended to move it in the opposite direction.

The forces on the bed in the present linear theory are given by (78) and so depend upon the square of the amplitude of the reflected wave, since  $a_r^2 + a_s^2 - a_i^2 = 2a_r^2$  by (71). Hence an upper bound may be placed on the mean force if the reflected wave amplitude is calculated from (44), or a more realistic result obtained if the correction procedure of § 5. is used. If the incident wave is totally reflected then  $a_r = a$ , and the force per unit width of wavefront becomes  $\frac{1}{2} \rho_w g a^2 (1 + 2kh / \sinh(2kh))$ . In terms of sediment transport, the mean force on the bedforms is likely to be of importance on geological timescales only, and quite possibly to be overshadowed by effects of the type discussed in § 6.1. It has been argued by Davies and Wilkinson (1978) that if surface waves are non-breaking, then, at the threshold of sediment motion, the force on a single sand grain due to pressure gradients in the flow is likely to be of secondary importance at most compared with the velocity-induced force. This is the relevant consideration in assessing the response of a sand bed to low waves. It is unlikely that the pressure gradients due to set-up and set-down will cause the bed to fail in its interior, and for shear to take place at some low level, resulting in the movement of bedforms as solid bodies. The most realistic way in which bedform migration can be envisaged as a result of the mean force (78) is by the gradual residual migration of individual mobile grains in one preferred direction - this direction being that of the propagation of the incident waves.

## § 7. CONCLUSIONS

In Part II of the report, a perturbation analysis has been developed to study the interaction of a given first order motion with a region of prescribed seabed topography. The analysis has been restricted to two dimensional irrotational flow,

and the first order motion has been taken as comprising surface waves of small amplitude in water of finite depth. The interaction of this motion with the bedforms has been assumed to be such that no flow separation occurs at the bed.

Although the perturbation solution enables the flow to be studied in the immediate vicinity of the bedforms, the general results produced in § 2. and § 3. are for the perturbation potentials well away from the bedforms, on both the up-wave and down-wave sides. These general results have been arrived at by two approaches, the first a steady-state analysis, the second the solution of an initial value problem. In each case a perturbing vertical velocity at the seabed, resulting from the interaction of the first order motion with the bedforms, gives rise to outgoing waves at the surface satisfying the radiation condition. Essentially, the general results relate the sizes of these outgoing waves to the Fourier transform of the perturbing vertical velocity.

The advantage of the present method over that proposed by, for example, Kreisel (1949) is that at no stage in the argument is a mapping of the complicated fluid domain required. Though, in theory, a conformal mapping exists for each of the cases discussed in § 4., in practice the mapping is not known, and so an alternative approach is desirable. The principal disadvantage of the approach described here is that it does not provide, at least at the outset, a proper balance between the incident, reflected and transmitted wave energy fluxes; in fact, the basic result merely provides an upper bound on the size of the reflected wave. However, an "ad hoc" correction procedure has been suggested in § 5. to establish a proper balance and achieve a more realistic result.

The principal applications of the method discussed here have concerned the cases of a patch of sinusoidal dunes and an isolated submerged hill, the latter being a special case of the former. In general terms, the results for the reflected wave have shown that the reflection coefficient is both a highly oscillatory function of the ratio of the overall length of the patch of dunes to the surface wavelength, and is also strongly dependent on the ratio of the surface to bed wavelengths. Examples have shown that, for realistic values of dune steepness and fairly small values of the ratio of dune amplitude to water depth, only a few dunes may be needed to produce quite a large reflection of incident energy, at least if  $2k/\ell \approx 1$ , where  $k$  and  $\ell$  are the surface and bed wavenumbers respectively. The greater the number of dunes, the narrower is the range of incident wavenumbers which are strongly reflected by the topography. An implication of the results is that if a spectrum of waves is incident on a patch of dunes of wavenumber  $\ell$ , there will be a selective reflection of wave energy

depending upon incident wavenumber, the preferred part of the spectrum for wave energy reflection being in the vicinity of  $k = \frac{\pi}{2}$ . It has been found also that there may be a small phase shift in the transmitted wave, even in cases of zero reflection. This has been noted also by Newman (1965b).

The wave reflection mechanism discussed in this report may be important in terms of the possible coupling which may exist between dune growth on an erodible bed and the reflection of incident wave energy. It is well known that partial wave reflection may occur from a beach face, with the consequent formation of a series of offshore bars which, in turn, shelter the beach from wave attack. It may be concluded from the present analysis that, under certain preferred conditions, a totally submerged series of bedforms may act as an effective reflector of incident wave energy, thereby reducing the wave height on the down-wave side of the bedforms, and possibly causing the growth of new bedforms on the up-wave side. The further reduction of the transmitted wave height by this process may be quite significant and have far-reaching implications, for example in the siting of wave power devices.



## ACKNOWLEDGEMENTS

The study in Part I was prompted by the suggestion of Dr S A Thorpe (IOS Wormley), while that in Part II was an adaptation of a suggestion made to the author by Dr J Breslin (Davidson Laboratory, Stevens Institute of Technology, New Jersey, USA) for the study of steady flows over bottom undulations. Both are thanked, as are Professor T V Davies and Dr S J Maskell for some helpful comments on Part II. Most of the numerical calculations for Part I were done by Mr J P Futcher, on a sandwich studentship from the University of Bath. Mr D N Langhorne kindly made available the sandwave profiles, and the diving team at IOS Taunton obtained the seabed ripple profiles. Finally, Mr R L Soulsby is thanked for his comments on the manuscript, as are Mrs Lynne Ellett and Mrs Jean Hooper for preparing the diagrams.

## REFERENCES

- ADAMS, J K and BUCHWALD, V T. 1969. The generation of continental shelf waves. Journal of Fluid Mechanics, 35 (4), 815-826.
- ALLEN, J R L, 1968. Current ripples. Their relation to patterns of water and sediment motion. Amsterdam: North-Holland, 433 pp.
- ALLEN, J S, 1976. Continental shelf waves and alongshore variations in bottom topography and coastline. Journal of Physical Oceanography, 6, 864-878.
- BAINES, P G, 1971. The reflexion of internal/inertial waves from bumpy surfaces Journal of Fluid Mechanics, 46 (2), 273-291.
- BAINES, P G, 1973. The generation of internal tides by flat-bump topography. Deep-Sea Research, 20, 179-205.
- BAINES, P G, 1974. The generation of internal tides over steep continental slopes. Philosophical Transactions of the Royal Society of London Series A, 277-(1263), 27-58.
- BARTHOLOMEUSZ, E F, 1958. The reflexion of long waves at a step. Proceedings of the Cambridge Philosophical Society, 54, 106-118.
- BERKHOFF, J C W, 1973. Computation of combined refraction-diffraction. Pp 471-490 in Proceedings of the 13th Conference on Coastal Engineering, Vancouver, 1972. New York: American Society of Civil Engineers.
- BIESEL, F and LE MÉHAUTE, B, 1955. Étude théorique de la reflexion de la houle sur certains obstacles. La Houille Blanche, 10, 130-138.
- BRINK, K H, 1980. Propagation of barotropic continental shelf waves over irregular bottom topography. Journal of Physical Oceanography, 10, 765-778.
- CARRIER, G F, 1966. Gravity waves on water of variable depth. Journal of Fluid Mechanics, 24 (4), 641-659.
- COX, C and SANDSTROM, H, 1962. Coupling of internal and surface waves in water of variable depth. Journal of the Oceanographical Society of Japan, 20th Anniversary Volume, 499-513.
- DAVIES, A G, 1979. The potential flow over ripples on the seabed. Journal of Marine Research, 37 (4), 743-759.
- DAVIES, A G and WILKINSON, R H, 1979. Sediment motion caused by surface water waves. Pp 1577-1595 in Proceedings of the 16th Conference on Coastal Engineering, Hamburg, 1978. Volume 2. New York: American Society of Civil Engineers.
- FITZ-GERALD, G F, 1976. The reflexion of plane gravity waves travelling in water of variable depth. Philosophical Transactions of the Royal Society of London Series A, 284 (1317), 49-89.

- FULLER, J D and MYSAK, L A, 1977. Edge waves in the presence of an irregular coastline. Journal of Physical Oceanography, 7, 846-855.
- HAMILTON, J, 1977. Differential equations for long-period gravity waves on fluid of rapidly varying depth. Journal of Fluid Mechanics, 83 (2), 289-310.
- HARBAND, J, 1977. Propagation of long waves over water of slowly varying depth. Journal of Engineering Mathematics, 11 (2), 97-119.
- HAVELOCK, T H, 1917. Some cases of wave motion due to a submerged obstacle. Proceedings of the Royal Society Series A, 93, 520-532.
- HOWE, M S and MYSAK, L A, 1973. Scattering of Poincaré waves by an irregular coastline. Journal of Fluid Mechanics, 57 (1), 111-128.
- HSUEH, Y, 1980. Scattering of continental shelf waves by longshore variations in bottom topography. Journal of Geophysical Research, 85 (C2), 1147-1150.
- JEFFREYS, H, 1944. Motion of waves in shallow water. Note on the offshore bar problem and reflexion from a bar. London: Ministry of Supply Wave Report, No 3.
- JOHNS, B, 1970. On the mass transport induced by oscillatory flow in a turbulent boundary layer. Journal of Fluid Mechanics, 43 (1), 177-185.
- JOLAS, P, 1960. Passage de la houle sur un seuil. La Houille Blanche, 15, 148-151.
- JONSSON, I G, SKOVGAARD, O and BRINK-KJAER, O, 1976. Diffraction and refraction calculations for waves incident on an island. Journal of Marine Research, 34 (3), 469-496.
- KAJIURA, K, 1961. On the partial reflection of water waves passing over a bottom of variable depth. I.U.G.G. Monograph No 24, 206-230.
- KREISEL, G, 1949. Surface waves. Quarterly of Applied Mathematics, 7 (1), 21-44.
- LAMB, H, 1932. Hydrodynamics. (6th ed) Cambridge University Press, 738 pp.
- LANGHORNE, D N, 1978. Offshore engineering and navigational problems: the relevance of sandwave research. London: Society for Underwater Technology in conjunction with the Institute of Oceanographic Sciences, 21 pp.
- LARSEN, L H, 1969. Internal waves incident upon a knife edge barrier. Deep-Sea Research, 16, 411-419.
- LeBLOND, P H and MYSAK, L A, 1978. Waves in the ocean. Amsterdam: Elsevier Scientific Publishing Company, 602 pp.
- LEWIS, J E, LAKE, B M and KO, D R S, 1974. On the interaction of internal waves and surface gravity waves. Journal of Fluid Mechanics, 63 (4), 773-800.

- LIGHTHILL, M J, 1965. Group velocity. Journal of the Institute of Mathematics and its Applications, 1, 1-28.
- LIGHTHILL, M J, 1978. Waves in fluids. Cambridge University Press, 504 pp.
- LONGUET-HIGGINS, M S, 1953. Mass transport in water waves. Philosophical Transactions of the Royal Society of London Series A, 245, 535-581.
- LONGUET-HIGGINS, M S, 1977. The mean forces exerted by waves on floating or submerged bodies with applications to sand bars and wave power machines. Proceedings of the Royal Society of London Series A, 352, 463-480.
- MAHONY, J J, 1967. The reflection of short waves in a variable medium. Quarterly of Applied Mathematics, 25 (3), 313-316.
- MCGOLDRICK, L F, 1968. Long waves over wavy bottoms. University of Chicago, Department of Geophysical Sciences, O.N.R. Ocean Science and Technology Group, Technical Report No 1., 67 pp.
- MCWILLIAMS, J C, 1974. Forced transient flow and small scale topography. Geophysical Fluid Dynamics, 6, 49-79.
- MEI, C C and BLACK, J L, 1969. Scattering of surface waves by rectangular obstacles in waters of finite depth. Journal of Fluid Mechanics, 38 (3), 499-511.
- MEYER, R E, 1979. Surface wave reflection by underwater ridges. Journal of Physical Oceanography, 9, 150-157.
- MILES, J W, 1967. Surface-wave scattering matrix for a shelf. Journal of Fluid Mechanics, 28 (4), 755-767.
- MILNE-THOMSON, L M, 1968. Theoretical hydrodynamics. (5th ed) London: Macmillan Press Limited, 743 pp.
- MYSAK, L A and TANG, C L, 1974. Kelvin wave propagation along an irregular coastline. Journal of Fluid Mechanics, 64 (2), 241-261.
- NIELSEN, P, 1979. Some basic concepts of wave sediment transport. Technical University of Denmark. Institute of Hydrodynamics and Hydraulic Engineering. Series Paper No 20, 160 pp.
- NEWMAN, J N, 1965a. Propagation of water waves over an infinite step. Journal of Fluid Mechanics, 23 (2), 399-415.
- NEWMAN, J N, 1965b. Propagation of water waves past long two-dimensional obstacles. Journal of Fluid Mechanics, 23 (1), 23-29.
- OGILVIE, T F, 1960. Propagation of waves over an obstacle in water of finite depth. University of California, Institute of Engineering Research Report No 82-14, 88 pp.
- PEREGRINE, D H, 1972. Equations for water waves and the approximations behind them. Pp 95-121 in Waves on beaches edited by R E Meyer. New York: Academic Press.

- PINSENT, H G, 1972. Kelvin wave attenuation along nearly straight boundaries. Journal of Fluid Mechanics, 53 (2), 273-286.
- RHINES, P B, 1970. Wave propagation in a periodic medium with application to the ocean. Reviews of Geophysics and Space Physics, 8 (2), 303-319.
- RHINES, P B and BRETHERTON, F, 1973. Topographic Rossby waves in a rough-bottomed ocean. Journal of Fluid Mechanics, 61 (3), 583-607.
- ROSEAU, M, 1952. Contribution a la théorie des ondes liquides de gravité en profondeur variable. Paris: Publications Scientifiques et Techniques du Ministère de l'Air, No 275.
- SANDTROM, H, 1976. On topographic generation and coupling of internal waves. Geophysical Fluid Dynamics, 7, 231-270.
- SHINBROT, M, 1980. Water waves over periodic bottoms in three dimensions. Journal of the Institute of Mathematics and its Applications, 25, 367-385.
- SLEATH, J F A, 1975. Transition in oscillatory flow over rippled beds. Proceedings of the Institution of Civil Engineers, 59 (2), 309-322.
- SLEATH, J F A, 1976. On rolling grain ripples. Journal of Hydraulic Research, 14 (1), 69-81.
- STOKER, J J, 1953. Some remarks on radiation conditions. Pp 97-102 in Proceedings of the Fifth Symposium in Applied Mathematics of the American Mathematical Society, Carnegie Institute of Technology, 1952. McGraw-Hill.
- STOKER, J J, 1957. Water waves. New York: Interscience, 567 pp.
- TAKANO, K, 1960. Effets d'un obstacle parallélépipédique sur la propagation de la houle. La Houille Blanche, 15, 247-267.
- THOMSON, R E, 1975. The propagation of planetary waves over a random topography. Journal of Fluid Mechanics, 70 (2), 267-285.
- URSELL, F, 1953. The long-wave paradox in the theory of gravity waves. Proceedings of the Cambridge Philosophical Society, 49, 685-694.
- U S ARMY. COASTAL ENGINEERING RESEARCH CENTER. 1973. Shore Protection Manual, Volume 2.
- WHITHAM, G B, 1974. Linear and nonlinear waves. New York: Wiley-Interscience, 636 pp.





*Printed by NERC/SRC Reprographic Services*

